

Seznam genů v panelech

Metabolický panel (237 genů)

Hyperhomocysteinémie (54 genů):

ABCD4, ADK, AHCY, ALDH7A1, AMN, CBS, CD320, CDO1, CTH, CUBN, DHFR, ETHE1, FOLH1, FOLR1, FOLR2, FOLR3, FTCD, FUT2, GIF, GNMT, GPHN, HCFC1, LMBRD1, LRP2, MAT1A, MAT2A, MAT2B, MCEE, MMAA, MMAB, MMACHC, MMADHC, MOCS1, MOCS2, MTHFD1, MTHFR, MTHFS, MTR, MTRR, MUT, PDXK, PDXP, PNPO, SLC19A1, SLC25A32, SLC46A1, SQOR, SUCLA2, SUOX, TCN1, TCN2, THAP11, TST, ZNF143

Leucinózy (4 geny): *BCKDHA, BCKDHB, DBT, DLD*

Neuronální ceroidlipofuscinózy (13 genů): *ATP13A2, CLN3, CLN5, CLN6, CLN8, CTSD, CTSF, DNAJC5, GRN, KCTD7, MFSD8, PPT1, TPP1*

Peroxisomální onemocnění (34 genů): *ABCD1, ABCD3, ACBD5, ACOX1, AGPS, AGXT, AMACR, BAAT, CAT, DNMIL, FAR1, GDAP1, GNPAT, HSD17B4, MFF, PEX1, PEX2, PEX26, PEX3, PEX5, PEX5L, PEX6, PEX7, PEX10, PEX11A, PEX11B, PEX11G, PEX12, PEX13, PEX14, PEX16, PEX19, PHYH, SCP2*

Poruchy metabolismu glykogenu (29 genů): *AGL, ALDOA, ALDOB, ALDOC, ENO3, FBP1, G6PC, GAA, GBE1, GYGI, GYS1, GYS2, KHK, PC, PFKM, PGAM2, PGMI, PHKA1, PHKA2, PHKB, PHKG2, PRKAB1, PRKAB2, PRKAG2, PYGL, PYGM, RBCK1, SLC2A2, SLC37A4*

Poruchy metabolismu neurotransmitterů (26 genů): *ABAT, ALDH5A1, ALDH7A1, AMT, DBH, DDC, DHFR, DNAJC12, FOLR1, GCH1, GCSH, GLDC, GLUL, MAOA, PCBD1, PHGDH, PNPO, PSAT1, PSPH, PTS, QDPR, SLC18A2, SLC46A1, SLC6A3, SPR, TH*

Poruchy cyklu močoviny, orotové acidurie (19 genů): *ARG1, ASL, ASS1, CAD, CPS1, DHODH, FTCD, NAGS, OTC, SHMT1, SHMT2, SLC25A13, SLC25A15, SLC25A2, SLC46A1, SLC7A7, TYMP, TYMS, UMPS*

Rhabdomyolýzy a poruchy metabolismu mastných kyselin (52 genů): *ACADM, ACADVL, AGL, ALDOA, AMPD1, ANO5, ATP2A1, CACNA1S, CASQ1, CAV3, CHKB, CPT1A, CPT2, CTDPI, CYP2C8, DGUOK, DYSF, ENO3, ETFA, ETFB, ETFDH, FDX1L, FKRP, FLAD1, HADHA, HADHB, HRAS, ISCU, LAMP2, LDHA, LPINI, PFKM, PGAM2, PGK1, PGMI,*

PHKA1, PHKB, POLG, PYGM, QARS, RYR1, SCN4A, SIL1, SLC16A1, SLC25A20, SLC25A32, SLC52A1, SLC52A2, SLC52A3, TANGO2, TSEN54, TSFM

Jiná onemocnění: CADASIL (*NOTCH3*), cystinurie (*SLC3A1, SLC7A9*), propionová acidurie (*PCCA, PCCB*), isovalerová acidurie (*IVD*)

Kardiologický panel (kardiomyopatie, aortopatie, arytmie, 177 genů):

ABCC9, ABCG5, ABCG8, ACTA1, ACTC1, ACTN2, AKAP9, ALMS1, ANK2, ANKRD1, APOA4, APOA5, APOB, APOC2, APOE, BAG3, BRAF, CACNA1C, CACNA2D1, CACNB2, CALR3, CASQ2, CAV3, CBL, CBS, CETP, COL3A1, COL4A5, COL5A1, COL5A2, CREB3L3, CRELD1, CRYAB, CSRP3, CTF1, CTNNA3, DES, DMD, DNAJC19, DOLK, DPP6, DSC2, DSG2, DSP, DTNA, EFEMP2, ELN, EMD, EYA4, FBN1, FBN2, FHL1, FHL2, FKRP, FKTN, FLNC, FXN, GAA, GATA4, GATAD1, GJA5, GLA, GPD1L, GPIHBP1, HADHA, HCN4, HFE, HRAS, ILK, JAG1, JPH2, JUP, KCNA5, KCND3, KCNE1, KCNE2, KCNE3, KCNE5, KCNH2, KCNJ2, KCNJ5, KCNJ8, KCNQ1, KLF10, KRAS, LAMA2, LAMA4, LAMP2, LDB3, LDLR, LDLRAP1, LMF1, LMNA, LOX, LPL, LTBP2, MAP2K1, MAP2K2, MIB1, MT-TL1, MURC, MYBPC3, MYH11, MYH6, MYH7, MYL2, MYL3, MYLK, MYLK2, MYOM1, MYOZ2, MYPN, NEBL, NEXN, NKX2-5, NODAL, NOS1AP, NOTCH1, NPPA, NRAS, OBSCN, PCSK9, PDLIM3, PKP2, PLN, PRDM16, PRKAG2, PTPN11, RAF1, RANGRF, RBM20, RIT1, RYR1, RYR2, SALL4, SCN10A, SCN1B, SCN2B, SCN3B, SCN4B, SCN5A, SDHA, SGCD, SGCG, SHOC2, SLC2A10, SLMAP, SMAD3, SMAD4, SNTA1, SOS1, SYNE1, SYNE2, TAZ, TBX20, TBX3, TBX5, TCAP, TGFB2, TGFB3, TGFBR1, TGFBR2, TMEM43, TMPO, TNNC1, TNNI3, TNNI3K, TNNT2, TPM1, TRDN, TRIM63, TRPM4, TTN, TTR, TXNRD2, VCL, ZIC3

Panel genů pro onemocnění skeletu (335 genů): *ACAN, ACP5, ACTB, ACTG1, ACVR1, ADAMTS10, ADAMTS17, ADAMTSL2, AGPS, AIFM1, AKT1, ALPL, ALX3, ALX4, AMER1, ANKH, ANKRD11, ANO5, ARHGAP31, ARSB, ARSE, ATP6V0A2, ATR, B3GALT6, B3GAT3, B4GALT7, BCS1L, BGN, BHLHA9, BMP1, BMP2, BMPER, BMPR1B, BRAF, BRCA2, BRIP1, CA2, CANT1, CASR, CBL, CCDC8, CDC6, CDC45, CDKN1C, CDT1, CENPJ, CEP63, CEP152, CHST3, CHST14, CHSY1, CKAP2L, CLCN5, CLCN7, COL1A1, COL1A2, COL2A1, COL3A1, COL5A1, COL5A2, COL9A1, COL9A2, COL9A3, COL10A1, COL11A1, COL11A2, COMP, CREB3L1, CREBBP, CRTAP, CSPP1, CTSK, CUL7, CYP27B1, DDR2, DHCR7, DHCR24, DHODH, DLL3, DLL4, DLX3, DLX5, DMP1, DOCK6, DVLI, DYM, DYNC2H1, EBP, EFN1, EFTUD2, EIF2AK3, ENAM, ENPP1, EOGT, EP300, ERCC4,*

ESCO2, EVC, EVC2, EXT1, EXT2, EXTL3, EZH2, FAM20A, FAM20C, FAM58A, FAM83H, FAM111A, FANCA, FANCB, FANCC, FANCD2, FANCE, FANCF, FANCG, FANCI, FANCL, FANCM, FBN1, FBN2, FGD1, FGF10, FGF23, FGFR1, FGFR2, FGFR3, FKBP10, FLNA, FLNB, GALNT3, GDF5, GHI, GHR, GHRHR, GJA1, GLI2, GLI3, GNAS, GNPAT, GPC6, HDAC8, HESX1, HOXA13, HOXD13, HRAS, HSPG2, IDS, IFITM5, IFT43, IFT80, IFT122, IFT140, IFT172, IGF1, IGF1R, IGFALS, IHH, IMPAD1, INPPL1, INSR, IRS1, KAT6B, KIF7, KIF22, KMT2A, KRAS, LARP7, LBR, LEMD3, LHX3, LHX4, LIFR, LMNA, LMX1B, LONP1, LRP4, LRP5, LTBP2, LTBP3, LZTR1, MAFB, MAP2K1, MAP2K2, MATN3, MBTPS2, MESP2, MGP, MMP2, MMP9, MMP13, MSX2, MYCN, NANS, NEK1, NF1, NFIX, NIPBL, NKX3-2, NOG, NOTCH1, NOTCH2, NPR2, NRAS, NSD1, NSDHL, OBSL1, ORC1, ORC4, ORC6, OSTM1, OTX2, P3H1, PALB2, PAPSS2, PCNT, PCYT1A, PDE4D, PEX7, PEX14, PEX19, PGM3, PHEX, PIK3CA, PITX2, PLOD2, PLS3, POC1A, POLR1C, POLR1D, POR, POU1F1, PPIB, PRKARIA, PROPI, PTDSS1, PTH1R, PTHLH, PTPN11, PYCRI, RAB33B, RAD21, RAD51C, RAF1, RASA2, RBBP8, RBM8A, RBPJ, RECQL4, RITI, RMRP, RNU4ATAC, ROR2, RRAS, RTTN, RUNX2, SALL1, SALL4, SBDS, SEC24D, SERPINF1, SERPINH1, SETBP1, SF3B4, SH3BP2, SH3PXD2B, SHOC2, SHOX, SKI, SLC26A2, SLC29A3, SLC34A3, SLC35D1, SLC39A13, SLCO2A1, SLX4, SMAD3, SMAD4, SMARCAL1, SMC1A, SMC3, SNX10, SOS1, SOST, SOX2, SOX3, SOX9, SP7, SPARC, SRCAP, STAMBP, STAT5B, TBX3, TBX4, TBX5, TBX6, TBX15, TBX19, TCF12, TCIRG1, TCOF1, TCTN3, TGFB1, TGFB2, TGFB3, TGFBR1, TGFBR2, TMEM38B, TNFRSF11A, TNFRSF11B, TNFSF11, TP63, TRAPPC2, TRIM37, TRIP11, TRPS1, TRPV4, TTC21B, TWIST1, TYROBP, VDR, VIPAS39, WDR19, WDR34, WDR35, WDR60, WISP3, WNT1, WNT5A, WNT7A, XRCC2, XRCC4, XYLT1, CYP24A1, GTF2I, TRPC3

Original Article

X-Chromosome Inactivation Analysis in Different Cell Types and Induced Pluripotent Stem Cells Elucidates the Disease Mechanism in a Rare Case of Mucopolysaccharidosis Type II in a Female

(mucopolysaccharidosis II / Hunter syndrome / iduronate sulphatase deficiency / X-chromosome inactivation / induced pluripotent stem cells)

M. ŘEBOUN¹, J. RYBOVÁ¹, R. DOBROVOLNÝ¹, J. VČELÁK³, T. VESELKOVÁ¹, G. ŠTORKÁNOVÁ¹, D. MUŠÁLKOVÁ¹, M. HŘEBÍČEK¹, J. LEDVINOVÁ¹, M. MAGNER², J. ZEMAN², K. PEŠKOVÁ¹, L. DVOŘÁKOVÁ¹

¹Institute of Inherited Metabolic Disorders, ²Department of Paediatrics and Adolescent Medicine, First Faculty of Medicine, Charles University in Prague and General University Hospital in Prague, Czech Republic

³Institute of Endocrinology, Prague, Czech Republic

Abstract. Mucopolysaccharidosis type II (MPS II) is an X-linked lysosomal storage disorder resulting from deficiency of iduronate-2-sulphatase activity. The disease manifests almost exclusively in males; only 16 symptomatic heterozygote girls have been reported so far. We describe the results of X-chromosome inactivation analysis in a 5-year-old girl with clinically severe disease and heterozygous mutation p.Arg468Gln in the *IDS* gene. X inactivation analysed at three X-chromosome loci showed extreme skewing (96/4 to 99/1) in two patient's cell types. This finding correlated with exclusive expression of the mutated allele. Induced pluripotent stem cells (iPSC) generated from the patient's peripheral blood demonstrated characteristic pluripotency markers, defi-

ciency of enzyme activity, and mutation in the *IDS* gene. These cells were capable of differentiation into other cell types (cardiomyocytes, neurons). In MPS II iPSC clones, the X inactivation ratio remained highly skewed in culture conditions that led to partial X inactivation reset in Fabry disease iPSC clones. Our data, in accordance with the literature, suggest that extremely skewed X inactivation favouring the mutated allele is a crucial condition for manifestation of MPS II in females. This suggests that the X inactivation status and enzyme activity have a prognostic value and should be used to evaluate MPS II in females. For the first time, we show generation of iPSC from a symptomatic MPS II female patient that can serve as a cellular model for further research of the pathogenesis and treatment of this disease.

Received December 22, 2015. Accepted February 16, 2016.

This study was supported by the Ministry of Health, Czech Republic (IGA MZ CR NT14015-3/2013, MZ CR – RVO VFN 64165, MZ CR – RVO EÚ, 00023761) and by project reg. No. CZ.2.16/3.1.00/24012 from OP Prague Competitiveness.

Corresponding author: Lenka Dvořáková, Institute of Inherited Metabolic Disorders, Laboratory of DNA Diagnostics, bldg E1a, Ke Karlovu 455/2, 128 08 Prague 2, Czech Republic. Phone: (+420) 224 967 701; Fax: (+420) 224 967 168; e-mail: lenka.dvorakova@lfl.cuni.cz

Abbreviations: DMB – dimethylmethylene blue, DMSO – dimethyl sulphoxide, ERT – enzyme replacement therapy, FBS – foetal bovine serum, IDS – iduronate-2-sulphatase, iPSC – induced pluripotent stem cells, LIF – leukaemia inhibitory factor, MPS II – mucopolysaccharidosis type II, PBMC – peripheral blood mononuclear cells, SNP – single-nucleotide polymorphism, XCI – X-chromosome inactivation.

Introduction

Mucopolysaccharidosis II (Hunter syndrome, MPS II, OMIM 309900) is an X-linked lysosomal storage disorder caused by deficiency of iduronate-2-sulphatase activity (IDS, EC 3.1.6.13). Iduronate-2-sulphatase encoded by the *IDS* gene (Xq27-q28) catalyses the first step in the sequential degradation of heparan sulphate and dermatan sulphate, and its deficiency leads to the lysosomal accumulation of these glycosaminoglycans (Neufeld and Muenzer, 2001).

Children with MPS II have a normal appearance at birth and the disease manifests usually in late infancy or toddler age. The signs and symptoms include coarse facial features, short stature with joint stiffness, dysostosis multiplex, hepatosplenomegaly, and cognitive decline. The prognosis depends on the severity of the disease,

and is poor especially in children with severe form associated with death in the second decade of life (Neufeld and Muenzer, 2001).

Enzyme replacement therapy improves the visceral disease; however, it has no effect on the CNS. The first study on intrathecal idursulfase-IT in children has been published recently (Muenzer et al., 2016) and lentiviral isogenic haematopoietic stem cell gene therapy was described as a promising approach for correction of neuronal manifestation in MPS II mice by ameliorating lysosomal storage and autophagic dysfunction in the brain (Wakabayashi et al., 2015).

Recently, the possibility of using autologous induced pluripotent stem cells (iPSC) instead of haematopoietic stem cells for cell-based therapy received a great deal of attention. In female heterozygotes with X-linked diseases, individual cells are either functionally normal or deficient based on the origin of inactivated X chromosome (mutant or normal), and the X-chromosome inactivation (XCI) remains conserved in daughter cells. Selected iPSC clones or differentiated cells with favourable XCI skewing could possibly serve as suitable material for cell therapy without the need for gene manipulations (Bhatnagar et al., 2014).

The prevalence of MPS II is estimated to be 0.43–1.09 per 100,000 live births in five different countries (Poupetova et al., 2010). The vast majority of MPS II patients are males, while only 16 symptomatic MPS II female patients have been reported in the literature so far.

Three of these affected females had structural abnormality of the X chromosome impairing *IDS* expression of the wild-type allele, while two others had both *IDS* alleles defective. In the remaining 11 patients, the cause of MPS II manifestation was the presence of one mutated *IDS* allele in combination with highly skewed XCI leaving only the mutated allele active (Jurecka et al., 2012; Pina-Aguilar et al., 2013; Lonardo et al., 2014); other cases are reviewed in Tuschl et al. (2005) and Scarpa et al. (2011).

Here, we describe the first MPS II female patient in the Czech Republic. We show extremely skewed XCI favouring the mutated allele as the apparent epigenetic cause of the clinical manifestation. For the first time we

demonstrate iPSC generated from the MPS II patient cells. This cellular model will serve for future research into the pathogenesis and treatment of MPS II.

Material and Methods

Ethics

The study was approved by the ethics committee of the General University Hospital in Prague (The Ethics Committee Approval number 41/12) and was conducted in agreement with institutional guidelines. Written informed consent was obtained from both adult study participants. On behalf of the patient, written informed consent was obtained from her parents.

Molecular analyses

Genomic DNA was extracted from whole blood and from the urinary sediment using a QIAamp DNA Blood Mini Kit (Qiagen, Valencia, CA). DNA from buccal swabs and total RNA were isolated using a QIAamp DNA Micro Kit (Qiagen) and a BiOstic Blood Total RNA Isolation Kit (MO BIO Laboratories, Inc., Carlsbad, CA), respectively. Reverse transcription of RNA to cDNA was performed using a High Capacity RNA to cDNA Kit (Applied Biosystems, Carlsbad, CA).

PCR and reverse transcription PCR (RT-PCR) products of the *IDS* (GenBank NC_000023.11, NM_000202.6) and *LAMP2* (NM_002294.2) genes were generated according to standard PCR protocols using primers shown in Table 1. The genotypes were analysed by Sanger sequencing using a Big Dye Terminator v3.1 Cycle Sequencing Kit and a 3500xL Genetic Analyzer (Applied Biosystems).

For amplicon-based deep sequencing, singleplex PCR and RT-PCR products were pooled and prepared under standard protocols using the NexteraXT kit and the MiSeq reagent kit (2×250), respectively. Paired-end sequence reads were generated using the MiSeq platform (Illumina, San Diego, CA). Sequencing data were demultiplexed and trimmed for low quality and duplicates using MiSeq reporter v.2.4. Secondary analysis of the cDNA data was performed using TopHat v2.0.13 (Kim

Table 1. Primer sequences used for PCR amplification

Gene		Fragment/ Exon	Sequence
<i>IDS</i>	cDNA	Fr. 4 U	TAATACGACTCACTATAG GGACCTTGTGGAACCTGTGT
		Fr. 4 L	TGAAACAGCTATGACCATG AAACGACCAGCTCTAACTCC
	gDNA	ex. 9a U	TAATACGACTCACTATAG TCCTGCTATTTGATTGGATG
		ex. 9a L	TGAAACAGCTATGACCATG GTCTATGGTGCATGGAAT
		ex. 9b U	TAATACGACTCACTATAG CGATTCCGTGACTTGGGA
		ex. 9b L	TGAAACAGCTATGACCATG ATGGGTAATCACAAAACGAC
<i>LAMP2</i>	cDNA	Fr.1 U	GGTCGGTGGTCATCAGTGCT
		Fr.1 L	ATTCTGATGGCCAAAAGTTTCAT
	gDNA	ex.2 U	TAATACGACTCACTATAG TTTAGAGCTGGTTGAACTTC
		ex.2 L	TGAAACAGCTATGACCATG TCTAAAGGATAAAGTCAATTA

Upper (U) and lower (L) primers (excepting *LAMP2* cDNA) contain a T7 and an RP sequence, respectively, at the 5' end.

et al., 2013). The human hg19 genome sequence was used as a reference.

X-chromosome inactivation analysis

Two independent methods were used to determine the XCI pattern: a DNA methylation-based assay and a transcript expression analysis. The methylation status of polymorphic repeat regions was examined at two loci, *AR* and *CNKSR2*, using digestion with methylation-sensitive enzyme *HpaII*, as described elsewhere (Racchi et al., 1998; Musalkova et al., 2015). The DNA of the patient's father was used as a male control.

The transcriptional assay was performed similarly as described previously (Mossner et al., 2013). The RT-PCR product containing the single-nucleotide polymorphism (SNP) was used for quantification of SNP allele frequencies, which reflected the XCI ratios. The *LAMP2* gene polymorphism c.156A>T (rs12097) was selected for the assay as *LAMP2* is subject to XCI (Cotton et al., 2013), and the patient is heterozygous for this polymorphism. Instead of pyrosequencing (Mossner et al., 2013), amplicon sequencing using the Illumina platform was applied. The same procedure was used for quantification of the wt/mutated allele in the *IDS* gene transcript.

Generation of iPSC lines

The iPSC lines were generated from mononuclear cells isolated with Histopaque (Sigma-Aldrich, St. Louis, MO) according to manufacturer's instructions from peripheral blood of the presented MPS II female patient. Isolated peripheral blood mononuclear cells (PBMC) were frozen in 10% dimethyl sulphoxide (DMSO) in inactivated foetal bovine serum (FBS, BenchMark™ Fetal Bovine Serum, Gemini Bio-Products, West Sacramento, CA) and kept in liquid nitrogen until further use. Thawed PBMCs were cultured in complete LGM medium (Lonza, Walkersville, MD) containing 0.4 µg/ml of purified no azide/low endotoxin NA/LE Mouse Anti-Human CD3 (BD Biosciences, San Jose, CA), 0.4 µg/ml of Mouse Anti-Human CD28 (BD Biosciences), and 50 ng/ml of interleukin 2 (IL2; Abbiotec, San Diego, CA) and were plated onto CD3-coated 6-well plates for five days. Reprogramming of the cells into iPSCs was performed using the CytoTune™-iPS 2.0 Sendai Reprogramming Kit (Invitrogen, Carlsbad, CA) according to manufacturer's instructions. In brief, the cells were transduced at an appropriate multiplicity of infection (MOI) with each of the three reprogramming vectors (KOS MOI = 5, hc-Myc MOI = 5, hKlf4 MOI = 3) in the complete LGM medium. The free virus was removed by replacing the medium on the second day. The cells were transferred onto the layer of feeder cells (irradiated mouse embryonic fibroblasts) in the presence of HES medium (KnockOut™ESC/iPSC Medium Kit) with 8 ng/ml basic fibroblast growth factor (bFGF; Life Technologies, New York, NY) on the 4th day after the transduction. The selected colonies were picked and placed in 12-well plates containing feeder cells and then passaged with Accutase (STEMCELL Technologies Inc.,

Vancouver, BC, Canada) and the StemPro EZPassage tool (Invitrogen, Carlsbad, CA, USA) until the creation of stable iPSC lines.

Expression of pluripotency markers in generated iPSC was confirmed by immunostaining as previously described (Lian et al., 2013). Primary antibodies used in this study were directed to Oct3/4 (Santa Cruz Biotechnology, Dallas, TX, cat# sc-5279), SSEA4 (Invitrogen, cat# 41-4000), anti-TRA-1-81 (Invitrogen, cat# 41-1100), Sox2 (Santa Cruz Biotechnology, cat# sc-365823), CD63 (Abcam, Cambridge, UK, cat# ab1318), heparan sulphate (Amsbio, Abingdon, UK, Cat# 370255-1) and Lin-28 (Proteintech Group, Chicago, IL, cat# 11724-1-AP). The cells were incubated with Alexa Fluor 488- and Alexa Fluor 568-conjugated secondary antibodies (Molecular Probes, Invitrogen) and the nuclei were counterstained with 4',6-diamidino-2-phenylindole (DAPI, Invitrogen).

Naïve iPSC lines were established by cultivation of generated iPSC in NHSM medium containing leukaemia inhibitory factor (LIF) and small molecule inhibition of ERK1/ERK2 and GSK3β signalling, which induce conversion of primed iPSC toward naïve pluripotency, as described previously (Gafni et al., 2013).

Determination of enzyme activities

Total leukocytes were isolated from the blood anticoagulated with EDTA within 24 h of drawing using the method described by Skoog and Beck (1956). The iPSC were re-plated onto Geltrex® (Life Technologies, Grand Island, NY)-coated 6-well plates and cultivated in mTeSR™1 medium (STEMCELL Technologies Inc.) for two passages for the removal of the feeder cells. The homogenates were prepared by sonication in water. The protein concentration was determined using the method described by Hartree (1972). Iduronate-2-sulphate sulphatase activity was assayed using fluorogenic substrate 4-methylumbelliferyl-α-L-iduronate-2-sulphate according to the method described by Voznyi et al. (2001).

Results

Clinical description

A 5-year-old girl was born in term as a first child of healthy, non-consanguineous Ukrainian parents. Post-natal adaptation and early development were uneventful. She used five words and started to walk at the age of 13 months. Snoring, hearing impairment and delayed speech were recognized at the age of two years. A mild improvement in hearing was observed with a hearing device; however, the speech problems persisted. Coarse facial features, gingival hyperplasia, mild hepatosplenomegaly, sternal protrusion, claw hands, lumbal hyperlordosis, large joint contractures and mild mental retardation were noted during the third year of life. At the age of 3.5 years, clinical and laboratory analyses revealed mild paleocerebellar symptoms, mild mitral regurgitation, and "dysostosis multiplex" on the X-ray survey.

Table 2. X-chromosome inactivation at three X-chromosome loci compared with a mutant allele in the *IDS* gene

Sample	Locus			
	Methyl sensitive		Transcript analysis	
	<i>AR</i> (Xq12) %	<i>CNSKR2</i> (Xp22.12) %	<i>LAMP2</i> (Xq24) A:T %	<i>IDS</i> (Xq28) G:A %
Proband (leukocytes)	98:2 ^a	99:1 ^a	100:0 ^b	0,5:99,5 ^b
Proband (buccal swabs)	96:4	n.d. ^c	n.d. ^c	n.d. ^c
Mother (leukocytes)	n.i. ^d	70:30	n.d. ^c	n.d. ^c

^a Maternal chromosome is preferentially inactivated, ^b transcript analysis using the amplicon-based deep sequencing: number of reads Q>30 *LAMP2* (c.156A>T, rs12097) A: 3910, T: 2. The A allele was inherited from the patient's father. *IDS* (c.1403G>A) G: 18, A: 3668. Only the mutated allele is expressed. ^c not determined, ^d non-informative marker

No corneal clouding was present. Urinary excretion of heparan and dermatan sulphates were increased (60.5–65.7 g/mol creatinine; controls < 15.5). The *IDS* activity was markedly decreased in leukocytes (0.46 nmol/4 h/mg, control range: 28.1–70.4 nmol/4 h/mg) and serum (19 nmol/4 h/ml, control range: 167–475 nmol/4 h/ml). Heterozygous mutation c.1403G>A (p.Arg468Gln) was identified in the *IDS* gene. The girl is treated with enzyme replacement therapy, the glycosaminoglycan excretion decreased (19.5–22.5 g/mol creatinine), but she still has speech problems, delay of fine motor functions and a moderate delay of the gross motor development.

X-chromosome inactivation and mutation analysis in patient's tissues

Examination of the methylation status at the *AR* locus (Xq12) showed extreme skewing in both blood leukocytes and buccal swabs; the maternal allele was almost completely inactivated. Complete inactivation of the maternal allele was also observed in *CNSKR2* and apparent homozygosity for the c.156A allele inherited from the patient's father was detected in the *LAMP2* transcript. Deep sequencing of the *IDS* gene transcript revealed exclusive expression of the mutated allele (Table 2).

As the maternal allele is completely inactivated and only the mutated *IDS* is expressed, it can be deduced that the patient inherited the mutated allele from her father. However, Sanger sequencing did not identify the mutation c.1403G>A in the patient's parents. To detect possible somatic mosaicism in the parental tissues, DNA isolated from three cell types (peripheral leukocytes, urinary sediment cells and buccal swabs) was subjected to amplicon-based deep sequencing. The number of reads corresponding to the mutated allele was below the detection limit (< 0.5%) when the total sequence depth was higher than 1300 in all analysed tissues. Thus, the somatic mosaicism was not demonstrated, while germline mosaicism could not be excluded as meiotic cells from the parents were not available for analysis.

Generation of iPSC lines

Two of the multiple generated patient's iPSC lines have been used for the study. The clones were positive

for the characteristic pluripotency markers Oct3/4, SSEA4, anti-TRA-1-81, Lin28, and Sox2 (Fig. 1). The patient's iPSC lines also expressed slightly higher amounts of heparan sulphate (Fig. 2); however, the quantitative determination of GAGs in the cell lysate using dimethyl methylene blue (DMB) with spectrophotometric detection (Lopez-Marín et al., 2013) did not show significant differences. The *IDS* activities in two

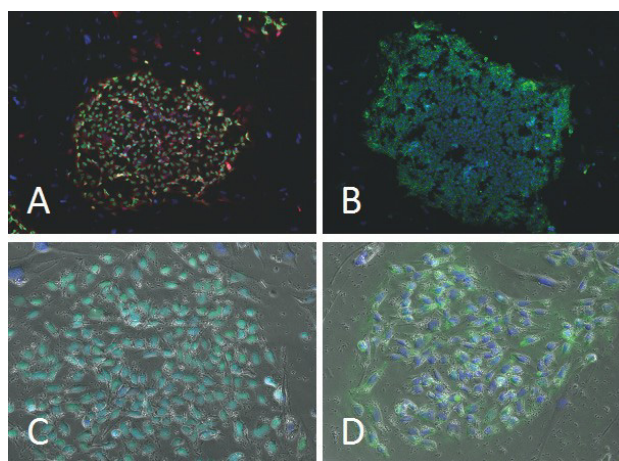


Fig 1. Characterization of iPSC colonies – pluripotency markers. **A:** Lin28 (red), Oct3/4 (green), DAPI (blue); **B:** SSEA4 (green), DAPI (blue); **C:** Sox2 (green), DAPI (blue) and **D:** anti-TRA-1-81 (green), DAPI (blue) in phase contrast image. A, B – 10× objective, C, D – 20× objective.

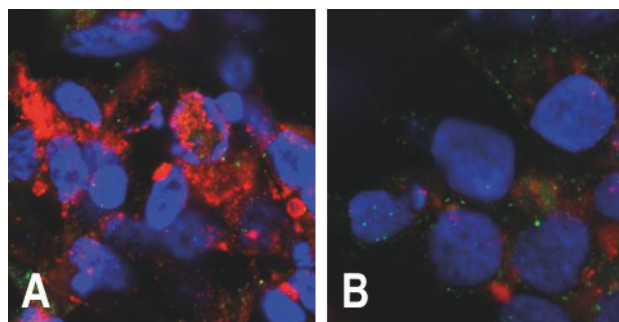


Fig 2. Detection of heparan sulphate in iPSC generated from an MPS II patient. Heparan sulphate (red), CD63 (green), DAPI (blue). **A:** MPS II patient; **B:** control; images were recorded with a laser scanning confocal microscope, 60× objective, NA 1.40

of the patient's iPSC clones were 1.49 and 2.32 nmol per mg of protein per hour, compared to 17.15 and 21.32 nmol/mg/h, respectively, in the controls. The potency to differentiate to cardiomyocytes and neuronal cells has been confirmed using previously published protocols (Stacpoole et al., 2011; Lian et al., 2013).

Analysis in two iPSC clones cultured in usual conditions showed the same XCI pattern with preferential inactivation of the maternal allele (98 : 2). Using cell culture conditions described to lead to the naïve state of iPSC with reset XCI did not result in a changed XCI ratio in the MPS II clones; however, in case of the Fabry disease heterozygote used as a control, the XCI ratio changed from 97 : 3 to 80 : 20 (Fig. 3).

Discussion

In this report we describe a 5-year-old girl with severe deficiency of IDS activity and clinical manifestation of the disease corresponding to the severe form of Hunter syndrome in boys. The disease in our patient is caused by the heterozygosity for the recurrent mutation p.Arg468Gln (Brusius-Facchin et al., 2014) in combination with highly skewed XCI resulting in exclusive expression of the mutated allele.

To reduce the risk of incorrect interpretation of the results due to chromosomal crossover or due to failure of the individual loci to correlate with XCI we performed XCI analysis using two independent methods at three X-chromosome loci. The results of methyl-sensitive methods (*AR*, *CNKSR2*) agreed well with the results of the transcription-based assay using the *LAMP2* gene polymorphism. Thus, unlike Swierczek et al. (2012), we did not observe any discrepancy among the used methods.

To date, two states of iPSC are known, referred to as primed and naïve, which differ mainly in XCI. Several attempts have been undertaken to generate a more naïve state (with two active X chromosomes in female cells) in established primed iPSC (with one inactive X chromosome) by different media formulation. In our study the XCI was analysed using the methyl-sensitive method (*AR*) in iPSC cultured in standard media and in naïve state-inducing media (Gafni et al., 2013). Cells derived from the MPS II patient did not show any change in the skewed XCI ratio in any culture conditions. There are three explanations for this finding: 1) the X chromosome remains inactive in the iPSC without going through the "reset" state when both X chromosomes in female cells are active, 2) the X chromosome is non-randomly inactivated after resetting XCI during iPSC reprogramming, or 3) a fraction of cells reached the stage of reprogramming in which both X chromosomes are active, but the used methyl-sensitive method is not able to detect these cells (Briggs and Reijo Pera, 2014). In any case, the iPSC derived from the MPS II patient differ from those derived from the Fabry disease heterozygote used as a control line, which responded to media change by partial change of the XCI ratio from 97 : 3 to 80 : 20.

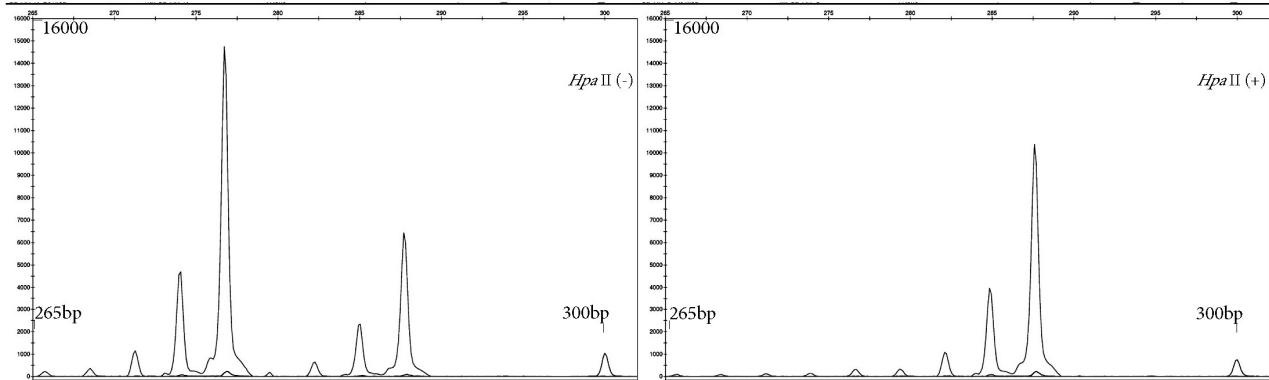
Extreme skewing of XCI in favour of the mutated allele (> 95/5) is a common feature shared by symptomatic MPS II female patients (Scarpa et al., 2011). In accordance with this XCI status, symptomatic MPS II in females is associated with profound IDS deficiency comparable to affected hemizygous males, confirming the recessive nature of the disease. A similar strict correlation is not found in Fabry disease, another X-linked lysosomal storage disorder, where the overwhelming majority of heterozygotes have intermediate levels of the deficient enzyme and develop some symptoms of the disease, although later in life than the hemizygous males (Echevarria et al., 2016). According to the threshold model of Conzelmann and Sandhoff, low levels of enzyme activity are compatible with normal levels of substrate degradation unless they cross a threshold, which, in lysosomal diseases, is usually lower than 10 % of the normal activity (Conzelmann and Sandhoff, 1983). It is important to note that in the tissues of heterozygotes of X-linked disorders, there are patches of deficient cells following the pattern of inactivation of the non-mutated chromosome. This illuminates the development of tissue pathology in Fabry heterozygotes, while carriers for autosomal recessive lysosomal diseases are free of it. The absence of symptoms in the majority of MPS II heterozygotes may be explained by the low threshold of the enzyme activity compatible with normal degradation of the substrate or by good uptake of the enzyme by the deficient cells from the surrounding cells. Notably, cultured fibroblasts from MPS II patients are able to cross-correct the IDS deficiency, unlike cultured skin fibroblasts from the Fabry patients (Fuller et al., 2015).

Our results and the review of the literature show that the clinical manifestation of MPS II in heterozygous females is associated with conditions leading to near monoallelic expression of the mutant allele and severe IDS deficiency, most often due to extremely skewed XCI. This suggests that girls with skewed XCI diagnosed postnatally might benefit from enzyme replacement therapy (ERT), which, if introduced early, may significantly improve further clinical course of the disease (Tyłki-Szymanska et al., 2012; Tajima et al., 2013).

To our knowledge, we generated the first iPSC model from a symptomatic MPS II heterozygote and generally from any MPS II patient. These models are valuable for further research of MPS II pathogenesis and testing of therapeutic approaches in various cell types differentiated from iPSC clones and relevant to the disease. The iPSC lines from the presented case can also be used for general research of the mechanisms leading to extremely skewed XCI ratios, as the MPS II clones we have studied retained their XCI skewing under naïve state culture conditions in contrast with control clones. Hypothetically, the iPSC clones from heterozygotes of X-linked disorders with favourable XCI and thus functionally normal can serve as a source of autologous material (haematopoietic progenitors, neurons, cardiomyocytes, etc.) for cell-based therapy (Bhatnagar et al.,

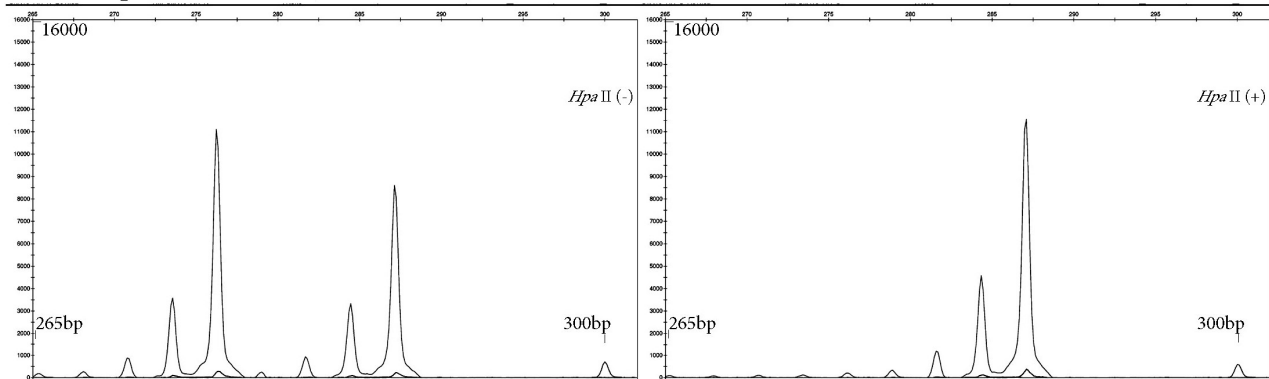
I. MPSII patient iPS cells (standard culture)

XCI value 98:2



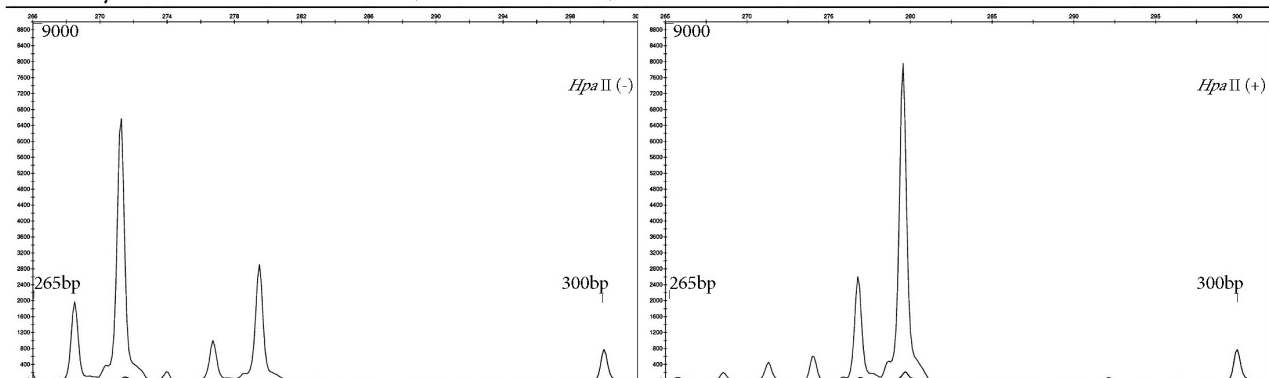
II. MPSII patient iPS cells (naïve culture)

XCI value 98:2



III. Fabry disease control iPS cells (standard culture)

XCI value 97:3



IV. Fabry disease control iPS cells (naïve culture)

XCI value 80:20

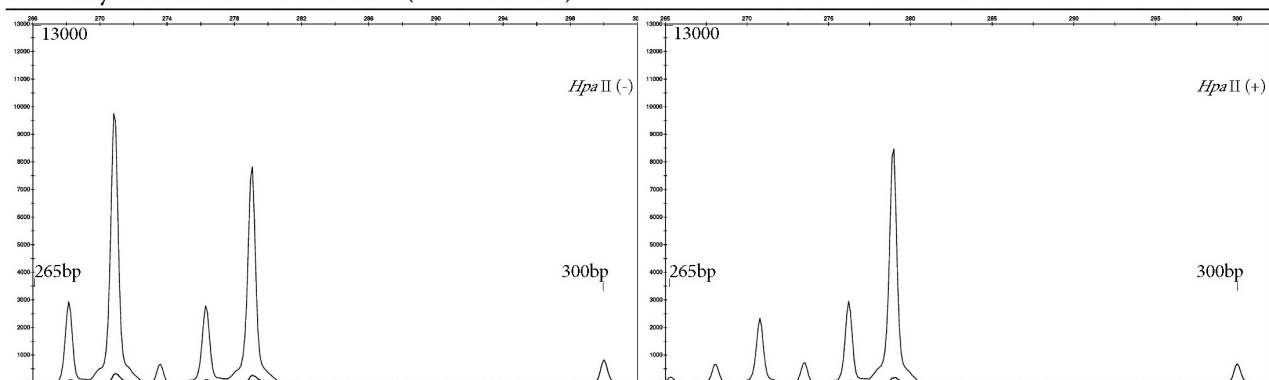


Fig 3. X-chromosome inactivation analysis in the patient's iPSC generated from the MPS II patient and a Fabry disease heterozygote serving as control. Standard and naïve culture conditions cells are compared. Methylation status analysis of the *AR* alleles before (*HpaII*-) and after (*HpaII*+) digestion is shown. The 300-bp peak belongs to the GeneScan 500 ROX size standard. The analysis was conducted using GeneMapper software (Applied Biosystems).

2014). These types of therapies, however, will need to await development of safe therapeutic protocols.

Acknowledgements

The authors would like to acknowledge Helena Pouřetová for enzyme analysis, Hana Vlášková for constructive discussion, and Michaela Hnízďová Boučková and Larisa Stolnaja for excellent laboratory work. The authors have no conflicts of interest to disclose.

References

- Bhatnagar, S., Zhu, X., Ou, J., Lin, L., Chamberlain, L., Zhu, L. J., Wajapeyee, N., Green, M. R. (2014) Genetic and pharmacological reactivation of the mammalian inactive X chromosome. *Proc. Natl. Acad. Sci. USA* **111**, 12591-12598.
- Briggs, S. F., Reijo Pera, R. A. (2014) X chromosome inactivation: recent advances and a look forward. *Curr. Opin. Genet. Dev.* **28**, 78-82.
- Brusius-Facchin, A. C., Schwartz, I. V., Zimmer, C., Ribeiro, M. G., Acosta, A. X., Horovitz, D., Monlleo, I. L., Fontes, M. I., Fett-Conte, A., Sobrinho, R. P., Duarte, A. R., Boy, R., Mabe, P., Ascurra, M., de Michelena, M., Tylee, K. L., Besley, G. T., Garreton, M. C., Giugliani, R., Leistner-Segal, S. (2014) Mucopolysaccharidosis type II: identification of 30 novel mutations among Latin American patients. *Mol. Genet. Metab.* **111**, 133-138.
- Conzelmann, E., Sandhoff, K. (1983) Partial enzyme deficiencies: residual activities and the development of neurological disorders. *Dev. Neurosci.* **6**, 58-71.
- Cotton, A. M., Ge, B., Light, N., Adoue, V., Pastinen, T., Brown, C. J. (2013) Analysis of expressed SNPs identifies variable extents of expression from the human inactive X chromosome. *Genome Biol.* **14**, R122.
- Echevarria, L., Benistan, K., Toussaint, A., Dubourg, O., Hagege, A. A., Eladari, D., Jabbour, F., Beldjord, C., De Mazancourt, P., Germain, D. P. (2016) X-chromosome inactivation in female patients with Fabry disease. *Clin. Genet.* **89**, 44-54.
- Fuller, M., Mellett, N., Hein, L. K., Brooks, D. A., Meikle, P. J. (2015) Absence of α -galactosidase cross-correction in Fabry heterozygote cultured skin fibroblasts. *Mol. Genet. Metab.* **114**, 268-273.
- Gafni, O., Weinberger, L., Mansour, A. A., Manor, Y. S., Chomsky, E., Ben-Yosef, D., Kalma, Y., Viukov, S., Maza, I., Zviran, A., Rais, Y., Shipony, Z., Mukamel, Z., Krupalnik, V., Zerbib, M., Geula, S., Caspi, I., Schneir, D., Shwartz, T., Gilad, S., Amann-Zalcenstein, D., Benjamin, S., Amit, I., Tanay, A., Massarwa, R., Novershtern, N., Hanna, J. H. (2013) Derivation of novel human ground state naive pluripotent stem cells. *Nature* **504**, 282-286.
- Hartree, E. F. (1972) Determination of protein: a modification of the Lowry method that gives a linear photometric response. *Anal. Biochem.* **48**, 422-427.
- Jurecka, A., Krumina, Z., Zuber, Z., Rozdzynska-Swiatkowska, A., Kloska, A., Czartoryska, B., Tylki-Szymanska, A. (2012) Mucopolysaccharidosis type II in females and response to enzyme replacement therapy. *Am. J. Med. Genet. A* **158A**, 450-454.
- Kim, D., Pertea, G., Trapnell, C., Pimentel, H., Kelley, R., Salzberg, S. L. (2013) TopHat2: accurate alignment of transcriptomes in the presence of insertions, deletions and gene fusions. *Genome Biol.* **14**, R36.
- Lian, X., Zhang, J., Azarin, S. M., Zhu, K., Hazeltine, L. B., Bao, X., Hsiao, C., Kamp, T. J., Palecek, S. P. (2013) Directed cardiomyocyte differentiation from human pluripotent stem cells by modulating Wnt/ β -catenin signaling under fully defined conditions. *Nat. Protoc.* **8**, 162-175.
- Lonardo, F., Di Natale, P., Lualdi, S., Acquaviva, F., Cuoco, C., Scarano, F., Maioli, M., Pavone, L. M., Di Gregorio, G., Filocamo, M., Scarano, G. (2014) Mucopolysaccharidosis type II in a female patient with a reciprocal X;9 translocation and skewed X chromosome inactivation. *Am. J. Med. Genet. A* **164A**, 2627-2632.
- Lopez-Marin, L., Gutierrez-Solana, L. G., Azuara, L. A., de Las Heras, R. S., Rodriguez, A. D., Extremera, V. C. (2013) Detection by urinary GAG testing of mucopolysaccharidosis type II in an at-risk Spanish population. *JIMD Rep.* **10**, 61-68.
- Mossner, M., Nolte, F., Hutter, G., Reins, J., Klaumunzer, M., Nowak, V., Oblander, J., Ackermann, K., Will, S., Rohl, H., Neumann, U., Neumann, M., Hopfer, O., Baldus, C. D., Hofmann, W. K., Nowak, D. (2013) Skewed X-inactivation patterns in ageing healthy and myelodysplastic haematopoiesis determined by a pyrosequencing based transcriptional clonality assay. *J. Med. Genet.* **50**, 108-117.
- Muenzer, J., Hendriksz, C. J., Fan, Z., Vijayaraghavan, S., Perry, V., Santra, S., Solanki, G. A., Mascelli, M. A., Pan, L., Wang, N., Sciarappa, K., Barbier, A. J. (2016) A phase I/II study of intrathecal idursulfase-IT in children with severe mucopolysaccharidosis II. *Genet. Med.* **18**, 73-81.
- Musalkova, D., Minks, J., Storkanova, G., Dvorakova, L., Hrebicek, M. (2015) Identification of novel informative loci for DNA-based X-inactivation analysis. *Blood Cells Mol. Dis.* **54**, 210-216.
- Neufeld, E. F., Muenzer, J. (2001) The mucopolysaccharidoses. In: *The Metabolic and Molecular Bases of Inherited Disease*, eds. Scriver, C. R., Beaudet, A. L., Sly, W. S., Valle, D., pp. 3421-3452, McGraw-Hill Co., New York
- Pina-Aguilar, R. E., Zaragoza-Arevalo, G. R., Rau, I., Gal, A., Alcantara-Ortigoza, M. A., Lopez-Martinez, M. S., Santillan-Hernandez, Y. (2013) Mucopolysaccharidosis type II in a female carrying a heterozygous stop mutation of the iduronate-2-sulfatase gene and showing a skewed X chromosome inactivation. *Eur. J. Med. Genet.* **56**, 159-162.
- Pouřetová, H., Ledvinová, J., Berna, L., Dvorakova, L., Kozich, V., Elleder, M. (2010) The birth prevalence of lysosomal storage disorders in the Czech Republic: comparison with data in different populations. *J. Inherit. Metab. Dis.* **33**, 387-396.
- Racchi, O., Mangerini, R., Rapezzi, D., Rolfo, M., Gaetani, G., Ferraris, A. M. (1998) X chromosome inactivation patterns in normal females. *Blood Cells Mol. Dis.* **24**, 439-447.
- Scarpa, M., Almasy, Z., Beck, M., Bodamer, O., Bruce, I. A., De Meirleir, L., Guffon, N., Guillen-Navarro, E., Hensman, P., Jones, S., Kamin, W., Kampmann, C., Lampe, C., Lavery, C. A., Teles, E. L., Link, B., Lund, A. M., Malm, G., Pitz, S., Rothera, M., Stewart, C., Tylki-Szymanska, A., van der Ploeg, A., Walker, R., Zeman, J., Wraith, J. E.,

- Hunter Syndrome European Expert Council (2011) Mucopolysaccharidosis type II: European recommendations for the diagnosis and multidisciplinary management of a rare disease. *Orphanet J. Rare Dis.* **6**, 72.
- Skoog, W. A., Beck, W. S. (1956) Studies on the fibrinogen, dextran and phytohemagglutinin methods of isolating leukocytes. *Blood* **11**, 436-454.
- Stacpoole, S. R., Bilican, B., Webber, D. J., Luzhynskaya, A., He, X. L., Compston, A., Karadottir, R., Franklin, R. J., Chandran, S. (2011) Efficient derivation of NPCs, spinal motor neurons and midbrain dopaminergic neurons from hESCs at 3% oxygen. *Nat. Protoc.* **6**, 1229-1240.
- Swierczek, S. I., Piterkova, L., Jelinek, J., Agarwal, N., Hammoud, S., Wilson, A., Hickman, K., Parker, C. J., Cairns, B. R., Prchal, J. T. (2012) Methylation of AR locus does not always reflect X chromosome inactivation state. *Blood* **119**, e100-109.
- Tajima, G., Sakura, N., Kosuga, M., Okuyama, T., Kobayashi, M. (2013) Effects of idursulfase enzyme replacement therapy for mucopolysaccharidosis type II when started in early infancy: comparison in two siblings. *Mol. Genet. Metab.* **108**, 172-177.
- Tuschl, K., Gal, A., Paschke, E., Kircher, S., Bodamer, O. A. (2005) Mucopolysaccharidosis type II in females: case report and review of literature. *Pediatr. Neurol.* **32**, 270-272.
- Tylki-Szymanska, A., Jurecka, A., Zuber, Z., Rozdzyńska, A., Marucha, J., Czartoryska, B. (2012) Enzyme replacement therapy for mucopolysaccharidosis II from 3 months of age: a 3-year follow-up. *Acta Paediatr.* **101**, e42-47.
- Voznyi, Y. V., Keulemans, J. L., van Diggelen, O. P. (2001) A fluorimetric enzyme assay for the diagnosis of MPS II (Hunter disease). *J. Inherit. Metab. Dis.* **24**, 675-680.
- Wakabayashi, T., Shimada, Y., Akiyama, K., Higuchi, T., Fukuda, T., Kobayashi, H., Eto, Y., Ida, H., Ohashi, T. (2015) Hematopoietic stem cell gene therapy corrects neuropathic phenotype in murine model of mucopolysaccharidosis type II. *Hum. Gene Ther.* **26**, 357-366.

Příloha: 3

Short Report

Genotype–phenotype correlation in 44 Czech, Slovak, Croatian and Serbian patients with mucopolysaccharidosis type II

Dvorakova L., Vlaskova H., Sarajlija A., Ramadza D.P., Poupetova H., Hrubá E., Hlavata A., Bzduch V., Peskova K., Storkanova G., Kecman B., Djordjevic M., Baric I., Fumic K., Barisic I., Reboun M., Kulhanek J., Zeman J., Magner M. Genotype–phenotype correlation in 44 Czech, Slovak, Croatian and Serbian patients with mucopolysaccharidosis type II. *Clin Genet* 2017; 91: 787–796. © John Wiley & Sons A/S. Published by John Wiley & Sons Ltd, 2016

Mucopolysaccharidosis type II (Hunter syndrome, MPS II, OMIM 309900) is an X-linked lysosomal storage disorder caused by deficiency of iduronate-2-sulfatase (IDS). We analyzed clinical and laboratory data from 44 Slavic patients with this disease. In total, 21 Czech, 7 Slovak, 9 Croatian and 7 Serbian patients (43 M/1 F) were included in the study (median age 11.0 years, range 1.2–43 years). Birth prevalence ranged from 1:69,223 (Serbia) to 1:192,626 (Czech Rep.). In the majority of patients (71%), the disease manifested in infancy. Cognitive functions were normal in 10 patients. Four, six and 24 patients had mild, moderate, and severe developmental delay, respectively, typically subsequent to developmental regression (59%). Residual enzyme activity showed no predictive value, and estimation of glycosaminoglycans (GAGs) had only limited importance for prognosis. Mutation analysis performed in 36 families led to the identification of 12 novel mutations, eight of which were small deletions/insertions. Large deletions/rearrangements and all but one small deletion/insertion led to a severe phenotype. This genotype–phenotype correlation was also identified in six cases with recurrent missense mutations. Based on patient genotype, the severity of the disease may be predicted with high probability in approximately half of MPS II patients.

Conflict of interest

Nothing to declare.

L. Dvorakova^a, H. Vlaskova^a,
A. Sarajlija^{b,c}, D. P. Ramadza^d,
H. Poupetova^a, E. Hrubá^a,
A. Hlavata^e, V. Bzduch^f,
K. Peskova^a, G. Storkanova^a,
B. Kecman^b, M. Djordjevic^{b,c},
I. Baric^g, K. Fumic^h, I. Barisicⁱ,
M. Reboun^a, J. Kulhanek^j,
J. Zeman^{a,j} and M. Magnerⁱ

^aInstitute of Inherited Metabolic Disorders, First Faculty of Medicine, Charles University and General University Hospital, Prague, Czech Republic,

^bDepartment of Metabolism and Clinical Genetics, Mother and Child Health Care Institute of Serbia, Belgrade, Serbia,

^cSchool of Medicine, University of Belgrade, Belgrade, Serbia, ^dDepartment of Pediatrics, University Hospital Center, Zagreb, Croatia, ^e2nd Department of Pediatrics, ^f1st Department of Pediatrics,

Comenius University Medical School in Bratislava University Children's Hospital, Bratislava, Slovakia, ^gDepartment of Pediatrics, University Hospital Center and University of Zagreb, School of Medicine,

Zagreb, Croatia, ^hDepartment of Laboratory Diagnostics, University Hospital Centre Zagreb and School of Medicine, Zagreb, Croatia, ⁱDepartment of Paediatrics, Children's Hospital Zagreb, School of Medicine, Zagreb,

Croatia, and ^jDepartment of Paediatrics and Adolescent Medicine, First Faculty of Medicine, Charles University and General University Hospital, Prague, Czech Republic

Key words: genotype–phenotype correlation – Hunter syndrome – MPS II – mucopolysaccharidosis type II – Slavic origin

Corresponding author: Martin Magner, MD, PhD, Department of Paediatrics and Adolescent Medicine, First Faculty of Medicine, Charles University and

General University Hospital in Prague,
Ke Karlovu 2, 128 08 Prague, Czech
Republic.
Tel.: +420224967791;
fax.: +420224911453;
e-mail: martin.magner@vfn.cz

Received 21 September 2016, revised
and accepted for publication 17
November 2016

Mucopolysaccharidosis type II (Hunter syndrome, MPS II, OMIM 309900) is an X-linked recessive lysosomal storage disorder caused by deficiency of iduronate-2-sulfatase (IDS, EC 3.1.6.13) (1, 2). IDS catalyzes the first step in degradation of the glycosaminoglycans (GAGs) dermatan sulfate and heparan sulfate. Characteristic clinical manifestations include hepatomegaly and splenomegaly, short stature, joint contractures, skeletal changes, inguinal and/or umbilical hernia, recurrent ear infections, coarse facial features, and variable cognitive impairment (1). This disease generally affects almost exclusively males, and only 17 female patients with MPS II have been described to date (3).

Iduronate-2-sulfatase is encoded by the *IDS* gene located on chromosome Xq28. The gene encompasses 28 kb and comprises 9 exons encoding the active IDS enzyme with 550 amino acid residues. A homologous non-functional pseudogene *IDS2* facilitating genetic rearrangements is located approximately 20 kb distal to the functional *IDS* gene (4). More than 550 different mutations have been described in the *IDS* gene to date (HGMD® Professional 2016.2, www.hgmd.cf.ac.uk).

Mutations in the *IDS* gene have been extensively studied in MPS II patients from various nations and ethnicities, including France, Portugal, Tunisia and Switzerland (5); Italy (6); Japan (7); Latin America (8); Mexico (9); Poland (10); Portugal (11); Russia (12); Spain (13); and Thailand (14). In this report, we describe detailed clinical phenotype, mutation spectrum and genotype – phenotype correlations of 44 patients from four Slavic countries, i.e. the Czech Republic, Slovakia, Croatia and Serbia.

Patients and methods

Referral metabolic centers for lysosomal storage disorders from all four countries have participated in the study. To our knowledge the presented 44 patients represent the absolute majority of Czech, Slovak, Croatian and Serbian patients, who have been diagnosed with mucopolysaccharidosis type II in observed time period. The details of birth prevalence calculation, used clinical classification, urine glycosaminoglycans and IDS activity analyses are shown in Appendix S1 (Supporting information). Molecular-genetic analyses of the *IDS* gene (GenBank NC_000023.11, NM_000202.6) in all Czech and Slovak patients and one patient from Croatia (Patient 44) were performed in Prague, other analyses at genetic institutions in Rostock (Germany), and Graz (Austria) (details

in Appendix S1). Study was approved by an Institutional Review Board of the General University Hospital in Prague (The Ethics Committee Approval Number 41/12).

Results

Clinical data

In total, 21 Czech, 7 Slovak, 9 Croatian and 7 Serbian patients (43 M/1 F) were included in the study (median age 11 years, range 1.2 – 43 years) (Table 1). The calculated birth prevalences were 1:69,223 in Serbia, 1:115,007 in Croatia, 1:132,915 in Slovakia, and 1:192,626 in the Czech Republic (Table S1). The symptoms consistent with MPS II occurred typically in the first year of life in 29 patients (71%). The most common signs at onset included inguinal hernias (13 patients), developmental delay (11 patients), macrocephaly, recurrent respiratory infections and joint contractures (4 patients), often in combination. The average delay between the first symptom and the diagnosis was 2.4 years (0 – 9 years). The disease severity could be specified in 42 patients as follows: attenuated form in six, intermediate form in four and severe form in 32 patients. Two boys were too young for the prediction of clinical outcome. Cognitive functions were normal or borderline in ten patients; four patients had mild, six had moderate and 24 had severe developmental delay/intellectual disability typically after developmental regression (59% patients). The only female, a 5-year-old patient (Patient 6) with moderate developmental delay manifested fully expressed visceral involvement (details in Ref. 3).

Enzyme replacement therapy was introduced in 23 patients, and haematopoietic stem cell transplantation was performed in one boy with poor outcome at the age of five years (Patient 26). Fifteen patients with the severe form died during the study period (median age at death 13 years, range 9 – 23 years), mostly due to cardiopulmonary failure related to pneumonia. Two patients with the intermediate form of the disease died at 17.5 and 32 years due to cardiac arrest during pneumonia and cardiomyopathy, respectively.

Laboratory findings

The values of GAG excretion were available in 30 patients (23, 3 and 4 patients with severe, intermediate and attenuated forms of the disease, respectively). Values

Table 1. Clinical manifestation in 44 Slavic patients with mucopolysaccharidosis type II^a

Patient	Age	Phenotype	Urine GAGs at dg. (mol/g creat)	First symptom	Age at first symptom	Age at diagnosis	Age at death	Developmental delay	Developmental regression	Dysostosis multiplex (100%)	Short stature (70%)	Coarse features	Macrocephaly (76%)	Macroglossia	Joint contractures (98%)
1	18	int.	68.1	Inguinal hernia	Birth	5 y.	Alive	Mild	-	+	+	++	+	+	+
2	14	sev.	90.3	Developmental delay	inf.	5 y.	14 y.	Severe	+	+	+	++	+	+	+
3	9	sev.	33.4	Developmental delay	inf.	2 y.	Alive	Severe	+	+	+	++	-	+	+
4	11	att.	43.7	Hearing impairment	3 y.	12 y.	Alive	Borderline	-	+	+	+	-	-	+
5	3	sev.	91.7	Macrocephaly	4 m.	3 y.	Alive	Moderate	+	+	-	++	-	+	+
6 ^b	5	sev.	46.2	Adenoid hypertrophy	2 y.	3.5 y.	Alive	Moderate	-	+	-	++	+	+	+
7	37	att.	12.6	Joint contractures	3 y.	5 y.	Alive	Above level	+	+	+	+	-	-	+
8	8	sev.	53.4	Laryngeal stridor, hepatomegaly	inf.	3 y.	Alive	Moderate	+	+	+	++	+	+	+
9	4	sev.	50.0	Kyphosis, developmental delay	inf.	2 y.	Alive	Moderate	-	+	-	+	-	-	+
10	9	sev.	87.5	Inguinal hernia, acute otitis media	inf.	2 y.	9 y.	Severe	+	+	+	++	+	+	+
11	22	int.	35.5	Chronic rhinorea	inf.	5 y.	Alive	Mild	-	+	+	++	+	-	+
12	9	sev.	58.8	Developmental delay	inf.	3 y.	9 y.	Severe	+	+	+	++	-	+	+
13	13	sev.	n.k.	Facial dysmorfism, joint contractures	inf.	3 y.	13 y.	Severe	+	+	+	++	-	+	+
14	15	sev.	29.6	Inguinal hernia	inf.	3 y.	15 y.	Severe	+	+	+	++	-	+	+
15	9	sev.	n.k.	Developmental delay	inf.	4 y.	n.k.	Mild	-	+	+	++	+	-	+
16	15	sev.	n.k.	Developmental delay	inf.	0.5 y.	15 y.	Severe	+	+	+	++	+	+	+
17	5	sev.	n.k.	Developmental delay	inf.	5 y.	13 y.	Moderate	-	+	+	++	n.k.	-	+
18	n.k.	int.	n.k.	N.k.	n.k.	n.k.	32 y.	Mild	-	+	+	++	+	+	+
19	9	sev.	n.k.	Developmental delay	inf.	3 y.	9 y.	Severe	+	+	n.k.	++	n.k.	+	n.k.
20	35	att.	n.k.	N.k.	n.k.	34 y.	Alive	Borderline	-	+	+	+	+	-	+
21	43	att.	n.k.	N.k.	n.k.	n.k.	Alive	Borderline	-	+	+	+	+	-	+
22	15	sev.	59.8	Inguinal hernia	3 m.	5 y.	15 y.	Borderline	-	+	+	++	+	+	+
23	10	sev.	n.k.	Inguinal hernia	8 m.	2 y.	Alive	Severe	+	+	-	++	+	-	+
24	12	sev.	99.9	Recc, resp. Inf.	23 m.	2.3 y.	Alive	Moderate	-	+	+	++	-	+	+
25	9	sev.	59.0	Speech delay	3 y.	5.5 y.	9 y.	Severe	+	+	+	++	+	+	+
26	25	sev.	n.k.	Cardiomyopathy	7 m.	2 y.	Alive	Severe	+	+	-	++	+	+	+
27	11.5	sev.	n.k.	Macrocephaly, inguinal hernia	1 m.	5 y.	11.5 y.	Severe	+	+	-	++	+	+	+
28	4	sev.	n.k.	Inguinal et umbilical hernia	inf.	4 y.	n.k.	Severe	+	+	-	++	+	n.k.	n.k.
29	10	sev.	33.0	Inguinal et umbilical hernia	6 m.	2.5 y.	10 y.	Severe	+	+	+	++	+	+	+
30	11	sev.	98.5	Macrocephaly	12 m.	2.5 y.	Alive	Severe	+	+	+	++	+	+	+
31	4.5	att.	35.0	Joint contractures	3 y.	3.5 y.	Alive	No	-	+	-	+	+	-	+
32	6	sev.	29.1	Bilateral inguinal hernia	2 m.	1.2 y.	Alive	Severe	+	+	+	++	+	+	+
33	8	sev.	59.2	Macrocephaly, macroglossia	18 m.	2 y.	Alive	Severe	+	+	+	++	+	+	+
34	6	sev.	15.2	Reccurent acute otitis media	12 m.	1.5 y.	Alive	Severe	+	+	+	++	+	+	+
35	5.5	sev.	63.9	Umbilical hernia	inf.	3 y.	Alive	Severe	-	+	-	++	+	-	+
36	14.5	sev.	64.0	Laryngeal strid., recc. Resp. Inf.	1.5 m.	2.5 y.	Alive	Severe	+	+	+	++	+	+	+
37	24	sev.	50.0	Hearing impairment, speech delay	toddl.	7 y.	Alive	Severe	+	+	-	++	+	+	+
38	23	sev.	50.0	Kyphosis, speech delay	18 m.	2.5 y.	23 y.	Severe	+	+	+	++	+	+	+
39	14	sev.	105.0	Bilateral inguinal hernia	1 m.	7 y.	14 y.	Severe	+	+	+	++	+	+	+
40	17	int.	54.0	Inguinal hernia	4.5 m.	3.5 y.	17.5 y.	No	-	+	+	++	+	-	+
41	13	sev.	44.0	Inguinal hernia	3 y.	7 y.	13 y.	Severe	+	+	-	++	+	+	+
42	1.2	n.d.	78.0	Inguinal hernia	7 m.	0.75 y.	Alive	No	-	+	-	+	-	-	-
43	14.5	att.	50.0	Recc. Resp. Inf., hearing impairment	4.5 y.	6.5 y.	Alive	No	-	+	+	+	+	-	+
44	2.5	n.d.	77.0	Inguinal hernia	2 m.	2.5 y.	Alive	No	-	+	-	++	+	+	+

Table 1. continued

Patient	Age	Phenotype	Urine GAGs at dg. (mol/g creat)	Capral tunnel syndrome	Inguinal (72%)/umbilical hernia (60%)	Hepato-(93%)/splenomegaly (69%)	Obesity	Heart valve involvement (85%)	Cardiomyopathy (37%)	Adenotomy/tonsillectomy	Acute otitis media	Hearing impairment (79%)	Seizures (21%)	Hydrocephalus	Comments; imaging
1	18	int.	68.1	n.k.	+/+	6/6	+	+	-	+/+	+	+	-	-	ERT; MRI: WMC, CS
2	14	sev.	90.3	n.k.	+/+	10/4	+	+	+	+/-	-	+	+	+	Subdural hydromia surgery
3	9	sev.	33.4	n.k.	+/-	1/0	+	+	-	+/-	+	+	-	-	ERT
4	11	att.	43.7	n.k.	-/+	7/4	-	+	-	+/-	-	+	-	-	ERT; MRI: without CS
5	3	sev.	91.7	n.k.	-/-	9/2	+	-	-	+/-	+	+	-	-	
6 ^b	5	sev.	46.2	+	-/-	3/2	+	-	-	+/-	+	+	-	-	ERT; MRI: without CS
7	37	att.	12.6	+	+/-	0/0	-	+	-	n.k.	+	-	+	-	ERT
8	8	sev.	53.4	+	-/+	5/2	+	+	-	+/-	+	+	-	+	ERT; MRI: CS
9	4	sev.	50.0	n.k.	+/+	2/2	-	-	+	-/-	-	+	-	-	ERT
10	9	sev.	87.5	+	+/+	6/7	+	+	+	-/-	+	+	-	+	MRI: WMC, CS
11	22	int.	35.5	n.k.	+/+	10/4	-	+	-	-	+	+	-	-	
12	9	sev.	58.8	-	+/-	3/0	-	+	-	-	+	+	+	+	MRI: WMC, CS
13	13	sev.	n.k.	n.k.	+/-	10/8	+	+	-	-	-	+	-	n.k.	MRI: CS
14	15	sev.	29.6	n.k.	+/-	3/3	+	+	-	-	-	+	+	+	Gastrostomy
15	9	sev.	n.k.	n.k.	+/-	2/0	-	+	-	-	+	-	-	-	
16	15	sev.	n.k.	n.k.	n.k.	n.k.	-	-	-	n.k.	n.k.	+	-	n.k.	
17	5	sev.	n.k.	n.k.	+/+	n.k.	n.k.	n.k.	n.k.	-/-	-	+	-	+	
18	n.k.	int.	n.k.	+	n.k.	+/+	+	+	+	n.k.	n.k.	+	-	n.k.	
19	9	sev.	n.k.	n.k.	n.k.	10/8	n.k.	+	+	n.k.	n.k.	n.k.	-	n.k.	
20	35	att.	n.k.	+	n.k/+	4/0	-	n.k.	n.k.	n.k.	n.k.	+	-	n.k.	
21	43	att.	n.k.	+	+/+	4/0	-	n.k.	n.k.	n.k.	n.k.	+	-	n.k.	
22	15	sev.	59.8	n.k.	+/+	4/6	-	+	-	-/-	n.k.	-	+	+	
23	10	sev.	n.k.	-	+/+	3/0	-	+	-	-/-	n.k.	-	-	-	ERT; MRI: WMC
24	12	sev.	99.9	-	-/+	2/0	-	+	-	+/+	n.k.	+	-	+	ERT; MRI: WMC
25	9	sev.	59.0	-	-/+	4/1	-	+	-	-/-	n.k.	+	+	+	MRI: WMC
26	25	sev.	n.k.	+	n.k.	3/4	+	+	+	n.k.	n.k.	-	-	+	MRI: WMC; HSCT
27	11.5	sev.	n.k.	-	+/+	5/4	+	-	+	+/-	n.k.	+	+	+	MRI: WMC; recc. subdural heatomas
28	4	sev.	n.k.	n.k.	+/+	2/0	n.k.	+	-	n.k.	n.k.	n.k.	n.k.	n.k.	
29	10	sev.	33.0	+	+/+	4/2	-	+	-	-/-	-	+	-	-	ERT
30	11	sev.	98.5	-	-/+	6/3	+	-	-	-/+	-	+	-	-	ERT; MRI: WMC; D-W sy
31	4.5	att.	35.0	-	-/-	5/2	-	+	-	-/-	-	-	-	-	ERT
32	6	sev.	29.1	-	+/+	8/2	+	+	-	+/+	+	+	+	-	ERT
33	8	sev.	59.2	-	-/-	3/2	-	+	-	-/-	-	-	-	-	ERT; MRI: WMC
34	6	sev.	15.2	+	-/-	2/1	+	+	+	+/-	+	+	-	-	ERT
35	5.5	sev.	63.9	+	+/-	4/5	+	+	+	-/-	+	+	-	-	ERT
36	14.5	sev.	64.0	-	-/+	4/-	-	+	-	+/+	+	+	-	-	ERT; MRI: WMC, CS
37	24	sev.	50.0	n.k.	+/+	+/+	-	+	+	+/+	+	+	-	-	MRI: WMC
38	23	sev.	50.0	-	+/-	+/+	-	+	+	-/+	n.k.	+	+	+	ERT; CT: WMC; MRI: CS
39	14	sev.	105.0	-	+/+	+/+	-	+	-	+/+	+	-	-	+	MRI: WMC
40	17	int.	54.0	+	+/+	+/+	-	+	+	+/+	+	+	-	-	ERT; MRI: WMC
41	13	sev.	44.0	+	+/-	+/+	-	+	+	+/+	+	+	-	-	ERT; MRI: WMC
42	1.2	n.d.	78.0	-	+/-	-/-	-	+	+	-/-	-	+	-	-	ERT
43	14.5	att.	50.0	+	+/+	+/-	-	+	+	-/-	-	+	-	-	ERT; MRI: WMC, CS
44	2.5	n.d.	77.0	-	+/-	-/-	-	+	-	-/-	+	-	-	-	ERT

att., attenuated; creat., creatinine; CS., cervical stenosis; D-W sy, Dandy–Walker syndrome; ERT, enzyme replacement therapy; GAGs, glycosaminoglycans; inf., infancy; int., intermediate; MRI, magnetic resonance imaging; n.d., not determined; n.k., not known; sev., severe; toddl., toddler age; WMC, white matter changes.

^aCzech patients: 1–21, Slovak: 22–28, Serbian: 29–35, Croatian: 36–44; GAGs – controls: 0–2 years <26.4; 2–5 years <16.1; 5–10 years <8.8 g/mol creatinine.

^bPatient 6 is a female, the other patients are males.

Table 2. Mutations in the *IDS* gene in 38 Slavic patients with mucopolysaccharidosis II^{a, b}

Patient	Mutation	Consequences	Localization	Inherited allele	Phenotype	HGMD accession or citation
Nucleotide substitutions						
4	c. [187A > G]; [0]	p.Asn63Asp	Exon 2	Yes	Attenuated	CM960853
15	c. [239A > G]; [0]	p.Gln80Arg	Exon 2	Yes	Severe	CM128173
43	c. [253G > A]; [0]	p.Ala85Thr	Exon 3	N.d.	Attenuated	CM960855
5	c. [257C > T]; [0], r. [257c > u, 241_284del]	p.[Pro86Leu, Gln81Glufs*3]	Exon 3	Yes	Severe	CM950659
22, 23 (siblings)	c. [257C > T]; [0]	p.[Pro86Leu, Gln81Glufs*3]	Exon 3	Yes	Severe	CM950659
33	c. [262C > T]; [0]	p.Arg88Cys	Exon 3	n.d.	Severe	CM950661
37	c. [263G > A]; [0]	p.Arg88His	Exon 3	n.d.	Severe	CM960857
31	c. [286A > T]; [0] (AGA > TGA)	p.Arg96*	Exon 3	n.d.	Attenuated	–
13	c. [998C > G]; [0]	p.Ser333Trp	Exon 7	Yes	Severe	Froissart et al., 2007 (5)
36	c. [998C > T]; [0]	p.Ser333Leu	Exon 7	n.d.	Severe	CM920367
9	c. [998C > T]; [0]	p.Ser333Leu	Exon 7	n.d.	n.d.	CM920367
28	c. [1004A > T]; [0]	p.His335Leu	Exon 7	n.d.	Severe	–
14	c. [1010G > A]; [0] (TGG > TAG)	p.Trp337*	Exon 8	n.d.	Severe	CM128194
7	c. [1037C > T]; [0]	p.Ala346Val	Exon 8	n.d.	Attenuated	CM950669
29	c. [1040A > G]; [0]	p.Lys347Arg	Exon 8	n.d.	Severe	–
11	c. [1122C > T]; [0], r. [1121_1180del]	p.Glu375_Gly394del20	Exon 8	n.d.	Intermediate	CS963080
1	c. [1181 - 1G > A]; [0], r. [1181_1184del]	p.Arg395Asnfs*44	int 8	Yes	Intermediate	CS951450
18	c. [1327C > T]; [0] (CGA > TGA)	p.Arg443*	Exon 9	No	Intermediate	CM920368
6	c. [1403G > A]; [=]	p.Arg468Gln	Exon 9	No	Severe	CM930422
Small deletions/duplications/insertions/indels						
2	c. [121_123delCTC]; [0]	p.Leu41del	Exon 2	Yes	Severe	CD941707
12	c. [416dupC]; [0]	p.Gly140Trpfs*5	Exon 3	Yes	Severe	–
44	c. [510_511delAT]; [0]	p.Cys171Serfs*27	Exon 5	No	n.d.	–
25	c. [559delG]; [0]	p.Asp187Metfs*26	Exon 5	Yes	Severe	–
3	c. [1038delC]; [0]	p.Lys347Asnfs*13	Exon 8	Yes	Severe	–
19	c. [1212_1215dupGTCT]; [0]	p.Leu406Valfs*26	Exon 9	n.d.	Severe	–
24	c. [1234_1460del227]; [0]	p.Gly412Hisfs*11	Exon 9	n.d.	Severe	–
20, 21 (siblings)	c. [1353_1354insATCG]; [0]	p.Tyr452Ilefs*6	Exon 9	Yes	Attenuated	–
10	c. [1409_1410delCA]; [0]	p.Ser470*	Exon 9	Yes	Severe	–

Table 2. Continued.

Patient	Mutation	Consequences	Localization	Inherited allele	Phenotype	HGMD accession or citation
Major structural alternations						
27	[c.1181-1203_*262del]; [0] (a 1938 bp deletion encompassing a part of intron 8, entire exon 9 and a part of 3'UTR region)			Yes	Severe	The same type in CG116295
32	Hemizygous deletion encompassing entire IDS gene			n.d.	Severe	E.g. Brusius-Facchin et al., 2014 (8)
34	Hemizygous deletion encompassing entire IDS gene			n.d.	Severe	E.g. Brusius-Facchin et al., 2014 (8)
8	Recombination between intron 7 of the IDS gene and the IDS2 pseudogen			Yes	Severe	CP052806
26	Recombination between intron 7 of the IDS gene and the IDS2 pseudogene			Yes	Severe	CP052806
30	Recombination between int3/int 7 of the IDS gene and int3/int7 of the IDS2 pseudogene + duplication encompassing exons 1 to 7 of the IDS gene			n.d.	Severe	–
35	Recombination between int3/int 7 of the IDS gene and int3/int 7 of the IDS2 pseudogene			n.d.	Severe	CP052805
38	Recombination between intron 7 of the IDS gene and the IDS 2 pseudogene			n.d.	Severe	CP052806

^aNovel variants are depicted in bold; HGMD[®]: www.hgmd.cf.ac.uk.

^bNovel nucleotide substitutions predicting missense mutations (p.His335Leu and p.Lys347Arg) are listed neither in Exome Aggregation Consortium (ExAC) (<http://exac.broadinstitute.org>) nor in 1000 Genomes project (<http://browser.1000genomes.org/>). The other aminoacid exchange, p.His335Arg, led to MPS II phenotype (4). At position p.Lys347 four other exchanges (p.Lys347Gln, p.Lys347Thr, Lys347Ile, p.Lys347Glu) were described in patients with MPS II (16, 20–22).

Table 3. Comparison of published phenotypes in recurrent point mutations in the *IDS* gene^a

Mutation	Phenotype in patient described in present report	Phenotype published		
		Attenuated	Intermediate	Severe
c.[187A > G]; [0] p.Asn63Asp	Attenuated in Patient 4	Goldenfum et al., 1996 (23) Villani et al., 1997 (20) Gort et al., 1998 (13) Kosuga et al., 2016 (7)	Rathmann et al. 1996 (21) Karsten et al. 1998 (12)	
c.[253G > A]; [0] p.Ala85Thr c.[257C > T];[0], r.[257c > u, 241_284del] p.[Pro86Leu, Gln81Glufs*3]	Attenuated in Patient 43 Severe in Patients 5, 22, 23	Gort et al., 1998 (13) Kosuga et al., 2016 (7), four patients	Rathmann et al. 1996 (21) Isogai et al., 1998 (25) Popowska et al., 1995 (10)	Li et al., 1999 (24) Froissart et al., 1998 (4)
c.[262C > T]; [0] p.Arg88Cys	Severe in Patient 33			Isogai et al., 1998 (25) Alves et al., 2006 (11) Keeratchamroen et al., 2008 (14) Kosuga et al., 2016 (7), two patients Rathmann et al., 1996 (21), three patients Karsten et al., 1998 (12), two patients Moreira da Silva et al., 2001 (18) Alves et al., 2006 (11)
c.[263G > A];[0] p.Arg88His	Severe in Patient 37		Gort et al., 1998 (13)	Karsten et al., 1998 (12) Filocamo et al., 2001 (6), two patients Zhang et al., 2011 (26) Galvis et al., 2015 (16)
c.[998C > T]; [0] p.Ser333Leu	Severe in Patient 36 n.d. in Patient 9			Isogai et al., 1998 (25) Karsten et al., 1998 (12) Li et al., 1999 (24) Zhang et al., 2011 (26)
c.[1403G > A]; [=] p.Arg468Gln	Severe in Patient 6	Villani et al., 1997 (20)		Kosuga et al., 2016 (7), two patients Goldenfum et al., 1996 (23) (S/I) ^b Rathmann et al., 1996 (21) Isogai et al., 1998 (25), three patients Li et al., 1999 (24) Filocamo et al., 2001 (6), four patients Moreira da Silva et al., 2001 (18) Keeratchamroen et al., 2008 (14) Zhang et al., 2011 (26) Galvis et al., 2015 (16)
c.[1122C > T]; [0] r.[1121_1180del]	Intermediate in Patient 11	Rathmann et al., 1996 (21) Gort et al., 1998 (13), three patients	Filocamo et al., 2001 (6), two patients	Kosuga et al., 2016 (7), three patients Karsten et al., 1998 (12), two patients Zhang et al., 2011 (26)

Table 3. Continued.

Mutation	Phenotype in patient described in present report	Phenotype published attenuated	Intermediate	Severe
p.Glu375_Gly394del20		Moreira da Silva et al., 2001 (18), three patients Alves et al., 2006 (11) Brusius-Facchin et al., 2014 (8), 25 patients Kosuga et al., 2016 (7) Gort et al., 1998 (13) Zhang et al., 2011 (26) Sohn et al., 2012 (27) Kosuna et al. 2016 (7)		Sohn et al., 2012 (27)
c.[1327C > T];[0] p.Arg443*	Intermediate in Patient 18		Rathmann et al., 1996 (21) Froissart et al., 1998 (4) Froissart et al., 1998 (4) (S/I) ^b Isogai et al., 1998 (25) Karsten et al., 1998 (12) Filocamo et al., 2001 (6)	Froissart et al., 1998 (4), two patients Moreira da Silva et al., 2001 (18) Keeratichamroen et al., 2008 (14)

^aEach reference represents one patient if not further specified.

^b(S/I) – patient with borderline severe/intermediate form.

greater than 70 g/mol creatinine at the time of diagnosis were identified in six patients with the severe form of the disease. The residual enzyme activity analyzed in leukocytes from 24 patients ranged from 0% to 5% regardless of the phenotype. The only exception was Patient 7 with the attenuated form, who showed a residual enzyme activity of 14.6%.

The samples for molecular-genetic testing were available in 38 patients from 36 families (Table 2). Twelve novel mutations were identified. Among 17 different nucleotide substitutions, only two mutations leading to amino acid exchange and one creating a stop codon were novel. On the contrary, out of 9 small deletions/insertions, only one deletion was described in the literature. Nucleotide substitutions were the most frequent in exons 3, 7, and 8.

mRNA was analyzed in three patients (1, 5, 11) (Table 2). The intronic mutation c.1181-1G>A led to deletion of the first 4 bp of exon 9 in Patient 1. Two transcripts, one containing a missense mutation and the other exhibiting aberrant splicing with deletion of part of exon 3 (r.[257c>u, 241_284del]), were detected in Patient 5. In Patient 11 hemizygous for c.1122C>T, only the aberrantly spliced allele leading to deletion of 60 bp from the distal part of exon 8 was detected by Sanger sequencing (Table 2). This finding was supported by amplicon-based deep sequencing when 776 reads of the RT-PCR product revealed only the deleted allele, whereas the correctly spliced allele was not identified (MiSeq, Illumina platform, data not shown).

Molecular-genetic data were available from 17 mothers of male patients, and 15 of them were carriers of the pathogenic mutations (rate of *de novo* mutations approximately 10–15%).

Discussion

We evaluated clinical, biochemical and molecular-genetic data of 44 patients with Hunter syndrome from four countries populated mostly by inhabitants of Slavic origin.

Our patients manifested more severe phenotypes, with cognitive impairment in 77% of patients in comparison to 37% described in the literature (1). No prediction based on the age of clinical manifestation could be made. It is important to emphasize that symptoms in our group of patients occurred earlier with median <1 year than in other cohorts of patients described in the literature with median of 1.5 years and 2.5 years, respectively (1, 15).

Major structural alterations (large deletions or rearrangements), consistently associated with the severe form of the disease, were detected in 21% of patients in our cohort (comparable with 10 to 30% in (5–8, 13, 16)). This unequivocal correlation was not observed in other types of apparently null mutations (small deletions/insertions) when a 4-bp insertion was associated with attenuated phenotype in two brothers (Patients 20, 21). The predicted effect of this mutation is a frameshift and premature stop codon leading to loss of the entire smaller *IDS* subunit (a 14 kDa chain). Mutations within this region have been associated with severe phenotype

in patients presented here (Patients 6, 10) and in the literature (7). We have no explanation for this fact except for possible role of genetic background on clinical phenotype of the patients.

Single nucleotide changes comprised 53% of identified mutations. Within this group, the most predictable phenotype could be observed in several recurrent missense mutations (p.Asn63Asp, p.Pro86Leu, p.Arg88Cys, p.Arg88His, p.Ser333Leu, and p.Arg468Gln), which exhibited quite stable associations with certain phenotypes (Table 3). Nucleotide substitutions leading to premature stop codons in the Czech patient (p.Arg443*) and Serbian patient (p.Arg96*) led to an attenuated phenotype in both cases. These findings may be explained by the highest natural read-through potential of the stop codon TGA in comparison with the other two TAA and TAG termination codons (17). In accordance with this premise, the third nonsense mutation (p.Trp337*) with formation of the termination codon TAG led to a severe phenotype in the Czech patient and in a previously described Thai patient (14). However, the correlation is not straightforward, as the recurrent mutation p.Arg443* was described in patients with severe, intermediate and attenuated phenotypes (Table 3).

The silent mutation c.1122C>T causes an alternative splice site resulting in a 20-amino acid deletion in the major abnormal transcript (18). This mutation was described in patients with variable outcomes, but less severe phenotypes were predominant (Table 3). The mild phenotype was further explained by the detection of a small amount of correctly spliced transcript (11). The absence of normal transcript in our patient suggests individual differences in transcriptional machinery (19) and may explain variable phenotypes associated with this mutation.

Conclusion

In the majority of patients (>70%), MPS II manifested in infancy. GAG values greater than 70 g/mol creatinine are potentially associated with the severe form of disease. Large rearrangements and the majority of small deletions/insertions led to the severe phenotype. Genotype – phenotype correlation was also identified in several recurrent missense mutations. Summarizing the laboratory findings, the phenotype can be predicted with high probability in approximately half of MPS II patients.

Supporting Information

Additional supporting information may be found in the online version of this article at the publisher's web-site.

Acknowledgements

We would like to thank to Prof. Eduard Paschke (University Hospital of Youth and Adolescence Medicine, Medical University of Graz, Austria), Dr. Anne-Kartin Giese (Albrecht-Kossel-Institute

for Neurodegeneration, University of Rostock, Germany) for providing the molecular-genetic analyses of some Croatian and Serbian patients. Institutional support was provided by PRVOUK P24/LF1/3 (Charles University), UNCE 204011 (Charles University), RVO-VFN 64165/2012 (Ministry of Health, Czech Republic), and GAUK 580716 (Charles University). All contributors have reviewed the manuscript, approved the final version, consented to its submission to the journal, and agreed with the presented data analyses and conclusions. M. M. has received lecture honoraria, consultancy fee and travel expenses from Shire Human Genetic Therapies. This support did not have any influence on the study design, the data collection, the data analysis, the writing of the report, or the decision to submit the article for publication.


References

1. Wraith JE, Beck M, Giugliani R et al. Initial report from the Hunter Outcome Survey. *Genet Med* 2008; 10 (7): 508–516.
2. Pinto LL, Vieira TA, Giugliani R, Schwartz IV. Expression of the disease on female carriers of X-linked lysosomal disorders: a brief review. *Orphanet J Rare Dis* 2010; 5: 14.
3. Rebound M, Rybova J, Dobrovolny R et al. X-chromosome inactivation analysis in different cell types and induced pluripotent stem cells elucidates the disease mechanism in a rare case of mucopolysaccharidosis type II in a female. *Folia Biol (Praha)* 2016; 62 (2): 82–89.
4. Froissart R, Maire I, Millat G et al. Identification of iduronate sulfatase gene alterations in 70 unrelated Hunter patients. *Clin Genet* 1998; 53 (5): 362–368.
5. Froissart R, Da Silva IM, Maire I. Mucopolysaccharidosis type II: an update on mutation spectrum. *Acta Paediatr* 2007; 96 (455): 71–77.
6. Filocamo M, Bonuccelli G, Corsolini F, Mazzotti R, Cusano R, Gatti R. Molecular analysis of 40 Italian patients with mucopolysaccharidosis type II: new mutations in the iduronate-2-sulfatase (IDS) gene. *Hum Mutat* 2001; 18 (2): 164–165.
7. Kosuga M, Mashima R, Hirakiyama A et al. Molecular diagnosis of 65 families with mucopolysaccharidosis type II (Hunter syndrome) characterized by 16 novel mutations in the IDS gene: Genetic, pathological, and structural studies on iduronate-2-sulfatase. *Mol Genet Metab* 2016; 118 (3): 190–197.
8. Brusius-Facchin AC, Schwartz IV, Zimmer C et al. Mucopolysaccharidosis type II: identification of 30 novel mutations among Latin American patients. *Mol Genet Metab* 2014; 111 (2): 133–138.
9. Alcantara-Ortigoza MA, Garcia-de Teresa B, Gonzalez-Del Angel A et al. Wide allelic heterogeneity with predominance of large IDS gene complex rearrangements in a sample of Mexican patients with Hunter syndrome. *Clin Genet* 2016; 89 (5): 574–583.
10. Popowska E, Rathmann M, Tyłki-Szymanska A et al. Mutations of the iduronate-2-sulfatase gene in 12 Polish patients with mucopolysaccharidosis type II (Hunter syndrome). *Hum Mutat* 1995; 5 (1): 97–100.
11. Alves S, Mangas M, Prata MJ et al. Molecular characterization of Portuguese patients with mucopolysaccharidosis type II shows evidence that the IDS gene is prone to splicing mutations. *J Inher Metab Dis* 2006; 29 (6): 743–754.
12. Karsten S, Voskoboeva E, Tishkanina S, Pettersson U, Krasnopolskaja X, Bondeson ML. Mutational spectrum of the iduronate-2-sulfatase (IDS) gene in 36 unrelated Russian MPS II patients. *Hum Genet* 1998; 103 (6): 732–735.
13. Gort L, Chabas A, Coll MJ. Hunter disease in the Spanish population: molecular analysis in 31 families. *J Inher Metab Dis* 1998; 21 (6): 655–661.
14. Keeratchamroen S, Cairns JR, Wattanasirichaigoon D et al. Molecular analysis of the iduronate-2-sulfatase gene in Thai patients with Hunter syndrome. *J Inher Metab Dis* 2008; 31 (Suppl 2): S303–S311.
15. Young ID, Harper PS. The natural history of the severe form of Hunter's syndrome: a study based on 52 cases. *Dev Med Child Neurol* 1983; 25 (4): 481–489.
16. Galvis J, Gonzalez J, Uribe A, Velasco H. Deep genotyping of the IDS gene in Colombian patients with Hunter syndrome. *JIMD Rep* 2015; 19: 101–109.
17. Hein LK, Bawden M, Muller VJ, Sillence D, Hopwood JJ, Brooks DA. alpha-L-iduronidase premature stop codons and potential read-through in mucopolysaccharidosis type I patients. *J Mol Biol* 2004; 338 (3): 453–462.

18. Moreira da Silva I, Froissart R, Marques dos Santos H, Caseiro C, Maire I, Bozon D. Molecular basis of mucopolysaccharidosis type II in Portugal: identification of four novel mutations. *Clin Genet* 2001; 60 (4): 316–318.
19. Zhou Z, Fu XD. Regulation of splicing by SR proteins and SR protein-specific kinases. *Chromosoma* 2013; 122 (3): 191–207.
20. Villani GR, Balzano N, Grosso M, Salvatore F, Izzo P, Di Natale P. Mucopolysaccharidosis type II: identification of six novel mutations in Italian patients. *Hum Mutat* 1997; 10 (1): 71–75.
21. Rathmann M, Bunge S, Beck M, Kresse H, Tylki-Szymanska A, Gal A. Mucopolysaccharidosis type II (Hunter syndrome): mutation “hot spots” in the iduronate-2-sulfatase gene. *Am J Hum Genet* 1996; 59 (6): 1202–1209.
22. Chang JH, Lin SP, Lin SC et al. Expression studies of mutations underlying Taiwanese Hunter syndrome (mucopolysaccharidosis type II). *Hum Genet* 2005; 116 (3): 160–166.
23. Goldenfum SL, Young E, Michelakakis H, Tsagarakis S, Winchester B. Mutation analysis in 20 patients with Hunter disease. *Hum Mutat* 1996; 7 (1): 76–78.
24. Li P, Bellows AB, Thompson JN. Molecular basis of iduronate-2-sulphatase gene mutations in patients with mucopolysaccharidosis type II (Hunter syndrome). *J Med Genet* 1999; 36 (1): 21–27.
25. Isogai K, Sukegawa K, Tomatsu S et al. Mutation analysis in the iduronate-2-sulphatase gene in 43 Japanese patients with mucopolysaccharidosis type II (Hunter disease). *J Inher Metab Dis*. 1998; 21 (1): 60–70.
26. Zhang H, Li J, Zhang X et al. Analysis of the IDS gene in 38 patients with Hunter syndrome: the c.879G>A (p.Gln293Gln) synonymous variation in a female create exonic splicing. *PLoS One* 2011; 6 (8): e22951.
27. Sohn YB, Ki CS, Kim CH et al. Identification of 11 novel mutations in 49 Korean patients with mucopolysaccharidosis type II. *Clin Genet* 2012; 81 (2): 185–190.

CLINICAL REPORT

LAMP2 exon-copy number variations in Danon disease heterozygote female probands: Infrequent or underdetected?

Filip Majer^{1†} | Lenka Piherova^{1†} | Martin Reboun¹ | Veronika Stara² | Ondrej Pelak³ | Patricia Norambuena⁴ | Viktor Stranecky¹ | Alice Krebsova⁵ | Hana Vlaskova¹ | Lenka Dvorakova¹ | Stanislav Kmoch¹ | Tomas Kalina³ | Milos Kubanek⁵ | Jakub Sikora¹ 

¹Research Unit for Rare Diseases, Department of Pediatrics and Adolescent Medicine, 1st Faculty of Medicine, Charles University and General University Hospital, Prague, Czech Republic

²Department of Pediatrics, 2nd Faculty of Medicine, Charles University and University Hospital Motol, Prague, Czech Republic

³Department of Paediatric Haematology and Oncology, Childhood Leukaemia Investigation Prague, 2nd Faculty of Medicine, Charles University and University Hospital Motol, Prague, Czech Republic

⁴Department of Biology and Medical Genetics, 2nd Faculty of Medicine, Charles University and University Hospital Motol, Prague, Czech Republic

⁵Department of Cardiology, Institute for Clinical and Experimental Medicine, Prague, Czech Republic

Correspondence

Jakub Sikora, Research Unit for Rare Diseases, Department of Pediatrics and Adolescent Medicine, 1st Faculty of Medicine, Charles University and General University Hospital, Ke Karlovu 2, 128 00, Prague 2, Czech Republic. Email: jakub.sikora@lf1.cuni.cz

Funding information

Grantová Agentura, Univerzita Karlova, Grant/Award Number: GAUK 580716; Ministerstvo Školství, Mládeže a Tělovýchovy, Grant/Award Number: NCMG LM2015091, NPU I no. LO1604; Ministerstvo Zdravotnictví České Republiky, Grant/Award Number: AZV-MZ ČR 15-27682A, AZV-MZ ČR 15-33297A, RVO-VFN 64165/2012, VZ IKEM (00023001); Univerzita Karlova v Praze, Grant/Award Number: PROGRESS Q26, PRVOUK P24

Danon disease (DD) is an X-linked disorder caused by mutations in the lysosomal-associated membrane protein 2 (*LAMP2*) gene (*Xq24*). DD is characterized by cognitive deficit, myopathy, and cardiomyopathy in male patients. The phenotype is variable and mitigated in females. The timely identification of *de-novo* *LAMP2* mutated family members, many of whom are heterozygous females, remains critical for their treatment and family counseling. DD laboratory testing builds on minimally invasive quantification of the *LAMP2* protein in white blood cells and characterization of the specific mutation. This integrative approach is particularly helpful when assessing suspect female heterozygotes. *LAMP2* exon-copy number variations (eCNVs) were so far reported only in X-hemizygous male DD probands. In heterozygous female DD probands, the wild-type allele may hamper the identification of an eCNV even if it results in the complete abolition of *LAMP2* transcription and/or translation. To document the likely underappreciated rate of occurrence and point out numerous potential pitfalls of detection of the *LAMP2* eCNVs, we present the first two DD heterozygote female probands who harbor novel multi-exon *LAMP2* deletions. Critical for counseling and recurrence prediction, we also highlight the need to search for somatic-germlinal mosaicism in DD families.

KEY WORDS

Danon disease, X-chromosome, lysosomal-associated membrane protein 2, female heterozygotes, flow cytometry, exon-copy number variations

1 | INTRODUCTION

Danon disease (DD, MIM #300257) is a rare X-linked disorder characterized by cognitive deficit, cardiomyopathy and skeletal myopathy in males. DD is caused by mutations in the lysosomal-associated

membrane protein 2 (*LAMP2*, *Xq24*) (Nishino et al., 2000). The alternative *LAMP2* exons 9 (B, A, and C) code three protein variants differing in C-termini. The majority of the mutations affect the isoform shared regions (exons 1–8) of the gene and result in the complete and uniformly distributed absence of the *LAMP2* protein in tissues of male DD patients (Boucek, Jirikowic, & Taylor, 2011; D'Souza et al., 2014). *LAMP2* exon-copy number variations (eCNVs) have, thus far, all been

[†]These authors contributed equally to the work

reported in X-hemizygous male probands (Lines et al., 2014; Majer et al., 2014; Yang et al., 2010).

Heterozygous females for *LAMP2* mutations also develop DD. However, the tissue expression of their two *LAMP2* alleles is mosaic due to X-chromosome inactivation (XCI). In fact, the healthy allele may actually hamper characterization of the complementary *LAMP2* mutation in tissue homogenates from DD females, making eCNVs particularly difficult to identify during molecular genetic and/or genomic diagnostics.

To document the probable higher frequency of occurrence and demonstrate the numerous potential pitfalls posed by X-heterozygosity, we present the first two heterozygote female DD probands who harbor novel multi-exon deletions in the *LAMP2* gene.

2 | CLINICAL REPORTS

2.1 | Family 1—Proband II.1^{F1}

II.1^{F1} (Figure 1a) was diagnosed with hypertrophic cardiomyopathy at 12 years old. By 16 years of age, the patient's left ventricular (LV) hypertrophy had reached 22–25 mm, however the systolic function remained preserved. At 21 years, II.1^{F1} developed end-stage heart failure with severe LV systolic dysfunction and underwent

cardiac transplantation. A recent re-evaluation of her pretransplant electrocardiogram identified sinus rhythm and delta waves in most limb leads. Unfortunately, myocardial samples from her explanted heart were not available for histological, immunohistochemical, or ultrastructural testing. The plasma/serum activity levels of aminotransferases and creatine kinase were/are normal. II.1^{F1} has a mild cognitive deficit and normal muscle strength and is currently 42 years old.

2.2 | Family 2—Proband II.1^{F2}

II.1^{F2} (Figure 2a) was diagnosed with hypertrophic cardiomyopathy and pre-excitation at 11 years of age. The patient's electrocardiogram showed sinus rhythm with delta waves in inferior and precordial leads. At 14 years, the patient underwent radiofrequency ablation of two right-sided atrio-ventricular accessory pathways with a high capacity of antegrade conduction. At 15 years, the concentric LV hypertrophy (without obstruction of the outflow tract) reached 15–16 mm. Plasma/serum aspartate aminotransferase activity (0.95–1.45 μ kat/l; normal range 0.16–0.78 μ kat/l) and myoglobin levels (62–66 μ g/l; normal range 19–51 μ g/l) were slightly elevated throughout the patient's late childhood/adolescence. The patient experienced two episodes of palpitations at 17 and 18 years of age. Electrocardiography showed no arrhythmia at that time. At 19 years, the concentric LV hypertrophy

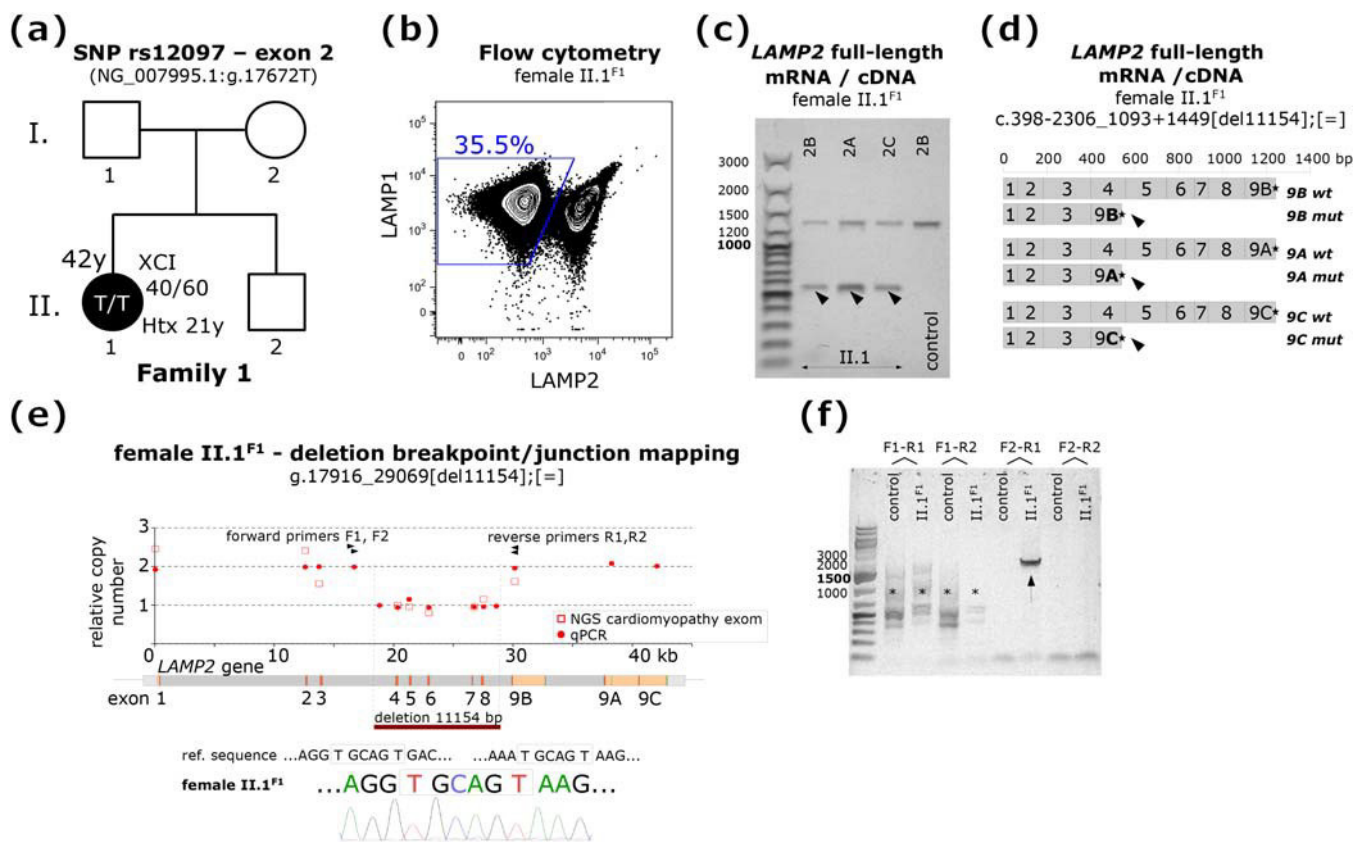


FIGURE 1 DD family 1—proband II.1^{F1}. (a) Current age, setup of the *LAMP2* exon 2 rs12097 SNP, and WBC XCI ratio are given for II.1^{F1}. I.1, I.2, and II.2 were not available for analyses. (b) LAMP1/LAMP2 coexpression FC profile shows LAMP2def granulocytes (blue gate) in II.1^{F1}. (c, d) Short aberrant *LAMP2* mRNA/cDNA isoforms (black arrowheads) lack exons 4–8. (e) qPCR (red dots) and NGS (red squares) values of *LAMP2* exon-copy number in II.1^{F1}. Black arrowheads mark positions and orientation of primers used to map the deletion breakpoint/junction. The deletion is flanked by short identical sequences. (f) Specific detection of the deletion junction (arrow), the wild-type allele, and/or the length of the product(s) may compromise PCR efficiency and specificity (*) [Color figure can be viewed at wileyonlinelibrary.com]

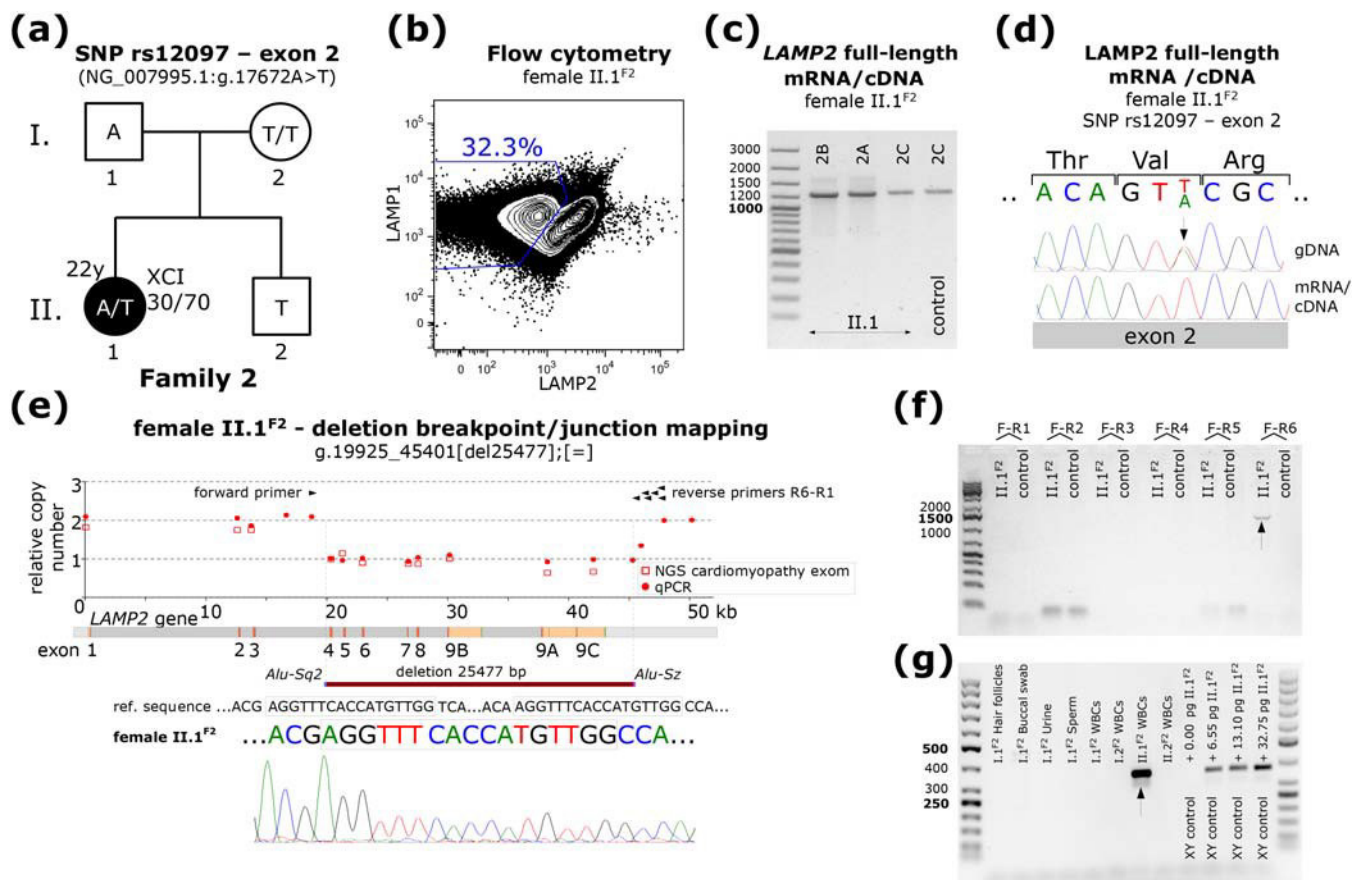


FIGURE 2 DD family 2—proband II.1^{F2}. (a) Current age and WBC XCI ratio are given for II.1^{F2}. Setup of the *LAMP2* exon 2 rs12097 SNP is shown for all family members. (b) LAMP1/LAMP2 coexpression FC profile shows LAMP2def granulocytes (blue gate) in II.1^{F2}. (c) Profile of the full-length *LAMP2* mRNA/cDNA isoforms (B, A, and C) in II.1^{F2} is normal. (d) gDNA and mRNA/cDNA sequence analyses of the exon 2 rs12097 SNP show exclusive expression of the maternal *LAMP2* allele in WBCs of II.1^{F2} (see also Supporting information Table S2 for NGS data). (e) qPCR (red dots) and NGS (red squares) values of *LAMP2* exon-copy number in II.1^{F2}. Black arrowheads mark positions and orientation of primers used to map the deletion breakpoint/junction site. The deletion is flanked by *Alu-Sq2* and *Alu-Sz* sequences. (f) Specific detection of the deletion junction (arrow) in II.1^{F2}. (g) PCR screening in the family identified the mutation only in WBCs of II.1^{F2}. 0.00, 6.55, 13.10, or 32.75 pg of II.1^{F2} WBC gDNA were mixed with 50 ng of XY control gDNA to demonstrate the efficiency of the nested PCR (Supporting information Table S1). These ratios correspond (Dolezel, Bartos, Voglmayr, & Greilhuber, 2003) to 0, 1, 2, or 5 mutant X-chromosome templates in the reaction mix and suggest that 1 cell carrying the mutation can be identified in ~7800 diploid or ~15600 haploid cells [Color figure can be viewed at wileyonlinelibrary.com]

progressed to 21–22 mm, nonetheless the LV systolic function remained normal. Recurrent syncope and nonsustained ventricular tachycardia were treated by implantation of a dual-chamber cardioverted defibrillator. II.1^{F2} is currently 22 years old and has normal intellect and skeletal muscle strength.

Parents and brothers of both probands are without symptoms of DD.

3 | MATERIALS AND METHODS

To diagnose DD in both probands, *LAMP2* expression was tested by flow cytometry (FC) in peripheral white blood cells (WBCs), and *LAMP2* molecular genetic analyses were performed. Informed consent (approved by the Ethics Committee of the authors' home institution) for participation and presentation of results was obtained from all tested individuals.

LAMP1/LAMP2 FC, polymerase chain reaction (PCR), and sequence analyses of the coding gDNA and full-length *LAMP2* mRNA/cDNAs, quantitative PCR (qPCR) *LAMP2* exon-copy number testing,

and XCI HUMARA assay were performed in WBCs as previously described (Majer et al., 2012, 2014).

Primers used for *LAMP2* exon dosage qPCR assessment, mapping of the breakpoint/junctions, and mutation-specific screening in Family 2 are listed in Table S1 (Supporting information).

LAMP2 exon dosage was also tested by next generation sequencing (NGS) using targeted enrichment panels and sequenced using the MiSeq platform (Illumina, San Diego, CA). The maternal/paternal *LAMP2* gDNA and mRNA/cDNA ratios, as well as the presence of the paternal wild-type *LAMP2* allele in II.1^{F2}, were tested by NGS. For additional details see Supporting Materials and Methods (Supporting information).

4 | RESULTS

4.1 | Flow cytometry

FC identified ~35% (Figure 1b) and ~33% (Figure 2b) of LAMP2 deficient (*LAMP2*def) granulocytes in II.1^{F1} and II.1^{F2}, respectively.

LAMP2 profiles were retested after one year in II.1^{F2} with the same result. FC findings corresponded with the XCI ratios by HUMARA assay in both probands (Figures 1a and 2a).

4.2 | Full-length *LAMP2* isoform mRNA/cDNA analyses and comparison to gDNA

In II.1^{F1}, a shorter (~550 bp) variant was detected in all three isoform mRNA/cDNAs in addition to the normal *LAMP2* splicing products (Figure 1c). Direct sequencing showed that these abnormal *LAMP2* mRNAs/cDNAs lack exons 4–8 (Figure 1d).

In II.1^{F2}, the profile of the *LAMP2* full-length mRNA/cDNAs was usual (Figure 2c), and the sequencing of all three isoforms did not identify any abnormality. However, analyses of her *LAMP2* gDNA coding regions revealed heterozygosity (A/T) for a known single nucleotide polymorphism (SNP) (rs12097) in exon 2. Comparison to the mRNA/cDNA sequences (using both direct sequencing and NGS) showed exclusive expression of the maternal *LAMP2* allele in II.1^{F2} (Figure 2a,d and Supporting information Table S2).

4.3 | *LAMP2* gDNA exon-copy number testing, deletion breakpoint/junction mapping, and mutation specific screening

gDNA qPCR eCNV analyses revealed abnormal (1 instead of 2) relative copy number of *LAMP2* exons 4–8 and 4–9C in II.1^{F1} and II.1^{F2}, respectively. Identical results were observed by NGS when evaluating normalized read depth coverage (Figures 1e and 2e and Supporting Materials and Methods in Supporting information).

To characterize the breakpoint/junctions in both probands, primer pairs were designed to span the presumed deleted gDNA regions. Alignment of the resultant PCR products (Figure 1f and 2f) to the reference *LAMP2* gene sequence (NG_007995.1) identified the TGCAGT motif to flank the breakpoint/junction in II.1^{F1} (Figure 1e) and *Alu-Sq2* and *Alu-Sz* repeats in II.1^{F2} (Figure 2e).

Mutation-specific screening was performed in gDNA from WBCs of I.1^{F2}, I.2^{F2}, and II.2^{F2}. To test for somatic-germlinal mosaicism, hair folliculi, buccal swabs, urine epithelia, and sperm were tested in I.1^{F2}. The deletion found in II.1^{F2} was not detected in any of these samples (Figure 2g). Similarly, the wild-type paternal *LAMP2* allele was not detected (using three SNPs in *LAMP2* intron 5) in WBCs of II.1^{F2} by NGS (Table S3, Supporting information).

These analyses were not performed in Family 1 because of advanced age of I.1^{F1} and I.2^{F1}.

5 | DISCUSSION

Heterozygous females for *LAMP2* mutations still likely remain an underdiagnosed DD patient group despite the growing body of information about their phenotype. Clinical presentation in heterozygous females is more variable (Toib et al., 2010) and mitigated in comparison to male DD patients (Boucek et al., 2011). Yet, early onset and/or malignant DD was documented in a number of females (Bottillo et al., 2016; Samad et al., 2017; Sugie et al., 2016). DD females were also

reported at risk of sudden death and timely ICD implantation was suggested as an appropriate therapeutic intervention (Miani et al., 2012).

To minimize late or retrospective (postmortem included) diagnosis, the clinical and laboratory DD workup should therefore account for pitfalls posed by X-chromosome heterozygosity. Minimally invasive and quantitative analyses of the cellular *LAMP2* protein content in WBCs combined with comparative gDNA and full-length isoform *LAMP2* mRNAs/cDNAs testing meet such requirements (Fanin et al., 2006; Majer et al., 2012, 2014; Regelsberger et al., 2009; Sikora, Majer, & Kalina, 2015). To further document the robustness of this protocol and highlight additional potential detection problems, we present the first two female DD probands affected by *LAMP2* eCNVs.

Clinical presentation was indicative of DD in the patients. However, it was the discrete populations of *LAMP2*def WBCs found by *LAMP2* FC that provided unambiguous evidence and advocated further *LAMP2* molecular genetic analyses in both females. Whereas the deletion of exons 4–8 in II.1^{F1} was anticipated based on the presence of the abnormally short PCR products while testing full-length *LAMP2* isoform mRNAs/cDNAs, II.1^{F2} unexpectedly showed a normal profile. The absence of the aberrant mRNA/cDNA species (lacking exons 4–9C) in II.1^{F2} is likely the result of decay of the truncated *LAMP2* mRNAs. Rationale for continued exploration of an eCNV was based on results from the *LAMP2* exon 2 SNP genotyping of the parents that suggested exclusive expression of the maternal *LAMP2* allele in II.1^{F2}.

Although unable to categorize the flanking elements (TGCAGT) of the breakpoint/junction in II.1^{F1}, the results suggest that the underlying mutagenic mechanism in both patients is a recombination mediated by repetitive sequences. Both deletions start/end in *LAMP2* intron 3. This localization is identical to four out of five *LAMP2* eCNVs reported in male DD patients (Lines et al., 2014; Majer et al., 2014; Yang et al., 2010). Moreover, the rearrangement in II.1^{F2} encompasses the same *AluSq2* repeat as that involved in an earlier reported duplication of *LAMP2* exons 4 and 5 (Lines et al., 2014). Collectively, these data imply that the *LAMP2* intron 3 could be a recombination hotspot and therefore warrants specific analysis of eCNVs in suspected patients.

DD is an important differential diagnostic option among patients with (hereditary) cardiomyopathies. The current diagnostic schemes for such patient cohorts frequently employ nonselective NGS-based approaches (Fu et al., 2016). Our findings document that *LAMP2* eCNVs not only occur in female DD probands but also constitute at least 10% of all reported (78–80 in March 2018 by the authors' review of the literature) *LAMP2* mutations. To avoid false-negative diagnostic conclusions and similar to others (Mates et al., 2018), we strongly suggest systematic (re)evaluation of NGS datasets for this type of molecular *LAMP2* pathology in suspected individuals.

Although frequent and critical for determining risk of recurrence in the siblings and progenies of the affected probands, mosaicism remains generally under-recognized in counseling practice (Campbell et al., 2014). For example, instances of maternal somatic-germlinal mosaicism were previously shown (Chen et al., 2012; Majer et al., 2014; Takahashi et al., 2002) but also missed in DD (Sikora et al., 2015). To the best of our knowledge, a paternal variant of this phenomenon has never been presented in DD. As II.1^{F2} carries the

mutation on the paternal *LAMP2* allele, we examined an array of the father's somatic tissues and sperm but did not identify the deletion-specific sequence. Moreover, high-resolution analyses of WBCs from II.1^{F2} did not detect the paternal wild-type *LAMP2* allele, suggesting homogenous distribution of the abnormal variant.

To conclude, *LAMP2* eCNVs are an important type of mutation causing DD and can be found in female probands. To avoid missing such variants, the outlined integrative approach to clinical, protein, and molecular genetic/genomic DD diagnostics is fully advocated, particularly in suspect females.

ACKNOWLEDGMENTS

This project was supported by the research grants AZV-MZ ČR 15-33297A, AZV-MZ ČR 15-27682A, GAUK 580716, and institutionally funded by VZ IKEM (00023001), NPU I no. LO1604, RVO-VFN 64165/2012, NCMG LM2015091, PRVOUK P24, and PROGRESS Q26 projects. The authors would like to thank Dr. Cristin Davidson for critical discussions and language proofing.

CONFLICT OF INTEREST

The authors declared that they have no conflict of interest.

ORCID

Jakub Sikora  <https://orcid.org/0000-0003-4104-2023>

REFERENCES

- Bottillo, I., Giordano, C., Cerbelli, B., D'Angelantonio, D., Lipari, M., Polidori, T., ... Grammatico, P. (2016). A novel *LAMP2* mutation associated with severe cardiac hypertrophy and microvascular remodeling in a female with Danon disease: A case report and literature review. *Cardiovascular Pathology*, 25(5), 423–431.
- Boucek, D., Jirikowic, J., & Taylor, M. (2011). Natural history of Danon disease. *Genetics in Medicine*, 13(6), 563–568.
- Campbell, I. M., Yuan, B., Robberecht, C., Pfundt, R., Szafranski, P., McEntagart, M. E., ... Stankiewicz, P. (2014). Parental somatic mosaicism is underrecognized and influences recurrence risk of genomic disorders. *American Journal of Human Genetics*, 95(2), 173–182.
- Chen, X. L., Zhao, Y., Ke, H. P., Liu, W. T., Du, Z. F., & Zhang, X. N. (2012). Detection of somatic and germline mosaicism for the *LAMP2* gene mutation c.808dupG in a Chinese family with Danon disease. *Gene*, 507(2), 174–176.
- D'Souza, R. S., Levandowski, C., Slavov, D., Graw, S. L., Allen, L. A., Adler, E., ... Taylor, M. R. (2014). Danon disease: Clinical features, evaluation, and management. *Circulation. Heart Failure*, 7(5), 843–849.
- Dolezel, J., Bartos, J., Voglmayr, H., & Greilhuber, J. (2003). Nuclear DNA content and genome size of trout and human. *Cytometry. Part A*, 51(2), 127–128.
- Fanin, M., Nascimbeni, A. C., Fulizio, L., Spinazzi, M., Melacini, P., & Angelini, C. (2006). Generalized lysosome-associated membrane protein-2 defect explains multisystem clinical involvement and allows leukocyte diagnostic screening in Danon disease. *The American Journal of Pathology*, 168(4), 1309–1320.
- Fu, L., Luo, S., Cai, S., Hong, W., Guo, Y., Wu, J., ... Wang, J. (2016). Identification of *LAMP2* mutations in early-onset Danon disease with hypertrophic

- cardiomyopathy by targeted next-generation sequencing. *The American Journal of Cardiology*, 118(6), 888–894.
- Lines, M. A., Hewson, S., Halliday, W., Sabatini, P. J., Stockley, T., Dipchand, A. I., ... Siriwardena, K. (2014). Danon disease due to a novel *LAMP2* microduplication. *JIMD Report*, 14, 11–16.
- Majer, F., Pelak, O., Kalina, T., Vlaskova, H., Dvorakova, L., Honzik, T., ... Sikora, J. (2014). Mosaic tissue distribution of the tandem duplication of *LAMP2* exons 4 and 5 demonstrates the limits of Danon disease cellular and molecular diagnostics. *Journal of Inherited Metabolic Disease*, 37(1), 117–124.
- Majer, F., Vlaskova, H., Krol, L., Kalina, T., Kubanek, M., Stolnaya, L., ... Sikora, J. (2012). Danon disease: A focus on processing of the novel *LAMP2* mutation and comments on the beneficial use of peripheral white blood cells in the diagnosis of *LAMP2* deficiency. *Gene*, 498(2), 183–195.
- Mates, J., Mademont-Soler, I., Del Olmo, B., Ferrer-Costa, C., Coll, M., Perez-Serra, A., ... Brugada, R. (2018). Role of copy number variants in sudden cardiac death and related diseases: Genetic analysis and translation into clinical practice. *European Journal of Human Genetics*, 26(7), 1014–1025.
- Miani, D., Taylor, M., Mestroni, L., D'Aurizio, F., Finato, N., Fanin, M., ... Proclemer, A. (2012). Sudden death associated with Danon disease in women. *The American Journal of Cardiology*, 109(3), 406–411.
- Nishino, I., Fu, J., Tanji, K., Yamada, T., Shimojo, S., Koori, T., ... Hirano, M. (2000). Primary *LAMP2* deficiency causes X-linked vacuolar cardiomyopathy and myopathy (Danon disease). *Nature*, 406(6798), 906–910.
- Regelsberger, G., Hoftberger, R., Pickl, W. F., Zlabinger, G. J., Kormoczi, U., Salzer-Muhar, U., ... Bernheimer, H. (2009). Danon disease: Case report and detection of new mutation. *Journal of Inherited Metabolic Disease*, 32 Suppl 1, S115–22.
- Samad, F., Jain, R., Jan, M. F., Sulemanjee, N. Z., Menaria, P., Kalvin, L., ... Tajik, A. J. (2017). Malignant cardiac phenotypic expression of Danon disease (*LAMP2* cardiomyopathy). *International Journal of Cardiology*, 245, 201–206.
- Sikora, J., Majer, F., & Kalina, T. (2015). *LAMP2* flow cytometry in peripheral white blood cells is an established method that facilitates identification of heterozygous Danon disease female patients and mosaic mutation carriers. *Journal of Cardiology*, 66(1), 88–89.
- Sugie, K., Yoshizawa, H., Onoue, K., Nakanishi, Y., Eura, N., Ogawa, M., ... Ueno, S. (2016). Early onset of cardiomyopathy and intellectual disability in a girl with Danon disease associated with a de novo novel mutation of the *LAMP2* gene. *Neuropathology*, 36(6), 561–565.
- Takahashi, M., Yamamoto, A., Takano, K., Sudo, A., Wada, T., Goto, Y., ... Saitoh, S. (2002). Germline mosaicism of a novel mutation in lysosome-associated membrane protein-2 deficiency (Danon disease). *Annals of Neurology*, 52(1), 122–125.
- Toib, A., Grange, D. K., Kozel, B. A., Ewald, G. A., White, F. V., & Canter, C. E. (2010). Distinct clinical and histopathological presentations of Danon cardiomyopathy in young women. *Journal of the American College of Cardiology*, 55(4), 408–410.
- Yang, Z., Funke, B. H., Cripe, L. H., Vick, G. W., 3rd, Mancini-Dinardo, D., Pena, L. S., ... Vatta, M. (2010). *LAMP2* microdeletions in patients with Danon disease. *Circulation. Cardiovascular Genetics*, 3(2), 129–137.

SUPPORTING INFORMATION

Additional supporting information may be found online in the Supporting Information section at the end of the article.

How to cite this article: Majer F, Piheroval L, Reboun M, et al. *LAMP2* exon-copy number variations in Danon disease heterozygote female probands: Infrequent or underdetected? *Am J Med Genet Part A*. 2018;176A:2430–2434. <https://doi.org/10.1002/ajmg.a.40430>

Supporting Materials and Methods

Supp. Table 1

List of primers

Primer pairs for amplification of *LAMP2* isoform coding sequences (CDS) (**mRNA/cDNA** template)

Oligonucleotide name	Sequence (5'-3')	Oligonucleotide size [bp]	Product size in wt [bp]
LAMP2 SalI F	GTCGAC C ATGGTGTGCTTCCGCTCTTC	28	
LAMP2B 1230 BamHI R	GGATCC GC CAGAGTCTGATATCCAGCATAAC	31	1230+15
LAMP2A 1230 BamHI R	GGATCC GC AAATTGCTCATATCCAGCATGA	30	1230+15
LAMP2C 1233 BamHI R	GGATCC GC CACAGACTGATAACAGTACGAC	31	1233+15

Primer pairs for *LAMP2* exon dosage quantitative real-time PCR (**genomic DNA** template)

Oligonucleotide name	Sequence (5'-3')	Oligonucleotide size [bp]	Product size [bp]
LAMP2 intron 3 2843 F	GTGTTCCCAAGTGGTCTCT	22	61
LAMP2 intron 3 2903 R	TCTAACACACACTGAGCCTTCC	20	
UPL probe 63	CTCCTCCT	8	
LAMP2 intron 3 5008 F	TGCTTGCTACATGATGGAGAG	21	69
LAMP2 intron 3 5076 R	CAAGAAAGGAAAGTATCCAAGTCT	24	
UPL probe 8	GAAGGCAG	8	
LAMP2 intron 8 988 F	TGATCCTTTAGTAGCTTTATTTTGGG	27	72
LAMP2 intron 8 1059 R	TGGACTTAAAATTAGGGGAATAATGA	26	
UPL probe 36	CTGGCTCC	8	
LAMP2 ATP1B4 2075 F	ATGCCCTTCCCTCCTTATCT	20	75
LAMP2 ATP1B4 2149 R	TTAGCCAGGCGTAGCAAAAAG	20	
UPL probe 41	CTTCAGCC	8	
LAMP2 ATP1B4 2684 F	GCTGAGATCTTGCCACTGC	19	109
LAMP2 ATP1B4 2792 R	ACCCCATAGCTTCACAATTCA	21	
UPL probe 64	CCAGGCTG	8	
LAMP2 ATP1B4 3245 F	GCAGGTGGATCACTTTTAGGC	20	71
LAMP2 ATP1B4 3315 R	TTTGTGGAGATAGGGTCTTGC	21	
UPL probe 61	CTGGGCAA	8	
LAMP2 ATP1B4 4638 F	ACAGGCTTGGTACAGAGTCCA	21	67
LAMP2 ATP1B4 4704 R	GGCTCAACTGTAGAAGTAATGG	23	
UPL probe 50	GCTCCAGA	8	
LAMP2 ATP1B4 7327 F	GGGATGGAGGAAAGATACAGA	21	60
LAMP2 ATP1B4 7386 R	TGTATGTCAGGCGGTTTG	19	
UPL probe 87	CTGCCACC	8	
LAMP2 ATP1B4 17720 F	AGCAGCACAACTCACTAGTGC	20	64
LAMP2 ATP1B4 17783 R	TGGTGGTAAGCATGCACTTC	20	
UPL probe 40	CAGCAGGC	8	
LAMP2 ATP1B4 26176 F	GAACAAAAGAAAGCCTCAAGGTG	22	62
LAMP2 ATP1B4 26237 R	TCAACTTCTTTGGGAGAGATGA	23	
UPL probe 7	CTTCTCCC	8	
LAMP2 ATP1B4 42316 F	TGTTGGGATCAGGGATCTGT	20	67
LAMP2 ATP1B4 42382 R	TTTCTTCTTTCCTTGGAAAGC	21	
UPL probe 30	GGCTGAGG	8	

Primers for genomic DNA deletion breakpoint/junction mapping (**genomic DNA** template) - **the deletion of *LAMP2* exons 4-8** - Family 1

Oligonucleotide name	Sequence (5'-3')	Oligonucleotide size [bp]	Product size [bp]
F1 - LAMP2 intron 3 2722 F	GAGGCTCCAGTGAAGTGTGATC	25	maximum PCR product size
F2 - LAMP2 intron 3 2837 F	GTTCCT GTGTTCCCAAGTGGTCCCT GATTAG	32	was limited by PCR extension
R1 - LAMP2 exon 9B 1230 R	CAGAGTCTGATATCCAGCATAACTTT	21	step to maximum of
R2 - LAMP2 exon 9B 1230 BamHI R	GGATCC T CAGAGTCTGATATCCAGCATAAC	31	~4000 bases

Primers for genomic DNA deletion breakpoint/junction mapping (**genomic DNA** template) - **the deletion of *LAMP2* exons 4-9C** - Family 2

Oligonucleotide name	Sequence (5'-3')	Oligonucleotide size [bp]	Product size [bp]
F - LAMP2 intron 3 5008 F	TGCTTGCTACATGATGGAGAG	21	maximum PCR product size
R1 - LAMP2 ATP1B4 2809 R	TGGATTCTTTGAGACTTACCCCATAGCTTCAC	32	was limited by PCR extension
R2 - LAMP2 ATP1B4 3574 R	TGAAACAGCTATGACCATG AGGTAGGGACTAAGTGTA	38	step to maximum of
R3 - LAMP2 ATP1B4 3783 R	TTTGTGTCTGGTAGCATTTTAGTG	24	~2000 bases
R4 - LAMP2 ATP1B4 4267 R	CTTAGCCAGTTTGAAGATATCTTG	25	
R5 - LAMP2 ATP1B4 4707 R	GGCTCAACTGTAGAAGTAATGGCTCCAATCT	32	
R6 - LAMP2 ATP1B4 4714 R	ATTCTGTTGGCCCTCAACTGTAGAAGTAATG	32	

Primer pairs for detection of breakpoint/junction in the pedigree (**genomic DNA** template) - **the deletion of *LAMP2* exons 4-9C** - Family 2

Preamplification and nested PCR primer pairs

Oligonucleotide name	Sequence (5'-3')	Oligonucleotide size [bp]	Product size [bp]
LAMP2 intron 3 5008 F	TGCTTGCTACATGATGGAGAG	21	1534
LAMP2 ATP1B4 2809 R	TGGATTCTTTGAGACTTACCCCATAGCTTCAC	32	
LAMP2 intron 3 5743 F	GAGCAGAGTTTCTCTCTTCT	21	354
LAMP2 ATP1B4 2364 R	TATTATCTGAACAGCTGACATC	22	

Primers for identification of SNP variability in intron 5 (**genomic DNA** template) - **the deletion of *LAMP2* exons 4-9C** - Family 2

Oligonucleotide name	Sequence (5'-3')	Oligonucleotide size [bp]	Product size [bp]
LAMP2 exon 5 559 F	TTCTGTGTGATTAAGCAAACTTC	26	1676
LAMP2 exon 6 821 R	AGTCTAAGTAGAGCAGTGTGAGAAGC	26	

DNA concentration for all analyses was measured using a NanoDrop (ThermoScientific, USA) at 260 nm.

Next generation sequencing (NGS) – LAMP2 exon copy number analyses

Genomic DNA (II.1^{F1}) was isolated from whole blood using FlexiGene® DNA AGF3000 Kit (QIAGEN, Germany) on the AutoGen Flex 3000 (Autogen, Holliston, USA) according to the manufacturer's instructions.

TruSight Cardio gene enrichment kit was used for DNA library preparation (Illumina, San Diego, USA; 174 genes). DNA library preparation was performed according to the manufacturer's instructions. DNA libraries were sequenced by NGS with paired-ends reads (2x150bp cycles) on the MiSeq platform (Illumina, San Diego). Copy-number variant analysis was performed using the GenesearchNGS (PhenoSystems®, Switzerland) software.

For NGS in II.1^{F2}, the sequencing libraries were constructed using the Nextera DNA Library Preparation Kit according to the manufacturer's instructions. Libraries were combined into pools of twelve for the solution phase of the hybridization using the Illumina TruSight Cardiomyopathy Enrichment Kit (Illumina, San Diego, CA, USA).

Sequencing was performed using the Illumina MiSeq instrument and version 3 sequencing reagents to generate 250 bp paired-end reads. Sequence data were aligned to the human reference genome (hg19) in Novoalign software (v.2.08.02). Resulting SAM files were coordinate sorted and PCR duplicates were removed in Samtools package (v. 1.2) (Li et al., 2009).

Normalized read depth coverages for each target (exon) were calculated using the CalculateHSMetrics tool from Picard suite (v1.99; <http://broadinstitute.github.io/picard/>) and used to obtain the patient/male control ratios reflecting the variations in the copy number of individual exons.

Supp. Table 2

LAMP2 exon 2 SNP (rs12097) in II.1^{F2}

PCR or RT-PCR products targeting the *LAMP2* exon 2 that contains the rs12097 SNP were analyzed. gDNA or cDNA was obtained from WBCs of II.1^{F2}. The final concentration of DNA in samples was 10 ng/μl.

Sequencing was performed using the NexteraXT kit and the MiSeq reagent kit v2 (2x250), respectively. Paired-end sequence reads were generated using the MiSeq platform (Illumina, San Diego, CA). Sequencing data were demultiplexed and trimmed for low quality and duplicates using MiSeq reporter v.2.4. Sequence data were aligned to the human reference genome (hg19) in Bowtie2 (genomic DNA) (Langmead & Salzberg, 2012) or TopHat2 (cDNA) (Kim et al., 2013). The IGV browser was used for the visualization and evaluation of single-nucleotide variants (SNV) (Thorvaldsdottir, Robinson, & Mesirov, 2013).

Colored values (maternal in pink and paternal in blue) represent the % fractions of the total reads that contained the alternative bases of the rs12097 SNP. gDNA results (44.6% - maternal vs. 55.4% - paternal) contrast with those from the mRNA/cDNA template (99.5% - maternal vs. 0.1% - paternal). These results suggest absence of expression of the paternal *LAMP2* allele as a result of eCNV in II.1^{F2}.

The bases are coded according to the sequence of the plus gDNA strand.

II.1^{F2} - <i>LAMP2</i> exon 2 SNP (rs12097)			
gDNA	Total reads:	2048	
			%
	A	1134	55.4
	C	0	0.0
	G	0	0.0
	T	914	44.6
cDNA	Total reads:	18516	
			%
	A	26	0.1
	C	54	0.3
	G	19	0.1
	T	18417	99.5

Supp. Table 3

Family 2 - Testing the presence of the paternal wild-type LAMP2 allele to address the issue of somatic mosaicism in II.1^{F2}

LAMP2 intron 5 is affected by the deletion of exons 4 – 9C in II.1^{F2}. Three informative SNPs were selected in this intron and amplified as part of a 1676bp long PCR product. Paternal (I.1^{F2} – blue) and maternal (I.2^{F2} – pink) PCR products were mixed in various ratios and analyzed using MiSeq (Illumina). The procedure was the same as described in Supp. Table 2. By comparing the data in the mixed samples with those measured in the II.1^{F2} gDNA (bottom section of the Table), we show (with approximate sensitivity of 1%) that the wild-type paternal allele is not present in WBCs of II.1^{F2}. We therefore conclude that the mutation is uniformly present in the proband's (II.1^{F2}) WBCs.

Frequency of the alternative SNP variants is presented as % fractions identified in all the reads.

Family 2 - LAMP2 intron 5 SNPs					
mixing ratio		rs2072067	rs2072068	rs42893	
I.1 ^{F2} I.2 ^{F2}	100% 0%	Total reads: 8604		9302	12029
		A 0.2	A 0.1	A 0.2	
		C 99.6	C 0.0	C 99.7	
		G 0.0	G 99.8	G 0.0	
		T 0.2	T 0.1	T 0.1	
I.1 ^{F2} I.2 ^{F2}	50% 50%	Total reads: 6271		6655	7509
		A 0.2	A 58.5	A 58.7	
		C 42.0	C 0.1	C 41.2	
		G 0.2	G 41.3	G 0.0	
		T 57.6	T 0.1	T 0.0	
I.1 ^{F2} I.2 ^{F2}	20% 80%	Total reads: 10058		10481	10811
		A 0.0	A 80.9	A 80.5	
		C 19.0	C 0.1	C 19.5	
		G 0.1	G 19.0	G 0.0	
		T 80.9	T 0.0	T 0.0	
I.1 ^{F2} I.2 ^{F2}	10% 90%	Total reads: 10930		11598	12258
		A 0.0	A 91.8	A 91.5	
		C 8.0	C 0.1	C 8.5	
		G 0.1	G 8.0	G 0.0	
		T 91.8	T 0.1	T 0.0	
I.1 ^{F2} I.2 ^{F2}	5% 95%	Total reads: 12342		12960	13788
		A 0.1	A 96.0	A 95.5	
		C 4.0	C 0.1	C 4.5	
		G 0.1	G 3.9	G 0.0	
		T 95.9	T 0.0	T 0.0	
I.1 ^{F2} I.2 ^{F2}	3% 97%	Total reads: 6333		6787	8251
		A 0.1	A 96.9	A 97.2	
		C 3.0	C 0.2	C 2.7	
		G 0.1	G 2.9	G 0.0	
		T 96.8	T 0.0	T 0.0	
I.1 ^{F2} I.2 ^{F2}	2% 98%	Total reads: 11484		12008	13314
		A 0.1	A 98.2	A 98.2	
		C 1.7	C 0.1	C 1.6	
		G 0.3	G 1.6	G 0.0	
		T 97.9	T 0.1	T 0.1	
I.1 ^{F2} I.2 ^{F2}	1% 99%	Total reads: 10476		10924	11536
		A 0.1	A 99.1	A 99.1	
		C 0.7	C 0.1	C 0.9	
		G 0.1	G 0.8	G 0.0	
		T 99.1	T 0.0	T 0.0	
I.1 ^{F2} I.2 ^{F2}	0% 100%	Total reads: 14764		15402	15926
		A 0.0	A 99.9	A 99.9	
		C 0.1	C 0.1	C 0.1	
		G 0.1	G 0.0	G 0.0	
		T 99.8	T 0.0	T 0.0	
proband II.1 ^{F2}	100%	Total reads: 8740		9172	10200
		A 0.0	A 99.9	A 99.9	
		C 0.0	C 0.1	C 0.1	
		G 0.1	G 0.0	G 0.0	
		T 99.8	T 0.0	T 0.0	

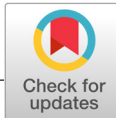
References

Kim, D., Pertea, G., Trapnell, C., Pimentel, H., Kelley, R., & Salzberg, S. L. (2013). TopHat2: accurate alignment of transcriptomes in the presence of insertions, deletions and gene fusions. *Genome Biol*, *14*(4), R36.

Langmead, B., & Salzberg, S. L. (2012). Fast gapped-read alignment with Bowtie 2. *Nat Methods*, *9*(4), 357-359.

Li, H., Handsaker, B., Wysoker, A., Fennell, T., Ruan, J., Homer, N., . . . Genome Project Data Processing, S. (2009). The Sequence Alignment/Map format and SAMtools. *Bioinformatics*, *25*(16), 2078-2079.


Thorvaldsdottir, H., Robinson, J. T., & Mesirov, J. P. (2013). Integrative Genomics Viewer (IGV): high-performance genomics data visualization and exploration. *Brief Bioinform*, *14*(2), 178-192.



CLINICAL REPORT

Příloha: 5

Alu-mediated *Xq24* deletion encompassing *CUL4B*, *LAMP2*, *ATP1B4*, *TMEM255A*, and *ZBTB33* genes causes Danon disease in a female patient

Filip Majer¹ | Bohdan Kousal^{1,2} | Petr Dusek^{3,4} | Lenka Piherova¹ |
 Martin Reboun¹ | Romana Mihalova⁵ | Jiri Gurka⁶ | Alice Krebsova⁶ |
 Hana Vlaskova¹ | Lenka Dvorakova¹ | Jana Krihova⁷ | Petra Liskova^{1,2} |
 Stanislav Kmoch¹ | Tomas Kalina⁸ | Milos Kubanek⁶ | Jakub Sikora^{1,9} 

¹Research Unit for Rare Diseases, Department of Pediatrics and Adolescent Medicine, 1st Faculty of Medicine, Charles University and General University Hospital, Prague, Czech Republic

²Department of Ophthalmology, 1st Faculty of Medicine, Charles University and General University Hospital, Prague, Czech Republic

³Department of Neurology and Center of Clinical Neuroscience, 1st Faculty of Medicine, Charles University and General University Hospital, Prague, Czech Republic

⁴Department of Radiology, 1st Faculty of Medicine, Charles University and General University Hospital, Prague, Czech Republic

⁵Institute of Biology and Medical Genetics, 1st Faculty of Medicine, Charles University and General University Hospital, Prague, Czech Republic

⁶Department of Cardiology, Institute for Clinical and Experimental Medicine, Prague, Czech Republic

⁷Department of Psychology, Thomayer Hospital, Prague, Czech Republic

⁸Department of Paediatric Haematology and Oncology, Childhood Leukaemia Investigation Prague, 2nd Faculty of Medicine, Charles University and University Hospital Motol, Prague, Czech Republic

⁹Institute of Pathology, 1st Faculty of Medicine, Charles University and General University Hospital, Prague, Czech Republic

Correspondence

Jakub Sikora, Research Unit for Rare Diseases, Department of Pediatrics and Adolescent Medicine, 1st Faculty of Medicine, Charles University and General University Hospital, Ke Karlovu 2, 128 00 Prague 2, Czech Republic. Email: jakub.sikora@lf1.cuni.cz

Funding information

Magistrát hlavního města Prahy, Česká Republika, Grant/Award Number: CZ.2.16/3.1.00/24505; Ministerstvo Školství, Mládeže a Tělovýchovy České Republiky, Grant/Award Numbers: NCMG LM2015091, LO1604; Ministerstvo Zdravotnictví České Republiky, Grant/Award Numbers: AZV-MZ ČR 15-27682A, NV19-08-00122, RVO-VFN 64165/2012, VZ IKEM (00023001); Univerzita Karlova v Praze, Grant/Award Numbers: PROGRESS Q25, PROGRESS Q26, SVV UK 260367/2017, UNCE 204064

Abstract

Cullin 4B (*CUL4B*), lysosomal-associated membrane protein Type 2 (*LAMP2*), *ATP1B4*, *TMEM255A*, and *ZBTB33* are neighboring genes on *Xq24*. Mutations in *CUL4B* result in Cabezas syndrome (CS). Male CS patients present with dysmorphic, neuropsychiatric, genitourinary, and endocrine abnormalities. Heterozygous CS females are clinically asymptomatic. *LAMP2* mutations cause Danon disease (DD). Cardiomyopathy is a dominant feature of DD present in both males and heterozygous females. No monogenic phenotypes have been associated with mutations in *ATP1B4*, *TMEM255A*, and *ZBTB33* genes. To facilitate diagnostics and counseling in CS and DD families, we present a female DD patient with a de novo *Alu*-mediated *Xq24* rearrangement causing a deletion encompassing *CUL4B*, *LAMP2*, and also the other three neighboring genes. Typical to females heterozygous for *CUL4B* mutations, the patient was CS asymptomatic, however, presented with extremely skewed X-chromosome inactivation (XCI) ratios in peripheral white blood cells. As a result of the likely selection against *CUL4B* deficient clones, only minimal populations (~3%) of *LAMP2* deficient leukocytes were identified by flow cytometry. On the contrary, myocardial *LAMP2* protein expression suggested random XCI. We demonstrate that contiguous *CUL4B* and *LAMP2* loss-of-function

copy number variations occur and speculate that male patients carrying similar defects could present with features of both CS and DD.

KEYWORDS

Cabezas syndrome, cullin 4B, Danon disease, female heterozygotes, lysosomal-associated membrane protein 2

1 | INTRODUCTION

Cullin 4B (*CUL4B*), lysosomal-associated membrane protein type 2 (*LAMP2*), ATPase Na⁺/K⁺ transporting family member beta 4 (*ATP1B4*), transmembrane protein 255A (*TMEM255A*), and KAISO (*ZBTB33*) are neighboring genes that occupy ~300 kb of *Xq24*.

Cabezas syndrome (CS, MIM #300354) is caused by mutations in *CUL4B* (Tarpey et al., 2007; Zou et al., 2007). Male CS patients express developmental, neuropsychiatric, genitourinary, endocrine, and dysmorphic symptoms. Females heterozygous for *CUL4B* mutations are clinically asymptomatic but skewed ratios of X-chromosome inactivation (XCI) in their peripheral blood suggest a selection against *CUL4B* deficient leukocyte clones (Ravn, Lindquist, Nielsen, Dahm, & Tumer, 2012; Zou et al., 2007).

Danon disease (DD, MIM #300257) results from mutations in *LAMP2*. DD is characterized by cognitive deficit, cardiomyopathy, and myopathy in male patients while delayed progression and cardiomyopathy dominate in heterozygous females (Brambatti et al., 2019).

No monogenic clinical phenotypes have been linked to variants in *ATP1B4*, *TMEM255A*, and *ZBTB33* genes.

Loss-of-function copy number variations (CNVs) in either *CUL4B* or *LAMP2* were reported in CS and DD families, respectively (Brambatti et al., 2019; Isidor, Pichon, Baron, David, & Le Caignec, 2010; Ravn et al., 2012). Despite their proximity, a simultaneous deficiency of the two genes has not yet been documented (Isidor et al., 2010).

To demonstrate the pitfalls of diagnostic assessment and facilitate counseling in CS and DD families, we present clinical, tissue and molecular findings in a female DD patient who carried a unique de novo *Alu*-mediated *Xq24* rearrangement causing a deletion encompassing *CUL4B*, *LAMP2*, *ATP1B4*, *TMEM255A*, and *ZBTB33* genes.

2 | CLINICAL REPORT

Aged 25 years, the proband (II.1) was diagnosed with dilated cardiomyopathy and severe bilateral heart failure. The left ventricle (LV) had normal wall thickness by echocardiography. LV ejection fraction was 20%. Moderate mitral and tricuspid valve regurgitation were also detected. A pulsatile biventricular assist device was implanted after 10 months of pharmacological treatment due to refractory cardiogenic shock with liver and kidney failure. Heart transplantation was performed 3 months later. Reevaluation (at the age of 36 years) of the

proband's pretransplantation electrocardiograph identified discrete delta waves in lateral leads (Figure S1a).

The Wechsler Adult Intelligence Scale-III test in the proband (performed at the age of 37 years) suggested mild mental retardation (verbal IQ—66, performance IQ—68, full-scale IQ—64), with verbal scores worse than performance subtest scores (see Supporting Materials and Methods for index and subtest scores). No additional psychiatric abnormalities were identified by the evaluation of anamnestic data.

No abnormalities were found by neurological examination and brain MRI (Figure S1b-e).

The patient has no subjective visual complaints. Best-corrected visual acuity is 1.0 in both eyes. Fundus examination in dilatation revealed salt and pepper retinopathy (Figure S2a-d), altered autofluorescence distribution that spared the foveal and parafoveal zones (Figure S2e,f) and mild visual field defects (Figure S2g,h). High-resolution spectral-domain optical coherence tomography detected deposits in the retinal pigment epithelium/Bruch's membrane layer and hyper-reflective foci in the outer nuclear layer. OCT angiography revealed normal retinal vasculature (Figure S2k,l). The hyperreflective signal was noted in the avascular central zone (Figure S2m,n) by automated segmentation. Retinal nerve fiber layer thickness of the right and left eye was normal (Figure S2o,p). The patient has a normal perception of colors, but her contrast sensitivity is bilaterally decreased to 1.20.

The cardiologic examination was normal in the proband's mother and brother. The father has mild hypertrophy (13 mm) of the interventricular septum as a likely consequence of arterial hypertension.

3 | MATERIALS AND METHODS

3.1 | Editorial policies and ethical considerations

The study was approved by the Ethics Committee of the authors' home institution. Informed consent (also approved by the Ethics Committee of the authors' home institution) for presentation of the results was obtained from all participants.

Standard laboratory protocol based on *LAMP2* protein assessment and molecular genetic studies (Majer et al., 2014; Majer et al., 2018; Sikora, Majer, & Kalina, 2015) confirmed DD in the clinically highly suspect proband (II.1, Figure 1a). Multicolor flow cytometry (FC) of the lysosomal-associated membrane protein Type 1 (*LAMP1*) and *LAMP2*, PCR and sequence analyses of the coding gDNA and full-length *LAMP2* mRNA/cDNAs, quantitative PCR (qPCR) *LAMP2* exon-copy number testing, and XCI HUMARA assay were performed in

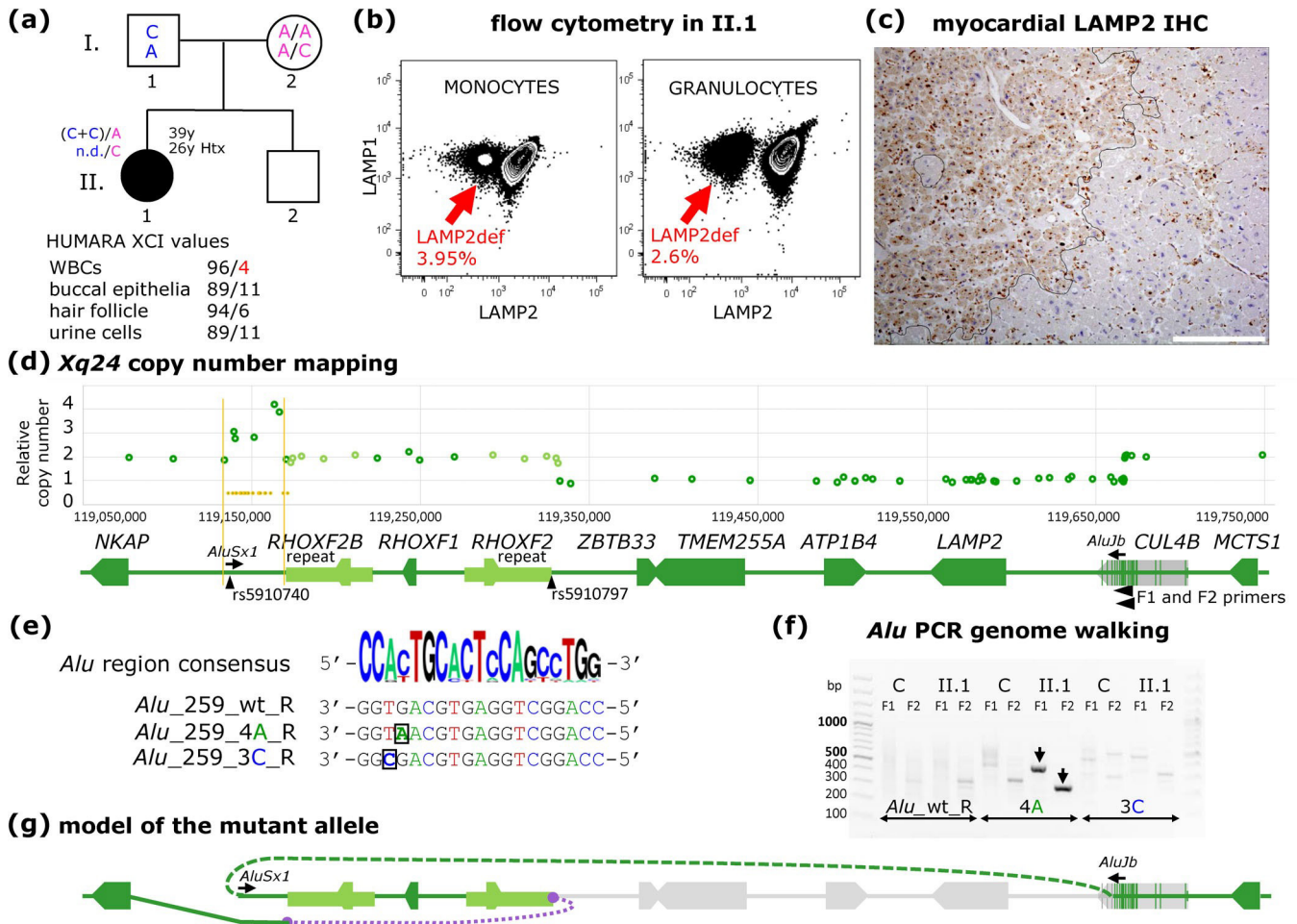


FIGURE 1 (a) Family pedigree. Current age and age at heart transplantation (Htx) are shown for II.1. Two SNPs (rs5910740 and rs5910797—positions are highlighted in Figure 1d and Figure S7) helped to identify, which of the parental alleles was affected by the rearrangement in the proband. The genetic setup of rs5910740 (upper) and rs5910797 (lower) is color-coded in both parents and the proband. rs5910740 localizes to a region with relative copy number 3 (Figure 1d). Paternal variant of rs5910797 was not detected (n.d.) in the proband (see also Figure S7). XCI ratios were assessed by the HUMARA assay. (b) FC dot plots show LAMP2^{def} monocytes and granulocytes (red arrows) with normal presence of LAMP1 in II.1. (c) representative image of the mosaic LAMP2 expression (brown signal) in the patient's myocardium of the interventricular septum (borderline of LAMP2^{def} and LAMP⁺ patches is highlighted, for further details see Figure S3), scale bar = 200 μ m. (d) qPCR relative copy number values (green circles) in the critical Xq24 region. Alu elements in the region with abnormally increased copy number values 3 and 4 are highlighted in orange. Black arrowheads indicate the position and orientation of the forward (F1 and F2) Alu PCR genome walking primers used to map the CUL4B breakpoint/junction site. Positions and orientation of AluJb and AluSx1 elements are shown by arrows. (e) Sequences of Alu elements in the Xq24 region with the copy number 3 or 4 were aligned (Figure S5) and three reverse primers for Alu PCR genome walking were designed. Alu_259_wt_R aligned to the most abundant and conserved part of the Alu sequence. Alu_259_4A_R and Alu_259_3C_R aligned to the most frequent 3^o Alu variants. (f) Agarose gel of Alu PCR genome walking reactions. Specific products (black arrows) were gained only with the Alu_259_4A_R primer (4A). The size difference (~177 bp), corresponds to the difference in position of primers F1 and F2 (Figure S6 shows the breakpoint junction sequence in detail). C—control sample. (g) A model of the complex rearrangement at the mutant allele. The orientation of the AluSx1 element that participates in the CUL4B breakpoint junction highlights the presumed inversion of the RHOXF gene cluster. Violet dotted line marks the breakpoint junction that was not characterized [Color figure can be viewed at wileyonlinelibrary.com]

peripheral white blood cells (WBCs) as previously described (Majer et al., 2012, 2014). Primers used for all the PCR-based analyses are listed in Table S1. Cytogenetic analyses of peripheral blood samples followed standard protocols (Verma & Babu, 1995).

Quantification of the ratio of LAMP2⁺ and LAMP2^{def} cardiomyocytes was performed on immunohistochemically (IHC) stained sections from the formalin-fixed and paraffin-embedded explanted heart. For additional details see Supporting Materials and Methods.

4 | RESULTS

4.1 | FC, XCI analyses, and myocardial (immuno) histopathology

FC detected small but distinct populations of LAMP2^{def} monocytes (~4%) and granulocytes (~3%) in the proband (Figure 1b). This corresponded with XCI ratios assessed by HUMARA (Figure 1a). HUMARA also showed that the inactive androgen receptor allele was of paternal origin.

Myocardial histopathology showed patchy hypertrophy and vacuolization of cardiomyocytes and fibrosis (Figure S3a,b). LAMP2 expression in cardiomyocytes was mosaic (Figure 1c) by IHC. The cell counts of the LAMP2^{def} and LAMP2⁺ cardiomyocytes were comparable (Figure 1c, Supplementary Materials and Methods and Figure S3c–f).

4.2 | LAMP2 molecular studies

Profile and sequence of the three full-length *LAMP2* isoform mRNAs/cDNAs were normal in the proband (Figure S4). gDNA qPCR analyses identified ~300 kb long *Xq24* region with abnormally reduced relative copy number (1 instead of 2). The deletion started in *CUL4B* intron 19 (see Figure S6 for details) and encompassed the distal part of *CUL4B* (including exons 20–22 that code the last 140 amino acids of the protein and also the 3' untranslated sequences with poly(A) sites), and the entire *LAMP2*, *ATP1B4*, *TMEM255A*, and *ZBTB33* genes. Five qPCR probes downstream of the *RHOXF2/RHOXF1/RHOXF2* homeobox gene cluster showed abnormally increased copy number values of 3 or 4 (Figure 1d). *Alu* PCR genome walking method was used to characterize the *CUL4B* breakpoint/junction site (Figure 1e,f). We identified residual sequences of *AluJb* (strand-) from intron 19 of *CUL4B* and *AluSx1* (strand+) (Figure S6) from the *Xq24* region with relative copy numbers of 3 and 4 (Figure 1d). G-banded chromosome analysis identified a normal female (46, XX) karyotype. Genotyping of two *Xq24* single nucleotide polymorphisms (SNPs; rs5910740 and rs5910797) in the proband and her parents (Figure 1a, Figure S7, and Table S1) suggested that the *Xq24* rearrangement affected the proband's paternal allele. The mutation-specific sequences were not identified in WBCs of either parent or the father's sperm (Figure S8).

5 | DISCUSSION

We present clinical findings and results of laboratory analyses in a female proband with a unique complex de novo *Xq24* rearrangement (Figure 1g) that caused a deletion impacting the distal part of *CUL4B* and the complete sequences of *LAMP2*, *ATP1B4*, *TMEM255A*, and *ZBTB33* genes.

The ophthalmic symptoms, myocardial histopathology, and mosaic LAMP2 expression corresponded to findings in DD female patients (Brambatti et al., 2019). In contrast to the latter study, however, the patient reached the end-stage heart failure more than 10 years earlier than DD females presenting with dilated cardiomyopathy.

Instability (and most probably also decay) of the putative *CUL4B* transcript is expected in the proband. Any truncated *CUL4B* protein (773 instead of 914 amino acids in length) would also likely not be stable, not complex with its partners, and fail the ubiquitination function (see Figure S9). Similar to other *CUL4B* female heterozygotes, our patient was asymptomatic in nonpsychiatric clinical domains that are usually impacted in male CS patients (Tarpey et al., 2007; Zou et al., 2007). Her mild mental retardation could be caused by the pathogenic effects of both *LAMP2* and *CUL4B* mutations. However, the

contribution of the pathogenic variants in either of the two genes to this particular phenotype is impossible to establish.

An additional finding typical for female CS heterozygotes, XCI ratios were extremely skewed (presumably due to selection against *CUL4B* deficient cellular clones) in several of the proband's tissues including peripheral blood (Zou et al., 2007). This phenomenon was reflected by minimal but distinct LAMP2^{def} populations of peripheral WBCs. On the contrary, the fraction of LAMP2^{def} cardiomyocytes was comparable to the number of cardiomyocytes that expressed LAMP2 normally. This tissue-specific discrepancy suggests that the selection may not be universal to all cell types/tissues. Interestingly, a similar phenomenon was suggested in heterozygous female *Cul4b* knock-out mice (Jiang et al., 2012).

Little is known about the function of the three other deleted genes (*ATP1B4*, *TMEM255A*, and *ZBTB33*). *ATP1B4* is a muscle-specific protein of the inner nuclear envelope (Zhao, Pestov, Korneenko, Shakhparonov, & Modyanov, 2004), *TMEM255A* is a predicted transmembrane protein (UniProtKB), and *ZBTB33* (KAISO) is a zinc-finger containing transcriptional factor involved in cell cycle regulation and cancer progression (Schackmann, Tenhagen, van de Ven, & Derksen, 2013). Variants in these three genes have not been associated with any defined human genetic phenotype. Contribution of their reduced copy number to the proband's phenotype is thus speculative.

As repetitive elements often contribute to *LAMP2* CNVs (Majer et al., 2018), we used the *Alu* PCR genome walking technique and identified residual *AluJb* and *AluSx1* sequences in the breakpoint junction (Figure 1e and Figures S5 and S6). Detailed analysis of this junctional sequence suggested an inversion of the *RHOXF2/RHOXF1/RHOXF2* homeobox cluster as part of the complex *Xq24* rearrangement. The full characterization of the other breakpoint(s) (violet dots in Figure 1g) was not completed because of the high content of repetitions in the region.

Overall, our data demonstrate that deletion CNVs contiguously affecting *CUL4B* and *LAMP2* occur. In reference to findings in the presented proband, the clinical phenotype in heterozygous females with similar genetic setup is expected to be dominated by cardiac DD symptoms. The values of XCI ratios in WBCs and quantitation of the LAMP2^{def} leukocyte populations in these patients should, however, be interpreted cautiously, because the results of these tests may be impacted by the (likely tissue-specific) effects of the *CUL4B* mutation. In male patients, on the contrary, a contiguous *CUL4B* and *LAMP2* loss-of-function CNV could result in a phenotype combining symptoms of CS and DD.

ACKNOWLEDGMENTS

This project was supported by the research Grants AZV-MZ ČR 15-27682A, NV19-08-00122 and institutionally funded by VZ IKEM (00023001), NPU I No. LO1604, CZ.2.16/3.1.00/24505, RVO-VFN 64165/2012, NCMG LM2015091, UNCE 204064, SVV UK 260367/2017, and PROGRESS Q26 and Q25 projects.

CONFLICT OF INTEREST

The authors have no conflict of interest.

DATA AVAILABILITY STATEMENT

The data that support the findings of this study are available on request from the corresponding author. The data are not publicly available due to privacy or ethical restrictions.

ORCID

Jakub Sikora  <https://orcid.org/0000-0003-4104-2023>

REFERENCES

- Brambatti, M., Caspi, O., Maolo, A., Koshi, E., Greenberg, B., Taylor, M. R. G., & Adler, E. D. (2019). Danon disease: Gender differences in presentation and outcomes. *International Journal of Cardiology*, 286, 92–98.
- Isidor, B., Pichon, O., Baron, S., David, A., & Le Caignec, C. (2010). Deletion of the CUL4B gene in a boy with mental retardation, minor facial anomalies, short stature, hypogonadism, and ataxia. *American Journal of Medical Genetics, Part A*, 152A(1), 175–180.
- Jiang, B., Zhao, W., Yuan, J., Qian, Y., Sun, W., Zou, Y., ... Gong, Y. (2012). Lack of Cul4b, an E3 ubiquitin ligase component, leads to embryonic lethality and abnormal placental development. *PLoS One*, 7(5), e37070.
- Majer, F., Pelak, O., Kalina, T., Vlaskova, H., Dvorakova, L., Honzik, T., ... Sikora, J. (2014). Mosaic tissue distribution of the tandem duplication of LAMP2 exons 4 and 5 demonstrates the limits of Danon disease cellular and molecular diagnostics. *Journal of Inherited Metabolic Disease*, 37(1), 117–124.
- Majer, F., Piherovala, L., Reboun, M., Stara, V., Pelak, O., Norambuena, P., ... Sikora, J. (2018). LAMP2 exon-copy number variations in Danon disease heterozygote female probands: Infrequent or underdetected? *American Journal of Medical Genetics, Part A*, 176(11), 2430–2434.
- Majer, F., Vlaskova, H., Krol, L., Kalina, T., Kubanek, M., Stolnaya, L., ... Sikora, J. (2012). Danon disease: A focus on processing of the novel LAMP2 mutation and comments on the beneficial use of peripheral white blood cells in the diagnosis of LAMP2 deficiency. *Gene*, 498(2), 183–195.
- Ravn, K., Lindquist, S. G., Nielsen, K., Dahm, T. L., & Tumer, Z. (2012). Deletion of CUL4B leads to concordant phenotype in a monozygotic twin pair. *Clinical Genetics*, 82(3), 292–294.
- Schackmann, R. C., Tenhagen, M., van de Ven, R. A., & Derksen, P. W. (2013). p120-catenin in cancer - Mechanisms, models and opportunities for intervention. *Journal of Cell Science*, 126(Pt 16), 3515–3525.
- Sikora, J., Majer, F., & Kalina, T. (2015). LAMP2 flow cytometry in peripheral white blood cells is an established method that facilitates identification of heterozygous Danon disease female patients and mosaic mutation carriers. *Journal of Cardiology*, 66(1), 88–89.
- Tarpey, P. S., Raymond, F. L., O'Meara, S., Edkins, S., Teague, J., Butler, A., ... Partington, M. (2007). Mutations in CUL4B, which encodes a ubiquitin E3 ligase subunit, cause an X-linked mental retardation syndrome associated with aggressive outbursts, seizures, relative macrocephaly, central obesity, hypogonadism, pes cavus, and tremor. *American Journal of Human Genetics*, 80(2), 345–352.
- UniProtKB. <https://www.uniprot.org/uniprot/Q5JRV8>.
- Verma, R., & Babu, A. (1995). *Human chromosomes: Principles & techniques* (2nd ed.). New York: McGraw-Hill, Inc.
- Zhao, H., Pestov, N. B., Korneenko, T. V., Shakhparonov, M. I., & Modyanov, N. N. (2004). Accumulation of beta (m), a structural member of X,K-ATPase beta-subunit family, in nuclear envelopes of perinatal myocytes. *American Journal of Physiology Cell Physiology*, 286(4), C757–C767.
- Zou, Y., Liu, Q., Chen, B., Zhang, X., Guo, C., Zhou, H., ... Gong, Y. (2007). Mutation in CUL4B, which encodes a member of cullin-RING ubiquitin ligase complex, causes X-linked mental retardation. *American Journal of Human Genetics*, 80(3), 561–566.

SUPPORTING INFORMATION

Additional supporting information may be found online in the Supporting Information section at the end of this article.

How to cite this article: Majer F, Kousal B, Dusek P, et al. *Alu-mediated Xq24 deletion encompassing CUL4B, LAMP2, ATP1B4, TMEM255A, and ZBTB33 genes causes Danon disease in a female patient. Am J Med Genet Part A*. 2020; 182A:219–223. <https://doi.org/10.1002/ajmg.a.61416>

Supporting Materials and Methods

Wechsler Adult Intelligence Scale-III test results

verbal IQ – 66, performance IQ – 68, full scale IQ – 64
verbal comprehension index – 62, perceptual organization index – 72, working memory index – 86, processing speed index – 80

Subtests (scaled scores):

vocabulary – 2, comprehension – 3, information – 4, picture arrangement – 4, similarities – 5, picture completion – 5, block design – 5, arithmetic – 5, digit symbol-coding – 5, matrix reasoning – 6, symbol search – 8, digit span - 9

Ophthalmic examination

The proband (II.1) underwent complex ocular examination. Measurements of the best corrected visual acuity were performed using the Early Treatment Diabetic Retinopathy Study charts and extrapolated to decimal values. The visual field was examined by standard automated testing of the perimeter (M700, Medmont International, Nunawading, Australia). Color vision discrimination was assessed by the Lanthony D-15 desaturated test (Shoji, Sakurai, Chihara, Nishikawa, & Omae, 2009) and contrast sensitivity with Pelli-Robson charts at 1 meter (Elliott, Sanderson, & Conkey, 1990). Fundus autofluorescence (scan angle 55°) and macular architecture were visualized by high resolution spectral domain optical coherence tomography (SD-OCT; Spectralis, Heidelberg Engineering GmbH, Heidelberg, Germany). OCT angiography was performed (OCT-A; AngioPlex, Carl Zeiss Meditec AG, Jena, Germany) with 8x8 mm field view with scans centered on the macula.

Myocardial histology, immunohistochemistry, and quantification of the LAMP2def and LAMP2+ cardiomyocytes

Histological and immunohistochemical assessment of the patient's explanted heart was performed in formalin fixed and paraffin embedded sections from 1 location of the right ventricle, 4 different locations of the left ventricle, and 1 location from the interventricular septum. The overall size of the stained tissue sections was ~ 770 mm². Tissue processing and staining protocols followed those previously reported (Majer et al., 2012). In brief, sections were stained for histology (H&E, Periodic Acid Schiff base (PAS), diastase treated PAS, and Masson's trichrome) and immunohistochemistry (IHC). Primary rabbit polyclonal anti-LAMP1 and anti-LAMP2 antibodies (kindly provided by Dr. Sven Carlsson, University of Umea, Umea, Sweden) were detected by the species specific Envision+ System-HRP kit (DAKO, Glostrup, Denmark). Quantification of the LAMP2def and LAMP2+ cardiomyocytes (modified from Majer et al. GENE 2012) was performed in LAMP2 IHC stained myocardial tissue sections from the aforementioned six anatomical localizations (*Figure S3*). A minimum of 19 images (129 in total) were acquired from each of the 6 IHC slides using Nikon Eclipse E800 microscope equipped with Plan Fluor 20x (N.A. 0.5) objective (both Nikon, Tokyo, Japan) and Olympus DP70 digital camera (Olympus, Tokyo, Japan). Each image was approximately 430x325 µm in size and had a resolution of 4080x3072 pixels. Single-nucleated cardiomyocytes were marked using Adobe Photoshop CS6 (v.13.0.1, Adobe Systems Inc., San Jose, CA, USA). LAMP2+ and LAMP2def cardiomyocytes were manually counted by two independent observers (JS and JG, *Figure S3*).

Cytogenetic analysis

Chromosome preparations were made from peripheral blood lymphocyte cultures using standard protocols (Verma & Babu, 1995). Karyotype analysis was performed on G-banded metaphases with resolution quality of 550 bphs.

Supporting Figures

Figure S1

Pre-transplantation electrocardiography and brain magnetic resonance imaging in the proband (II.1).

(a) Pre-transplantation electrocardiograph shows sinus rhythm with normal conduction intervals, q wave in leads I, aVL, QS wave in leads V1-V2, delta waves (arrows) in the lateral leads (V5-V6) and nonspecific abnormalities of repolarization. (b) sagittal and (c) axial T1-weighted image acquired using parameters TE = 4.4 ms, TR = 2300 ms. (d) axial and (e) coronal T2-weighted image acquired using parameters TE = 99 ms, TR = 4400 ms; brain MRI was performed using a 3T whole body system (Siemens Trio, Siemens Healthcare, Erlangen, Germany). No signs of parenchymal atrophy or signal abnormalities were detected.

Abbreviations: TE – echo time, TR – repetition time.

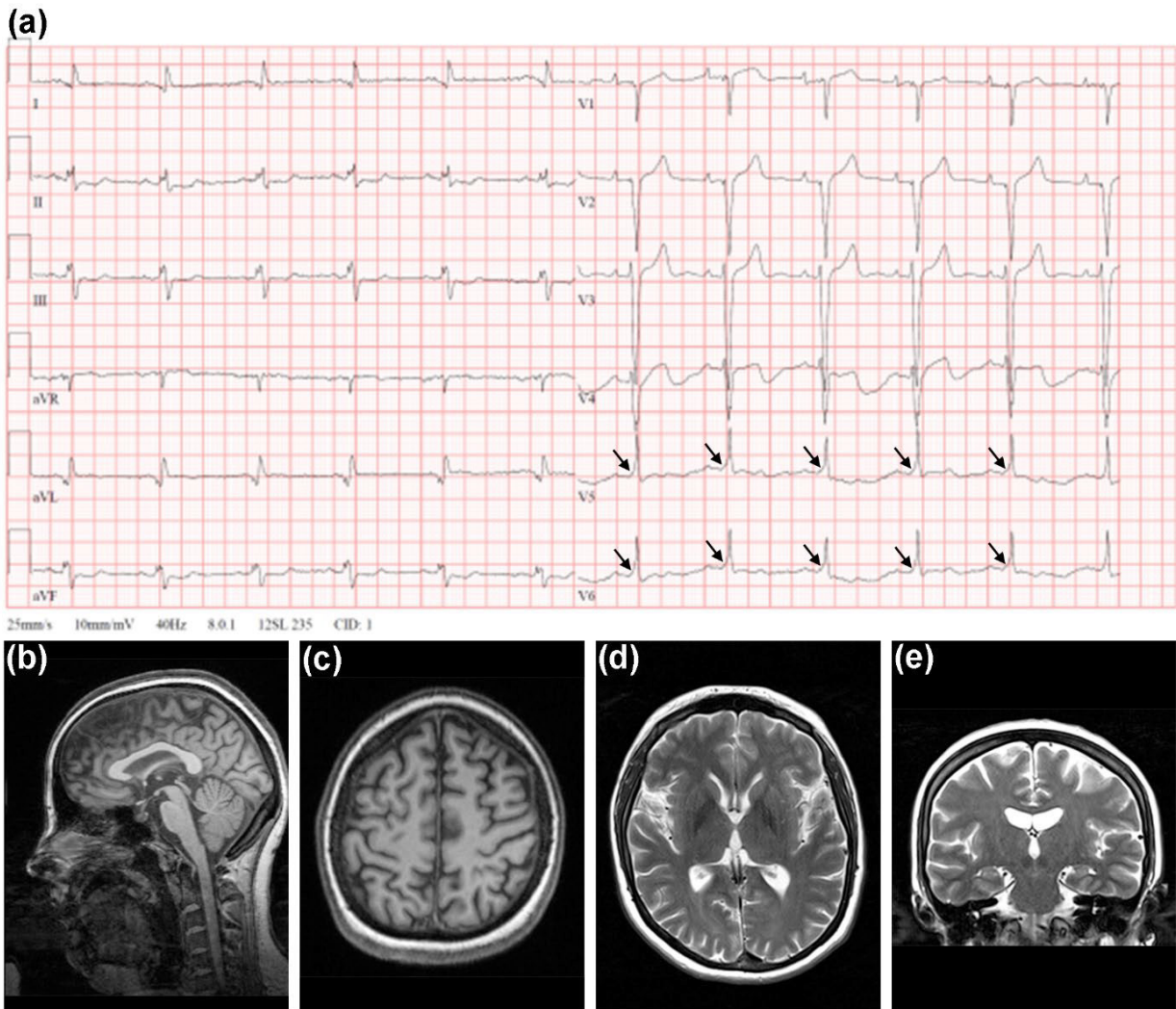


Figure S2

Ocular imaging in the proband (II.1).

Fundus photographs of the right **(a)** and left **(b)** eye, details of the retinal periphery of the right **(c)** and left **(d)** eye, fundus autofluorescence of the right **(e)** and left **(f)** eye. Note that the pigmentary retinopathy with the corresponding autofluorescence imaging abnormalities can be detected predominantly in the periphery of the fundus. Visual field (50°) of the right **(g)** and left **(h)** eye show mild diffuse loss of retinal sensitivity. SD-OCT images of the right **(i)** and left **(j)** eye demonstrate hyper-reflective areas in the inner photoreceptor layer (asterisks) and small hyper-reflective deposits (arrows) at the interface of the retinal pigment epithelium and the photoreceptor layer. OCT-A is shown as full depth color encoded image of the right **(k)** and left **(l)** eye. OCT-A of the avascular retinal layer of the right **(m)** and left **(n)** maps the vasculature between outer plexiform layer and retinal pigment epithelium. Retinal nerve fiber layer thickness of the right **(o)** and left **(p)** eye was normal.

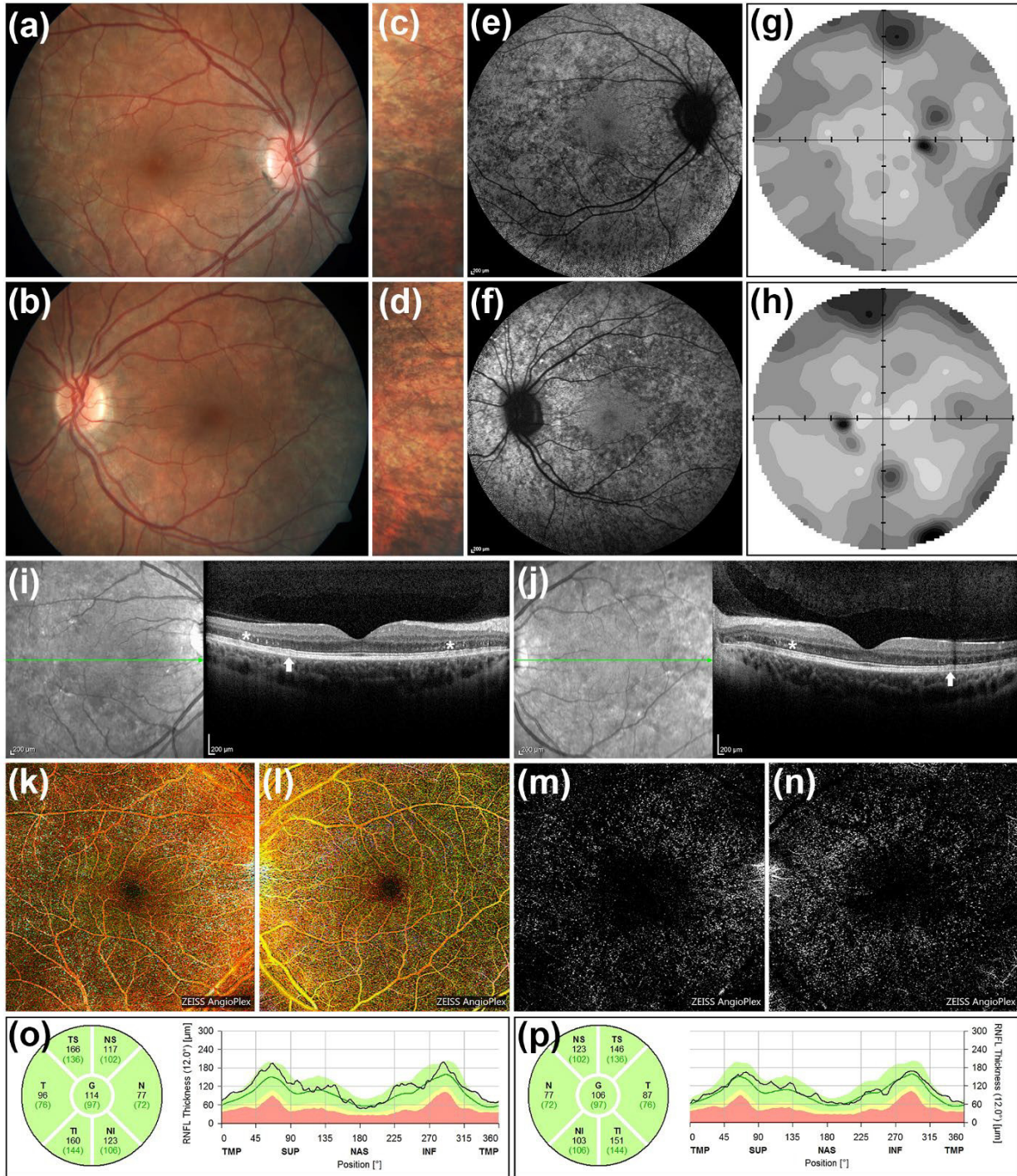


Figure S3

Myocardial histopathology, quantification of LAMP2^{def} and LAMP2⁺ cardiomyocytes in IHC stained tissue sections.

(a) Masson's trichrome staining shows patchy hypertrophy and cytoplasmic vacuolization of cardiomyocytes. Fibrosis stains blue. **(b)** Higher magnification detail (the image corresponds to the area outlined by the black rectangle in (a) of hypertrophy and vacuolization of cardiomyocytes). **(c-e)** Selected images of the IHC-stained myocardium of the interventricular septum demonstrate the variability of the mosaic LAMP2 expression in the cardiomyocytes. The numbers (10, 66, and 100%) represent the approximate size of the population of LAMP2^{def} cardiomyocytes in each particular image. Note that the interstitial cells (fibroblasts, vascular smooth muscle cells, endothelial cells, and other) are mostly LAMP2⁺. **(f)** Quantification of LAMP2^{def} cardiomyocytes in tissue sections from the individual anatomical locations - % fractions are shown. The number (n) of cardiomyocytes evaluated in each slide (and all together) are listed in the x axis legend. Values provided by both observers performing the analyses are compared. LV – left ventricle, RV – right ventricle, LCA – left coronary artery, RIA – *ramus interventricularis anterior*/anterior interventricular branch of LCA.

Scale bars in **a-e** = 200 μ m

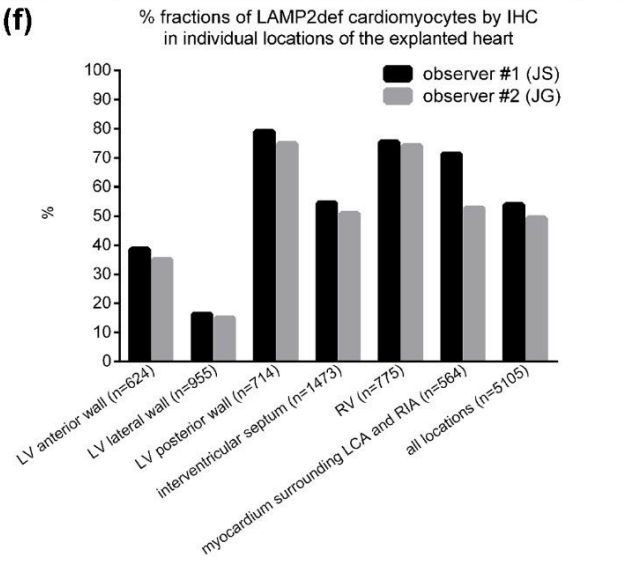
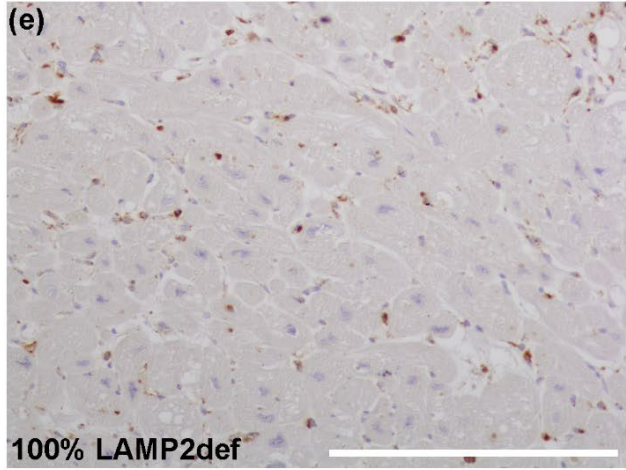
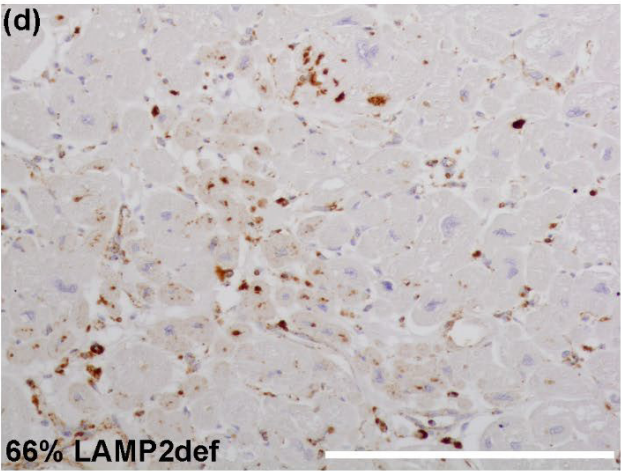
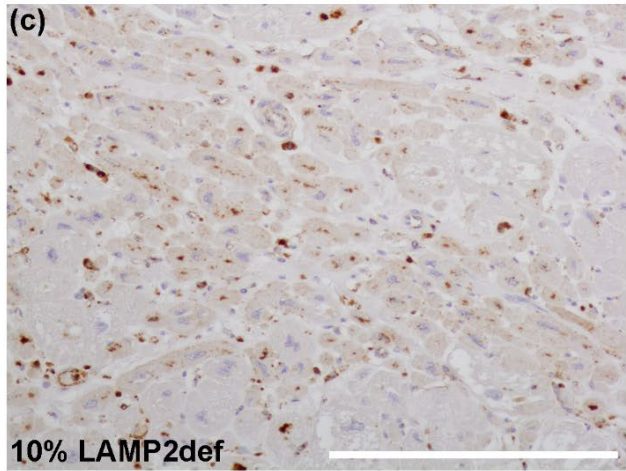
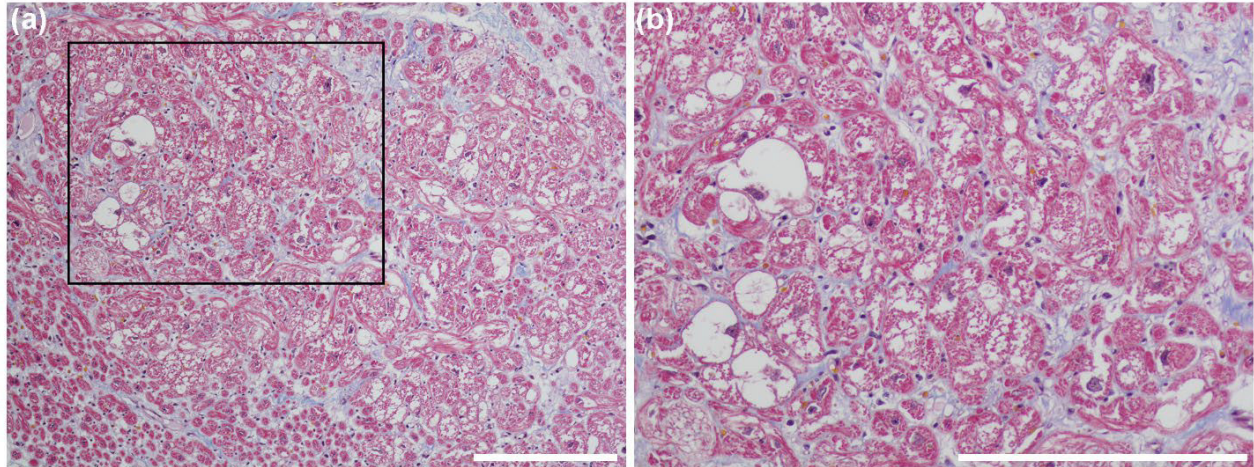


Figure S4

Analysis of the full-length *LAMP2* mRNA/cDNA isoforms in the proband (II.1).

Profile of the full-length *LAMP2* mRNA/cDNA isoforms is normal. All the PCR products were analyzed by direct Sanger sequencing. All PCR products encompass the coding sequence from the START ATG codon to the STOP codons of the three alternative *LAMP2* exons 9 (B, A, and C). Reverse transcription used oligo(dT) primer.

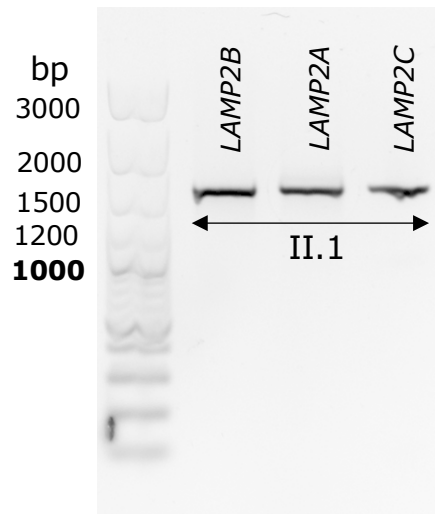


Figure S5

Sequence alignment of *Alu* retrotransposons within the *Xq24* region of the expected breakpoint junction (highlighted in orange in Figure 1d). *Alu* PCR genome walking primers (coding is identical to Figure 1e) are listed below the sequence alignment.

GRCh37 (hg19) assembly	strand	position	<i>Alu</i> sequence 5'→3'
<i>Alu</i> consensus (Price et al. 2004)		(222)	GCAGTGAGCCGAGATGCGCCACTGCCTCCAGCCTGGCGACA-GAGCGAGACTCCGTCTG-----
AluJr4 119135299_119135390	+	(20)	CGCCCCA-CTGCAATGCTCCACTGCCTCCAGCCTGGGAGAAA-AAGAGAGACCTGTACTTTAAA----AA
AluJb 119135408_119135646	+	(226)	GTAGTGAGCTATTT-----
AluJb 119136178_119136260	+	(1)	-----CTATGATGACACCCACTGCCTCCACTCCAGCCTGACTACA-GACTGAGAGCCTAGCTGTAAAAATAAA
AluSx1 119138647_119138945	+	(222)	GCAGTGAGCCATGATGTGTCCTATGGCCTCCAGCCTGGCAATG-GAGCGAGACTCTGTCTCAAAAAACAACA
AluY 119140644_119140941	-	(220)	GCAGTGAGCCGAGATGATGTCCTACTGCCTCCAGCCTGGCCACA-GAGCGAGACTCCGTCTGAAAAAATAAAA
AluJr 119140960_119141087	-	(129)	-----
AluJr4 119143201_119143335	-	(136)	-----
AluJb 119143422_119143709	+	(220)	GCAGTGAGCCATGATGTGTCCTACTGCCTCCAGCCTGGCAACA-GAGTGAGAGCCTAATCTGAAAAAATAAAA
AluJr 119144029_119144288	+	(181)	TCAGTGAGCTATGATGATCCACTGCCTCCAGCCTGGGTGACA-GACTGAGAGCCTGTCTCAAAAAAATAAAA
AluSz 119145360_119145636	-	(207)	---GTGAGCCGAGATGTGTCCTACTGCCTCCAGCCTGGGTGACA-GACTGAGAGCCTGTCTCAAAAAAATAAAA
AluY 119146114_119146420	+	(221)	GCAGTGAGCCGAGATGCGCCACTGCCTCCAGCCTGGCGACA-GAGCGAGACTCCATCTGAAAAAATAAAA
AluSx1 119147591_119147889	-	(218)	GCAGTGAGCCGAGATGTGTCCTACTGCCTCCAGCCTGGGTGACA-GTCCAGACTCTGTCTCAAAAAAATAAAA
AluJr4 119148000_119148265	-	(201)	TCAGTGAAGTGTGATGATCCACTGCCTCCACTTATGTGCCAGG-GAGCTGAGAGCCTAATCTGAAAAAATAAAA
AluJo 119150690_119150781	+	(15)	AGCGCCA-CTTCACTCAAGCCACTGCCTCCAGCCTGGCGACA-GAGTGAGAGCCTGACTCAAAAATAAAA
AluJo 119150800_119151111	+	(223)	ACAGTGAGCTATGATGATCCACTGCCTCCAGCCTGGCGACT-CAGTGAAGCCTGTCTCAAAAAAATAAAA
AluJo 119154061_119154359	-	(231)	GCAGTGAGCCATGATGATCCACTGCCTCCAGCCTGGCAACA-GAGTGAGATCTTGTCTGAAAAAATAAAA
AluSx 119154704_119154968	-	(222)	GCAGTGAGCCGAGATGATCCACTGCCTCCAGCCTGGCAACA-----
AluJr4 119155185_119155350	+	(86)	ACAGCGAGCTATGATGATCCACTGCCTCCAGCCTGGCGACA-BCGTGAGAGCCTGTCTGAAAAAATAAAA
AluJo 119157742_119157949	-	(136)	GCAGTGAGCTGTGATGATCCACTGCCTCCAGCCTGGGTGACA-GAGTGGATTCTGTCTCAAAAAAATAAAA
AluJb 119158224_119158514	-	(214)	GCAGTGAGCCGAGATGATCCACTGCCTCCAGCCTAGGTGACAG-----AGACTCAATCTGAAAAAATAAAA
AluSp 119161119_119161411	-	(221)	GGGGTGAGCCAAAATCGGATCCACTGCCTCCAGCCTGGCAACAAGAGTGAATTCCTCTGAAAAAATAAAA
AluSz 119168580_119168886	-	(228)	GCAGTGAGCTGAGATGTGTCCTACTGCCTCCAGCCTGGGTGACA-GAATGAGATTTCACTGAAAAAATAAAA
AluSp 119171159_119171467	-	(224)	GCAGTGAGCCGAGATGCGCCACTGCCTCCAGCCTGGCAACAAGAGTGAATTCCTCTGAAAAAATAAAA

3'-GGTGACGTGAGGTCGGACC-5' *Alu*_259_wt_R
3'-GGTACGTGAGGTCGGACC-5' *Alu*_259_4A_R
3'-GGCAGCTGAGGTCGGACC-5' *Alu*_259_3C_R

Figure S6

Detail of the gDNA sequence of the *CUL4B* breakpoint junction in the proband (II.1).

(a) Schematic showing the localization of gDNA qPCR probes with copy number 1 and 2 in *CUL4B* intron 19. The breakpoint junction is expected in the 428 bp region (highlighted in red) that contains *AluJb* element (arrow). (b) gDNA electrophoreogram of the breakpoint junction in intron 19 of *CUL4B* (Figure 1f). (c) Alignment of the reference sequence of the *AluJb* region (*in italics*), breakpoint junction sequence (in **bold** and corresponding to the electrophoreogram in b) in the proband (II.1) and the reference *AluSx1* sequence (*in italics*). There are two 2-nucleotide (TC and CT) overlaps at the junctions (outlined by the black rectangles). The binding site for the *Alu_259_4A_R* primer (see also Figure 1e, f and Figure S5) is also highlighted.

The putative impacts of the re-arrangement on the *CUL4B* transcript are:
CUL4B (NM_003588.3): c.2321-186_2742+2186del.

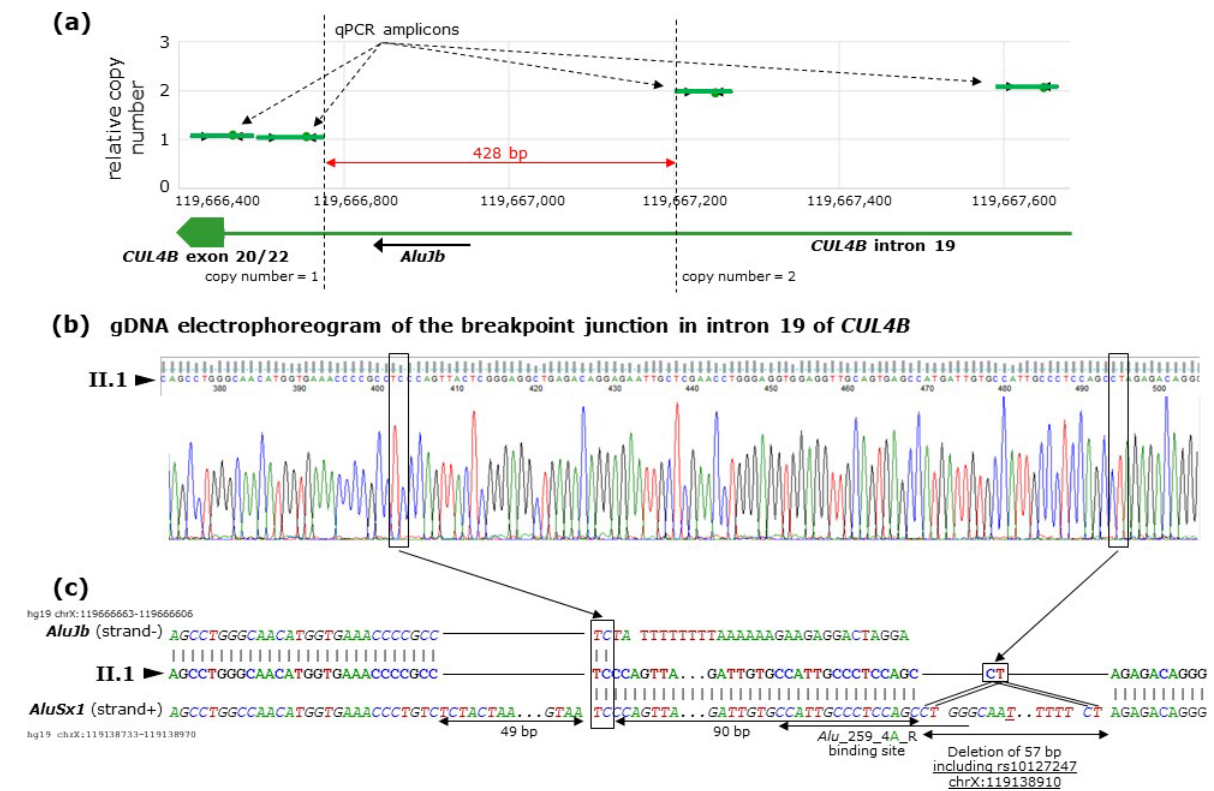


Figure S7

Parental configuration of the rs5910740 and rs5910797 SNPs (also shown in Figure 1a) was based on Sanger sequencing of the PCR products. Sequences of the listed PCR primers are included in *Table S1*. The abnormal re-arrangement (mutation) occurred on the paternal allele. Only the maternal variant of the rs5910797 (C) was detected in the proband.

rs5910797 localizes to a region (dotted violet line) that was not fully characterized in the proband (see Discussion and Figure 1g).

Undetectability of the paternal variant (A) of rs5910797 in the proband could either reflect its absence (deletion) or failure of the PCR assay in the abnormal (and undefined) region (e.g. primer binding site may be deleted or otherwise compromised).

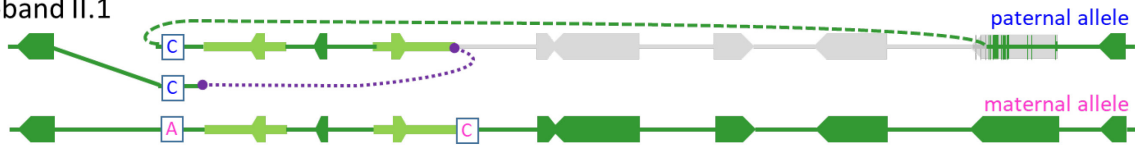
Father I.1



Mother I.2



Proband II.1



SNPs identified by Sanger sequencing of PCR products of primers:

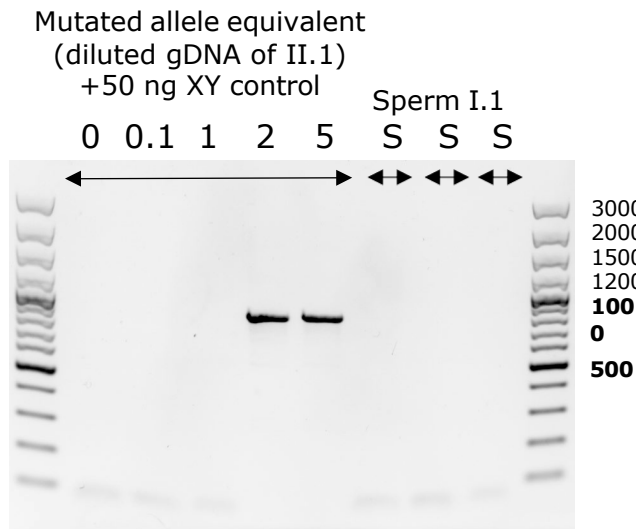
rs5910740 - chrX:119,139,139
 NKAP-61969_F - CUL4B_i19_1299F
 NKAP-61969_F - NKAP-60392_R

rs5910797 - chrX:119,331,643
 RHOXF2_38565_F - ZBTB33-54690_R

Figure S8

Detection of the mutant *LAMP2* allele by mutation-specific nested PCR in sperm of the father (I.1) (a) and peripheral blood of both parents (I.1 and I.2) (b). Serially diluted WBC gDNA of II.1 was used as positive control. 0.0, 0.065, 0.65, 1.3, 3.25 pg of II.1 gDNA were mixed with 50 ng of XY control gDNA. These ratios correspond to 0, 0.1, 1, 2 or 5 mutant X chromosome templates in the reaction mix. The result suggests that ~2 mutated alleles can be identified in a pool of ~7800 haploid cells. The primers have been preferentially designed outside the retrotransposons (Table S1).

(a)



(b)

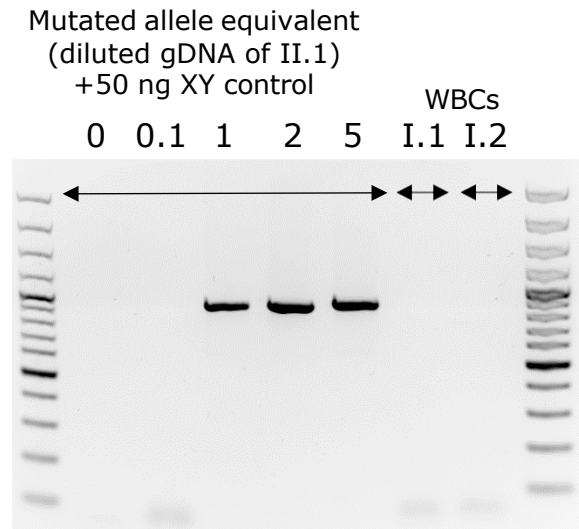
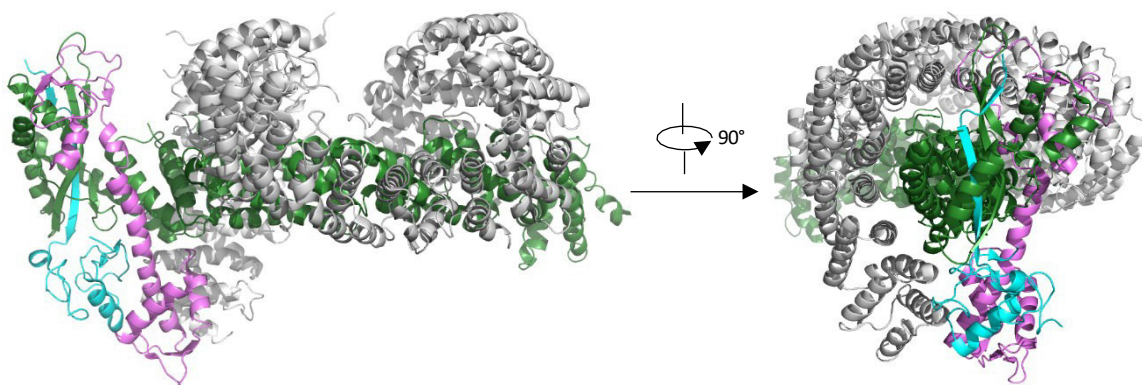


Figure S9

CAND1-CUL4B-RBX1 protein complex (PDB <http://www.rcsb.org/structure/4A0C>, (Fischer et al., 2011)).

Color legend: E3 ubiquitin-protein ligase RBX1 - light gray, cullin-associated NEDD8-dissociated protein 1 (CAND1) – cyan, cullin 4B (CUL4B) - forest green/purple (putative deletion of the 140 C-terminal amino acids)





References

- Elliott, D. B., Sanderson, K., & Conkey, A. (1990). The reliability of the Pelli-Robson contrast sensitivity chart. *Ophthalmic Physiol Opt*, *10*(1), 21-24.
- Fischer, E. S., Scrima, A., Bohm, K., Matsumoto, S., Lingaraju, G. M., Faty, M., . . . Thoma, N. H. (2011). The molecular basis of CRL4DDB2/CSA ubiquitin ligase architecture, targeting, and activation. *Cell*, *147*(5), 1024-1039.
- Majer, F., Vlaskova, H., Krol, L., Kalina, T., Kubanek, M., Stolnaya, L., . . . Sikora, J. (2012). Danon disease: a focus on processing of the novel LAMP2 mutation and comments on the beneficial use of peripheral white blood cells in the diagnosis of LAMP2 deficiency. *Gene*, *498*(2), 183-195.
- Shoji, T., Sakurai, Y., Chihara, E., Nishikawa, S., & Omae, K. (2009). Reference intervals and discrimination values of the Lanthony desaturated D-15 panel test in young to middle-aged Japanese army officials: the Okubo Color Study Report 1. *Eye (Lond)*, *23*(6), 1329-1335.
- Verma, R., & Babu, A. (1995). *Human Chromosomes: Principles & Techniques* (2nd ed.). New York: McGraw-Hill, Inc.

ORIGINAL ARTICLE

Příloha: 6

Pitfalls of X-chromosome inactivation testing in females with Fabry disease

Martin Řeboun¹ | Jakub Sikora^{2,3}  | Martin Magner^{1,4} | Helena Wiederlechnerová¹ | Alena Černá¹ | Helena Poupětová¹ | Gabriela Štorkánová¹ | Dita Mušálková² | Gabriela Dostálová⁵ | Lubor Golář⁵ | Aleš Linhart⁵  | Lenka Dvořáková¹

¹Diagnostic laboratories of IMD, Department of Pediatrics and Inherited Metabolic Disorders, First Faculty of Medicine, Charles University and General University Hospital, Prague, Czech Republic

²Research Unit for Rare Diseases, Department of Pediatrics and Inherited Metabolic Disorders, First Faculty of Medicine, Charles University and General University Hospital, Prague, Czech Republic

³Institute of Pathology, First Faculty of Medicine, Charles University and General University Hospital, Prague, Czech Republic

⁴Department of Pediatrics, Thomayer University Hospital and First Faculty of Medicine, Charles University, Prague, Czech Republic

⁵Second Department of Internal Cardiovascular Medicine, First Faculty of Medicine, Charles University and General University Hospital, Prague, Czech Republic

Correspondence

Lenka Dvorakova, Ph.D., Department of Pediatrics and Inherited Metabolic Disorders, First Faculty of Medicine, Charles University and General University Hospital in Prague, Ke Karlovu 455/2, Praha 2, 128 08, Czech Republic.
Email: lenka.dvorakova@lf1.cuni.cz

Funding information

Ministry of Health of the Czech Republic—conceptual development of research organization: a program of the General University Hospital in Prague RVO-VFN 64165/2012. Ministry of Health of the Czech Republic, Grant no. NU21-08-00324. All rights reserved.

Abstract

Fabry disease (FD) is an X-linked lysosomal storage disorder caused by mutations in the *GLA* gene encoding alpha-galactosidase A (AGAL). The impact of X-chromosome inactivation (XCI) on the phenotype of female FD patients remains unclear. In this study we aimed to determine pitfalls of XCI testing in a cohort of 35 female FD patients. XCI was assessed by two methylation-based and two allele-specific expression assays. The results correlated, although some variance among the four assays was observed. *GLA* transcript analyses identified crossing-over in three patients and detected mRNA instability in three out of four analyzed null alleles. AGAL activity correlated with XCI pattern and was not influenced by the mutation type or by reduced mRNA stability. Therefore, AGAL activity may help to detect crossing-over in patients with unstable *GLA* alleles. Tissue-specific XCI patterns in six patients, and age-related changes in two patients were observed. To avoid misinterpretation of XCI results in female FD patients we show that (i) a combination of several XCI assays generates more reliable results and minimizes possible biases; (ii) correlating XCI to *GLA* expression and AGAL activity facilitates identification of cross-over events; (iii) age- and tissue-related XCI specificities of XCI patterning should be considered.

KEYWORDS

alpha-galactosidase A activity, Fabry disease heterozygotes, *GLA* transcript expression, X chromosome inactivation assay

1 | INTRODUCTION

Fabry disease (FD, OMIM 301500) is an X-linked lysosomal storage disorder (LSD) caused by deficient activity of alpha-galactosidase A (AGAL, E.C. 3.2.1.22). This enzymatic defect is a consequence of pathogenic variants (mutations) in the *GLA* gene (Xq22.1) (Ortiz et al., 2018). Over 1000 disease causing *GLA* mutations (Stenson et al., 2020) have been associated with FD and approximately 70% are missense mutations.

AGAL cleaves substrates with terminal alpha D-galactose. The key unprocessed glycosphingolipid substrates are globotriaosylceramide (Gb3Cer), digalactosylceramide (diGalCer) and lipids bearing the antigenic blood group B determinant. As a result, these (and other) metabolites accumulate in lysosomes and trigger molecular cascades that cause further cellular, tissue and organ dysfunction and/or damage (Ortiz et al., 2018).

Clinical severity of FD depends on the sex, type of the *GLA* mutation and age of the patient(s). The majority of X-hemizygous male FD patients and sporadically detected homozygous female FD patients present with a complex clinical phenotype that, if untreated, leads to cardiac, renal and neurological involvement and reduced life expectancy (Ortiz et al., 2018). Additional symptoms include acroparesthesia, angiokeratomas, abnormal sweating (hypohidrosis and/or hyperhidrosis) and gastrointestinal symptoms (Lidove et al., 2006). A large proportion of FD patients present with late onset disease frequently limited to the heart (cardiac variant). Many specific *GLA* variants have been associated with relatively high residual AGAL activity and mild to moderate FD (Ortiz et al., 2018).

Females heterozygous for *GLA* mutations present with a variable clinical phenotype that ranges from asymptomatic course to severe clinical presentation comparable to that observed in male patients (Lenders et al., 2016). Besides common determinants (e.g., type of the *GLA* mutation or age), X-chromosome inactivation (XCI) has been suggested to contribute to the variable clinical course of the disease in this specific patient group.

Several studies suggested that women with XCI ratios skewed towards expression of the mutated *GLA* allele present with a more severe phenotype and exhibit faster disease progression (Dobrovolny et al., 2005; Echevarria et al., 2016). The larger proportion of cells mosaically expressing the mutant allele also makes these females more prone to develop organ damage (Mauer et al., 2014). Therefore, XCI assessment may represent a valuable read-out allowing prediction(s) of the course of the disease in heterozygous FD females. However, the impact of XCI on the variability of the clinical phenotype in FD female patients has not been proven by other authors (Elstein et al., 2012; Juchniewicz et al., 2018; Maier et al., 2006; Rossanti et al., 2021) and thus remains ambiguous partly owing to the limited number of studied samples and tissues and the choice of applied testing techniques. Moreover, it is unclear whether XCI ratios remain constant with age. Should the methodological issues be solved, XCI assessment represents a useful tool for risk stratification in FD females.

To identify potential technical problems with XCI testing, we therefore used a novel combination of methylation and allele-specific expression (ASE) assays to analyze a cohort of 35 female patients coming from 22 FD families. We correlated these results with *GLA*

mRNA analyses and AGAL enzymatic activity measurements. Additionally, we compared XCI in different tissues and tracked the XCI status over a prolonged period of time.

2 | MATERIALS AND METHODS

2.1 | Editorial policies and ethical considerations

The study was approved by the Ethics Committee of the General University Hospital in Prague, (decision no. 135/2015). Informed consent was obtained from all individuals.

2.2 | Patients

Thirty-five female patients (average age 52 years, median 56 years, range 24–72 years) from 22 families were included in the study. Twenty-nine females were diagnosed by family screening. Six females were probands in their families. Patients were included regardless of their clinical manifestations. These were heterogeneous and included neuropathic pain, gastrointestinal symptoms, cardiac, renal, and neurological involvement.

2.3 | Molecular genetic analyses

Genomic DNA (gDNA) was extracted from peripheral blood leukocytes, saliva and urinary sediment using the QIAamp DNA Blood Mini Kit DNA (Qiagen, Valencia, CA). gDNA from buccal swabs was isolated using the QIAamp DNA Micro Kit (Qiagen). Total RNA was isolated from peripheral blood using the BiOstic Blood Total RNA Isolation Kit (MO BIO Laboratories, Inc., Carlsbad, CA). Reverse transcription of RNA to cDNA was performed using the High Capacity RNA to cDNA Kit (Applied Biosystems, Carlsbad, CA).

GLA gene mutation analyses (LRG_672) in gDNA from peripheral blood leukocytes were performed by Sanger sequencing using the Big Dye Terminator v3.1 Cycle Sequencing Kit and the 3500xL Genetic Analyzer (Applied Biosystems). PCR primer sequences are shown in Table S1. If the female patient was a proband in the family, the entire *GLA* coding region and exon/intron boundaries were sequenced. For all other females, heterozygosity for the family-specific *GLA* mutation was tested.

2.4 | X-chromosome inactivation studies

XCI ratios/patterns were assessed using two different techniques – (i) testing the methylation status at the polymorphic repeat regions and (ii) analyzing the allele-specific expression (ASE) of heterozygous SNPs.

gDNA was digested at two loci, *AR* (Xq12) and *RP2* (Xp11.3), using methylation-sensitive enzyme HpaII, as described elsewhere (Machado et al., 2014; Musalkova et al., 2015; Racchi et al., 1998). Segregation of the *AR* and *RP2* allele(s) with the *GLA* mutant allele(s) was deduced from the results of gDNA analysis of a male proband and/or other family members (Dobrovolny et al., 2005).

Two frequent SNPs, rs1141608 and rs12097, localized in the *IDS* (*Xq28*) and the *LAMP2* (*Xq24*) genes, respectively, were used for the ASE assay (Carrel & Brown, 2017; Mossner et al., 2013). After detecting a heterozygous genomic SNP, reversely transcribed PCR products were subjected to amplicon sequencing (NEXTERA XT) using the Illumina MiSeq platform as described previously (Reboun et al., 2016). The average depth of coverage was 2132 reads per base and the variance ranged from 462 to 4928 reads. Sequences of the specific PCR primers are provided in Table S1. Segregation of the polymorphism(s) with the mutant *GLA* allele(s) was deduced from results of the transcript expression analyses of the *GLA* gene and/or from the value(s) of the residual AGAL activity.

XCI ratios outside the >25:75/<75:25 range were considered skewed (Dobrovolsky et al., 2005; Elstein et al., 2012).

2.5 | *GLA* transcript expression analyses

Similar to the ASE analyses, the relative expression of the mutated (*mut*) and wild-type (*wt*) *GLA* allele(s) was assessed. Reversely transcribed PCR products containing the *GLA* mutation were sequenced using (NEXTERA XT) and Illumina MiSeq platform(s). The number of reads corresponding to *mut* and *wt* alleles were used to calculate relative expression. The average depth of coverage was 712 reads per base and the variance ranged from 229 to 1872 reads.

2.6 | AGAL enzymatic activity studies

AGAL activity in the peripheral blood leucocytes was measured by fluorometric method using 4-methylumbelliferyl- α -D-galactopyranoside as substrate (final concentration 2.5 mM) in the presence of N-acetylgalactosamine (final concentration 0.1 M) as an inhibitor of α -D-galactosidase B (Mayes et al., 1981).

2.7 | Statistics

Statistical analyses were performed using RStudio (version 1.2.5001). Pearson's correlation and One-way analysis of variance followed by Tukey multiple pairwise-comparisons were used. Statistical significance was assumed at $p < 0.05$.

3 | RESULTS

3.1 | Molecular genetic studies and mutation classification

Genotypes of the female FD patients are shown in Table 1. We detected three novel *GLA* mutations: c.551A > G (p.Tyr184Cys), c.671A > C (p.Asn224Thr), c.1034dupT (p.Ser345Phefs*30).

Eight patients from six families were heterozygotes for null mutations (gross deletions or mutations leading to premature stop codons).

Four patients from three families carried splicing mutations. The pathogenic effects of the latter mutations were confirmed by analyzing the *GLA* mRNA. The remaining 23 patients from 13 families were heterozygotes for missense mutations.

We divided the missense and splicing mutations into two groups based on their severity (Table 1): (i) severe mutations leading to almost complete AGAL deficiency and (ii) hypomorphic mutations resulting in substantial residual AGAL activity in male patients. We based the categorization on previously published functional studies of *GLA* mutations (Lukas et al., 2013) and/or on the levels of the residual AGAL activity and clinical phenotype of the male patient(s) in the presented families.

The unpublished variant c.551A > G (p.Tyr184Cys) was classified as severe due to low residual AGAL activity in leukocytes (0.95 nmol $\text{mg}^{-1} \text{h}^{-1}$, mean control values \pm SD: 59.7 \pm 14.6 nmol $\text{mg}^{-1} \text{h}^{-1}$) and clinical phenotype of the son of Patient 15.

The second unpublished variant c.671A > C (p.Asn224Thr) was detected in two female patients with penetrant FD phenotype (patients 17 and 18, family 13). There was no X-hemizygous male patient in this family. Other variants in the same amino acid residue (p.Asn224Ser and p.Asn224Asp) were associated with classic FD phenotype (Saito et al., 2013). We therefore classified this novel *GLA* variant as a severe missense mutation.

3.2 | X-chromosome inactivation analyses in the peripheral blood—comparison of two methodological approaches

All patients were informative for at least one of the four loci detectable by DNA-methylation (*AR*, *RP2*) or ASE (*IDS*, *LAMP2*) assays. Twenty-four (69%) and 19 (54%) out of 35 analyzed FD female patients were heterozygous for the length polymorphism(s) in the *AR* and *RP2* loci, respectively. Seventeen (49%) and nine (26%) patients were heterozygous for the exonic SNPs in the *IDS* (rs1141608) and the *LAMP2* (rs12097) genes (Table 1).

XCI ratios obtained by both DNA-methylation and ASE assays correlated irrespective of the type of the *GLA* mutation (Figure S1). Comparable results were obtained for the four individual assays (*AR*, *RP2*, *IDS*, *LAMP2*) as documented in Table 1. The only exception was the *AR* assay in Patient 10. In this patient, the difference between *AR*/*RP2* assay and *AR*/*IDS* assay was 17% and 27%, respectively. Therefore, the *AR* result was excluded as an outlier and was not considered in the subsequent analyses. Average XCI values were calculated and used for further evaluations in patients informative for several loci. Twenty-six patients had random XCI, while skewed XCI was detected in nine patients (7, 8, 19, 20, 21, 26, 27, 34, and 35) (Table 1).

3.3 | Correlation of the *GLA* transcript expression to X-chromosome inactivation. Identification of crossing-over and *GLA* mRNA instability

Relative expression of the *wt* and *mut* *GLA* alleles was determined in the peripheral blood of 26 FD patients who carried point mutations

TABLE 1 *GLA* genotypes, AGAL activities, X chromosome inactivation patterns and relative *GLA* transcription assessed in leukocytes of 35 heterozygous females affected with Fabry disease

Patient	Family	<i>GLA</i> variant	Predicted effect on the protein	Age (years)	Enzyme activity (nmol/h/mg)	XCI: Methylation assay (% wt/mut) ^a		XCI: ASE assay (%) ^a		<i>GLA</i> expression (% wt/mut)	References
						<i>AR</i>	<i>RP2</i>	<i>IDS</i>	<i>LAMP2</i>		
NULL mutations											
1	1	c.195-1692_369 + 754del	p.Ser65Argfs*7	72	11.0	NI	60/40	50/50	NI	NI	Dobrovolny et al., 2005
2				34	36.5	42/58	35/65	NI	NI	NI	
3	2	c.559_560delAT ^b	p.Met187Valfs*6	62	39.8	36/64	46/54	NI	NI	100/0	Nowak et al., 2018
4	3	c.674_732del59	p.His225Leufs*5	72	16.5	52/48	51/49	62/38	NI	NI	Dobrovolny et al., 2005
5	4	c.881 T > G ^b	p.Leu294*	34	32.5	64/36	64/36	NI	70/30	88/12	Blaydon et al., 2001
6	5	c.1024C > T	p.Arg342*	24	49.0	65/35	69/31	60/40	74/26	56/44	Davies et al., 1993
7				52	0.5	5/95	NI	0/100	7/93	1/99	
8	6	c.1034dupT ^b	p.Ser345Phefs*30	68	20.6	18/82	14/86	NI	NI	44/56	Not published
Missense and splicing severe mutations											
9	7	c.194 + 2 T > C (r.194_195ins [194 + 1_194 + 14])	p.Ser65Argfs*61	32	32.5	NI	39/61	NI	NI	NI	Dobrovolny et al., 2005
10	8	c.277G > A	p.Asp93Asn	46	27.5	80/20	63/37	47/53	NI	45/55	Shabbeer et al., 2005
11	9	c.463G > C	p.Asp155His	63	34.8	44/56	41/59	NI	44/56	44/56	Dobrovolny et al., 2005
12				34	25.4	49/51	36/64	33/67	NI	47/53	
13	10	c.488G > T	p.Gly163Val	54	13.9	NI	26/74	67/33	NI	64/36	Eng et al., 1997
14	11	c.511G > C	p.Gly171Arg	59	17.9	51/49	NI	NI	NI	NA	Dobrovolny et al., 2005
15	12	c.551A > G	p.Tyr184Cys	60	25.9	37/63	55/45	NI	NI	71/29	Not published
16				50	39.9	30/70	NI	NI	NI	NA	
17	13	c.671A > C	p.Asn224Thr	60	14.1	NI	NI	37/63	NI	48/52	Not published
18				31	14.2	47/53	43/57	37/63	NI	36/64	
19	14	c.801 + 3A > G (r.801_802ins [801 + 1_801 + 36])	p.Leu268Valfs*4	56	8.6	NI	7/93	NI	NI	NI	Shabbeer et al., 2006
20	15	c.950 T > C	p.Ile317Thr	55	32.2	83/17	80/20	NI	NI	87/13	Shabbeer et al., 2002
21	16 ^c	c.1025G > A	p.Arg342Gln	70	57.4	NI	97/3	NI	99/1	100/0	Lukas et al., 2013; Ploos van Amstel et al., 1994
22				37	31.2	NI	NI	NI	51/49	53/47	
23	17 ^c	c.1025G > A	p.Arg342Gln	27	26.6	66/34	NI	NI	NI	80/20	Ploos van Amstel et al., 1994
24	18	c.1078G > A	p.Gly360Ser	49	31.6	56/44	NI	53/47	NI	58/42	Dobrovolny et al., 2005
25	19	c.1085C > T	p.Pro362Leu	38	26.2	NI	NI	48/52	37/63	49/51	Shabbeer et al., 2002
26				67	NA	21/79 ^d	22/78 ^d	68/32	NI	75/25 ^d	
27				59	34.7	NI	NI	77/23	77/23	69/31	

TABLE 1 (Continued)

Patient	Family	GLA variant	Predicted effect on the protein	Age (years)	Enzyme activity (nmol/h/mg)	XCI: Methylation assay (% wt/mut) ^a		XCI: ASE assay (%) ^a		GLA expression (% wt/mut)	References
						AR	RP2	IDS	LAMP2		
Missense and splicing hypomorphic mutations											
28	20	c.644A > G	p.Asn215Ser	59	29.2	NI	65/35	64/36	52/48	72/28	Davies et al., 1993; Lukas et al., 2013
29				69	27.8	43/57	NI	50/50	NI	55/45	
30				66	30.3	41/59	NI	NI	NI	50/50	
31				68	23.9	NI	NI	35/65	NI	29/71	
32	21	c.801 + 48 T > G (r.801_802ins [801 + 1_801 + 66])	p.Leu268Valfs*4	36	31.7	59/41	NI	NI	NI	NI	Palecek et al., 2014
33				70	56.6	64/36	NI	NI	NI	NI	
34	22	c.902G > A	p.Arg301Gln	72	13.9	76/24 ^d	NI	NI	NI	30/70 ^d	Lukas et al., 2013; Sakuraba et al., 1990
35				26	32.1	9/91 ^d	NI	89/11	NI	92/8 ^d	

Note: Patients 8, 15, 17, 24, 25, and 34 were index patients (probands) in their families. The result of mRNA transcript analysis is shown for patients 9, 19, 32, and 33 in parentheses the column *GLA* variant. NA—sample not available for analysis; NI—noninformative assay (i.e., nonpolymorphic locus for XCI analysis; *GLA* mutation type noncompatible with the expression analysis); in the case of methylation assays and *GLA* expression assays *wt* alleles in skewed XCI status are depicted in bold.

^aThe segregation of *AR* and *RP2* allele(s) with the mutant *GLA* allele(s) was based on the analysis of the proband and/or other family members. The relationships between the proband in the family and the patient with skewed XCI are: Patient 20: Sister of hemizygous male patient. Patient 21: Maternal aunt of hemizygous male patient. Patient 26: Mother of Patient 27, maternal aunt of Patient 25. Patient 34: Mother of hemizygous male patient. Patient 35: Niece of Patient 34, cousin of hemizygous male patient. The segregation of *IDS* and *LAMP2* allele(s) was deduced from results of *GLA* expression analyses for further purposes. Values of AGAL activities measured in leukocytes of 477 controls in 2003–2020 were as follows: mean 59.7 nmol mg⁻¹ h⁻¹, SD 14.6, range 24.8–103.0 nmol mg⁻¹ h⁻¹, median 58.7 nmol mg⁻¹ h⁻¹.

^bNonsense-mediated mRNA decay (NMD) effect observed.

^cFamilies 16 and 17 have the same mutation, the relationship is not known.

^dPatients, in whom crossing-over between the loci used for methylation assays and the *GLA* locus was detected.

(missense and nonsense) or small deletions and duplications. It was not possible to perform this assay in seven patients with large deletions or splicing *GLA* mutations.

The *wt GLA* expression was compared with XCI results obtained by methylation assays. As stated in the Materials and Methods section, segregation of the *AR* and *RP2* allele(s) with the *GLA* mutant allele(s) was deduced from the analyses of the proband and/or other members in the family (as specified in a legend of Table 1). Concordant values of XCI and *wt GLA* allele expression were observed in all patients with missense mutations who had random XCI. Similarly, corresponding data were detected in two patients with skewed XCI (Patients 20 and 21).

On the contrary, interpretation of data obtained from patients 26, 34, and 35 was problematic. In patients 26 (*AR*, *RP2*) and 35 (*AR*), the XCI pattern suggested skewing in favor of the mutated *GLA* allele. However, preferential expression of the *wt GLA* allele was identified. The opposite was found in Patient 34. While XCI (*AR*) results indicated silencing in favor of the wild type allele, preferential expression of the mutated *GLA* allele was detected in this patient (Table 1). These findings indicated cross-over event(s) between the loci used for XCI analyses and the *GLA* gene locus (Figure 1).

When corrected for crossing-over, XCI and *wt GLA* allele expression correlated in all patients with hypomorphic and severe missense mutations and in two patients (6 and 7) from a single family with a null

GLA mutation. In patients 3, 5, and 8, who carry null *GLA* mutations, the XCI status and the *wt GLA* allele expression differed by 59%, 24%, and 28%, respectively (Figure 2a, Table 1). This discrepancy can be explained by partial or full nonsense-mediated mRNA decay (NMD) of the mutated RNA transcripts. Although random XCI was detected, only *wt GLA* allele was expressed in Patient 3, who is a heterozygote for the c.559_560delAT mutation that leads to complete decay of the mutated *GLA* allele. Partial transcript instability was observed for the nonsense mutation (c.881 T > G; p.Leu294*) and a small duplication (c.1034dupT; p.Ser345Phefs*30) that were detected in Patients 5 and 8, respectively. On the contrary, the nonsense mutation c.1024C > T (p.Arg342*) does not appear to affect stability of the *GLA* mRNA. This can be documented in Patient 6 who shows random XCI as well as balanced expression of the *mut* and *wt* allele.

3.4 | Correlation of the AGAL activity and *GLA* transcript expression, X-chromosome inactivation, and the type of *GLA* mutation

AGAL activity was measured in peripheral blood leukocytes of female FD patients and ranged from 0.5 to 57.4 nmol mg⁻¹ h⁻¹ (healthy controls 24.8–103.0 nmol mg⁻¹ h⁻¹) (Table 1). Enzymatic activity was below the lower limit of healthy controls in 11 of 34 patients.

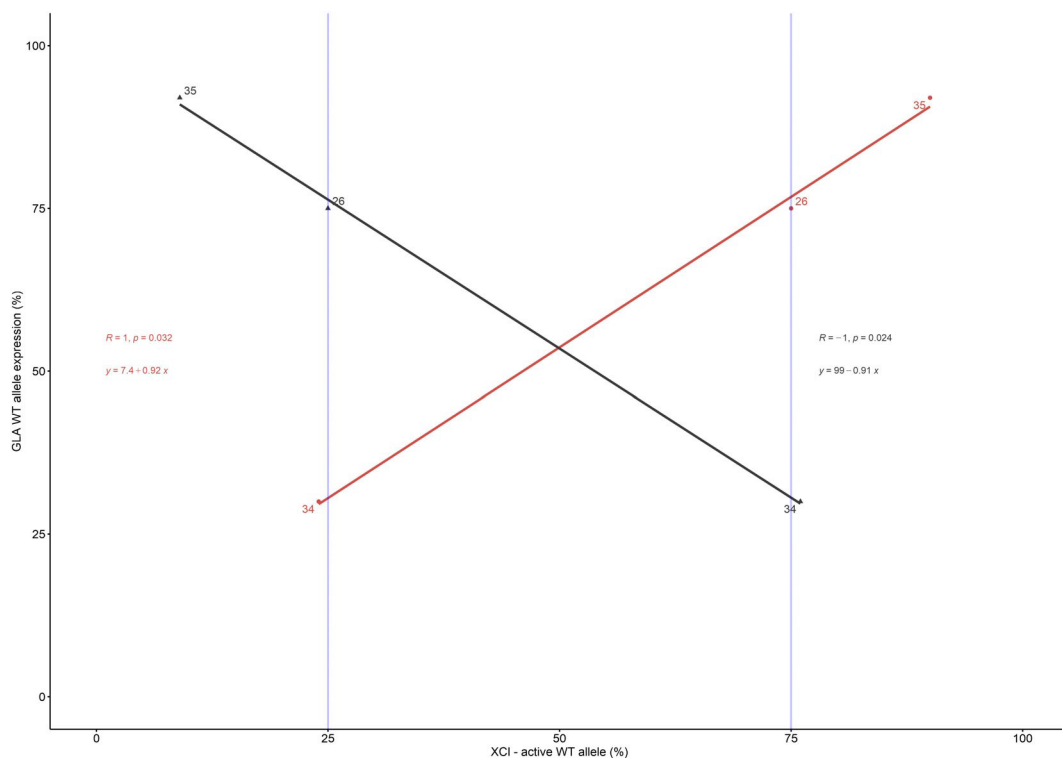


FIGURE 1 Demonstration of crossing-over. Cross-over events were detected in patients 26, 34, and 35 (Table 1). The segregation of *AR* and *RP2* allele(s) with the mutant *GLA* allele was based on the analysis of the proband and/or other family members as specified in a legend of Table 1. Noncorrected data (black triangles) of *wt* allele expression assessed by methylation assays is inversely proportional to the *wt GLA* allele relative expression. Red circles show data corrected for the crossing-over. Correlation coefficients (*R*), statistical significance (*p*), and linear regression equations are shown

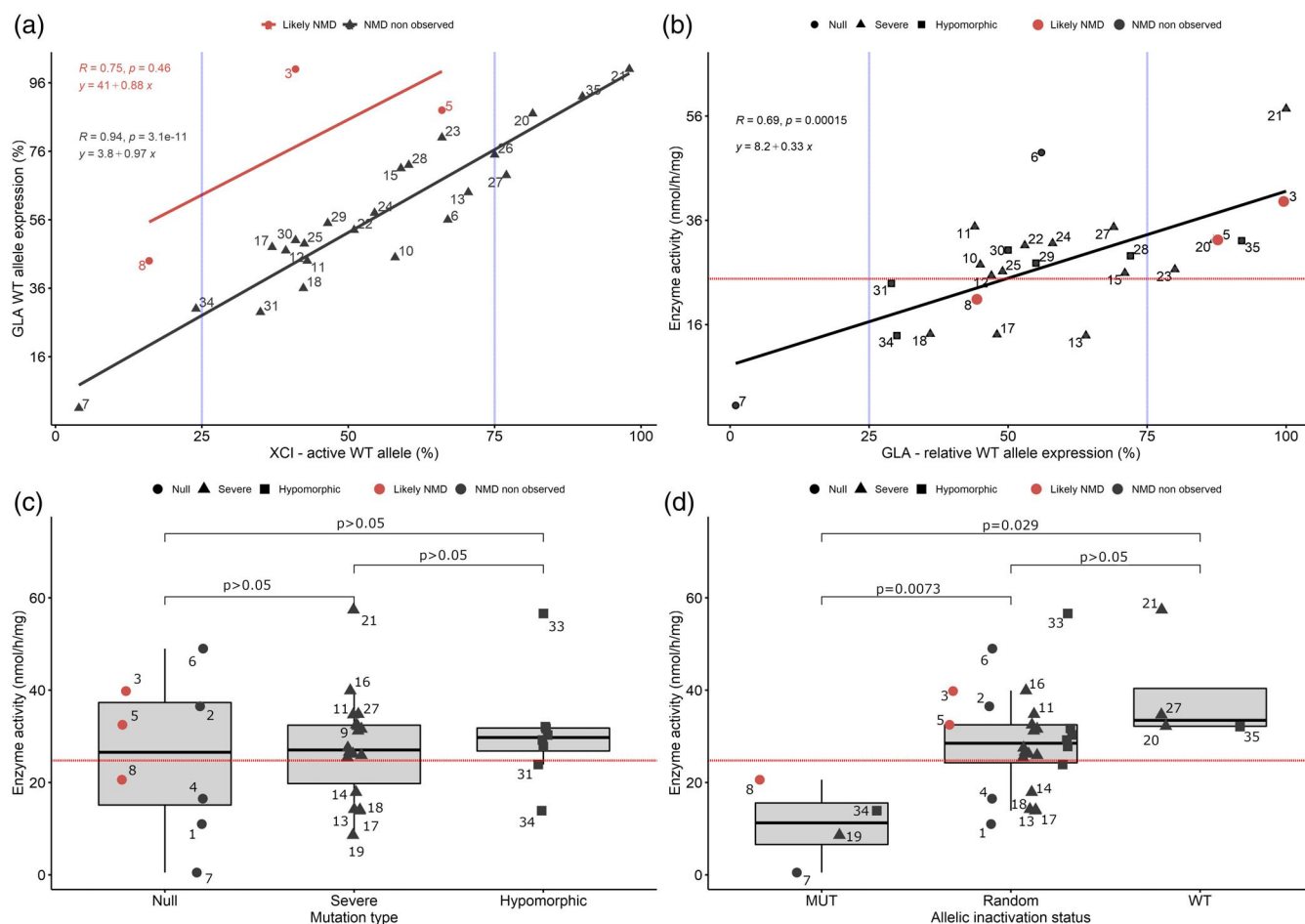


FIGURE 2 Relationships between XCI status, expression of the *wt* *GLA* allele, AGAL activity, and type of the *GLA* mutation. Patients in whom NMD is suspected are depicted in red. The red horizontal dotted line represents the lower limit of the AGAL activity in healthy controls. Average XCI values obtained from all the polymorphic loci (*AR*, *RP2*, *IDS*, and *LAMP2*) are shown. XCI data are corrected for the crossing-over. Table 1 provides summary information. Correlation coefficients and statistical significance are represented by *R* and *p* values, respectively. Equations represent linear regression. (a) Correlation of the relative expression of the *GLA* *wt* allele and XCI in 26 female FD patients. Black symbols represent patients who carry apparently stable *mut* *GLA* alleles. Red symbols correspond to partial (Patients 5 and 8) or complete (Patient 3) NMD. (b) Correlation of the AGAL activity and the relative expression of the *GLA* *wt* allele in 25 FD female patients. The enzymatic activity corresponds to the *wt* *GLA* expression independently of the type of the *GLA* mutation or NMD effect. (c) Correlation of the AGAL activity and the mutation type. No significant difference was detected. No NMD effect was observed. (d) Correlation of the AGAL activity and the XCI status. MUT column represent patients with *wt* *GLA* allele expression <25%, WT column represent patients with *wt* *GLA* allele expression >75%. Random column represents patients with *wt* *GLA* allele expression in range 25–75%

While AGAL activity correlated with the expression of the *wt* *GLA* allele, neither the type of *GLA* mutation nor the NMD affected the enzyme activity. In fact, remarkably high values of AGAL activity were detected in Patients 6 and 21 who carried a null and a severe missense mutation, respectively. Also, Patients 3, 5, and 8, who showed NMD, had AGAL activity values comparable to other patients (Figure 2b).

Twenty-three patients had the AGAL activity in the range of controls regardless of the mutation type (Figure 2c and Table 1). On the contrary, the correlation of XCI and AGAL activity could be identified (Figure 2d). If only the enzyme activity was considered, 19 of the 26 patients with random XCI (73%) and all patients with XCI favoring the *wt* allele would have escaped diagnosis. Thus, patients in whom

the *wt* allele is preferentially inactivated are the only group that can be unambiguously identified using the AGAL activity measurements.

3.5 | Effects of aging and tissue specificity of XCI

gDNA samples from tissues other than peripheral blood (i.e., urine sediment, buccal swabs, and saliva) were available in 15 patients. In addition, historical samples were available for comparative analyses in eight of these patients (Table 2).

XCI values in recent samples and samples of blood, saliva and urine collected 11 years ago were almost identical in Patient 21. Stable XCI patterns were observed also in blood of five other patients

TABLE 2 Tissue specificity of XCI and effects of aging

Patient	Age	Blood	Buccal swabs	Saliva	Urine
NULL mutations					
1	72	60/40	67/33	66/34	53/47
3	62	41/59 (8 years ago: 41/59)	82/18	64/36	50/50
5	34	64/36	43/57	68/32	62/38
7	52	5/95	10/90	NA	NA
8	68	16/84 (6 years ago: 45/55)	49/51	29/71	21/79
Missense and Splicing severe mutations					
10	46	63/37	55/45	NA	NA
11	63	43/57	54/46	40/60	43/57
14	59	51/49 (11 years ago: 46/54)	35/65	40/60	53/47
19	56	7/93 (15 years ago: 16/84)	23/77	NA	NA
20	55	82/18 (10 years ago: 36/64)	55/45	41/59	46/54
21	70	97/3 (11 years ago: 98/2)	54/46	96/4 (11 years ago: 85/15)	78/22 (11 years ago: 80/20)
23	27	66/34	60/40	63/37	50/50
26	67	78/22 (6 years ago: 68/32)	67/33	62/38	79/21
Missense and Splicing hypomorphic mutations					
34	72	76/24	78/22	81/19	69/31
35	26	9/91 (3 years ago: 2/98)	45/55	23/77	56/44

Note: NA—sample not available for analysis; Methylation assays were used; if both *AR* and *RP2* probes are informative, average values are shown. The shown data are corrected for crossing-over. *wt* alleles in skewed XCI status are depicted in bold.

(3, 14, 19, 26, and 35). The opposite was observed in Patients 8 and 20, who had random XCI in blood initially. XCI assessed 6 and 10 years later showed skewed patterns (Table 2) in both patients. Overall, the long-term instability of the XCI was documented in two of eight (25%) blood samples from tested patients.

XCI was random in all tissue samples analyzed from seven of 15 patients (including Patient 20 whose XCI in leukocytes became skewed with age). Patients 7 and 19 showed skewed XCI pattern favoring the mutated allele in both available tissue samples (blood and buccal swabs). Tissues of six other patients (3, 8, 21, 26, 34, and 35) showed discordant results. Random XCI was detected in some of their tissue samples while skewed patterns were found in other tissues (Table 2).

4 | DISCUSSION

To demonstrate previously underestimated pitfalls of XCI assessment in FD females, our study combined a set of XCI assays with *GLA* transcript and AGAL activity measurements. This approach allowed us to propose protocols minimizing misinterpretation of XCI results. We believe that our findings will substantially facilitate any future studies aimed at phenotype/XCI correlation in FD females.

FD females present with a more variable disease than X-hemizygous male patients (Lenders et al., 2016). As a result of this variability, the prediction of the disease course is problematic and initiation of treatment is often delayed. Characterization of XCI may help

the clinical/therapeutic decision-making process in FD females (Ortiz et al., 2018). However, data regarding impact of XCI status on severity of the disease is ambiguous. Significant correlation between the measures of the disease severity and XCI was reported in cohort studies (Dobrovlny et al., 2005; Echevarria et al., 2016) as well as in individual families (Hossain et al., 2017; Morrone et al., 2003; Redonnet-Vernhet et al., 1996; Yanagisawa et al., 2019). On the contrary, other authors did not confirm those findings (Elstein et al., 2012; Juchniewicz et al., 2018; Maier et al., 2006).

With few exceptions, the referenced studies used a single assay and XCI was evaluated in a single tissue. Echevarria et al. used two methylation assays in four different tissues, compared AGAL enzyme activity with the XCI results and found a significant impact of XCI on the phenotype in a cohort of 56 FD female patients (Echevarria et al., 2016). On the contrary, Rossanti et al. reported a study in which both ultra-deep RNA sequencing and methylation-based *AR* assays were used to examine XCI in blood leukocytes and urine sediment. This study tested a cohort of nine female FD patients and showed correlation between the results of the *AR* assay and the *GLA* transcript expression analyses. However, the XCI values gained by these two assays did not correspond to clinical symptoms of the patients (Rossanti et al., 2021).

The discordant results of the referenced studies may be explained either by methodological pitfalls of XCI testing or by the possibility that quantification of clinical impacts of XCI is biased by heterogeneity of symptoms, age, and variable organ manifestation among FD females.

In the present study we aimed solely at the methodological aspects of XCI testing.

Our study shows a good concordance of methylation and ASE assays for assessment of XCI in FD female patients. Despite the results of both types of assays differed by 10–15% in several patients, we consider these two techniques substitutable.

The use of methylation assays is limited by the finding that methylation of the tested loci may not reflect the correct XCI status in rare situations (Swierczek et al., 2012). In fact, findings in Patient 10 from our cohort exemplify this phenomenon. The *AR* assay showed skewed XCI, while *RP2* and *IDS* assays, in accordance with results of the *GLA* transcriptional analyses, showed a random XCI pattern.

The key drawback of the ASE assays is the uneven allele expression, which may be caused by a number of factors such as NMD or variants in expression regulatory sequences. NMD that reduced the transcript stability was identified in patients 3, 5, and 8 from our cohort. The regulatory variants have not yet been published in the *IDS* gene, however several variants modulating transcriptional efficacy were described in the promoter of the *LAMP2* gene (Pang et al., 2012) or in 5' UTR of the *GLA* gene (Ferreira et al., 2015). Use of a single assay, regardless whether ASE or methylation-based, could lead to incorrect results (as Patient 10 from our cohort).

The key limitation of both methylation and ASE assays is a considerable distance between the loci used for XCI analyses and the *GLA* gene locus. Assessing the correct phase is paramount. However, it is not straightforward, because of cross-over events occurring between maternal X chromosomes. A crossing-over occurs at least twice on each metacentric chromosome (Coop & Przeworski, 2007). This problem can be resolved by the analysis of the paternal sample and rigorous assessment of the segregation of the alleles in the family. However, samples for such meticulous analyses are rarely available and the information is often not stated in the published cohort studies. If the phasing is not established, preferential activation of either of the alleles (mutated or wild-type) cannot be distinguished based on XCI ratios.

We detected XCI skewing in seven FD females carrying a mis-sense mutation. Using the methylation assays, phasing of the alleles was based on the segregation analysis in the family, paternal samples were not available in any patient. Proper phasing of the alleles was, therefore, not feasible and correct interpretation of the XCI results was possible based on *GLA* expression analyses. By this approach we detected crossing-over between the loci used for methylation assays and the *GLA* locus in three patients.

Important, detection of crossing-over using *GLA* expression analyses is unreliable in patients with mutations affecting the mRNA stability. In the presented cohort, decreased mRNA stability was identified in three patients carrying a null *GLA* mutation. As the enzyme activity is not affected either by the type of the *GLA* mutation or by mRNA instability, AGAL activity assay, rather than the *GLA* expression analysis, is suitable for identification of potential crossing-over in these patients.

Our study further assessed tissue-specific patterns and age-related changes of XCI. These phenomena represent additional

potential bias to interpretation of XCI values and prediction of disease progression or proper treatment initiation. Tissue-specific variations of XCI were reported in a small number of FD female patients (Echevarria et al., 2016) as well as in healthy women (Hoon et al., 2015; Sharp et al., 2000). XCI in multiple tissue types was analyzed in 15 patients from our cohort, the full concordance of either the random or skewed patterns for all analyzed tissue samples was detected in just nine patients (60%). Aging, as well as some specific pathologies developing during life, may result in skewed XCI (Amos-Landgraf et al., 2006; Busque et al., 1996; Sandovici et al., 2004). We documented aging effects on XCI in two (25%) of eight patients from whom samples were collected over the time span of 3–15 years.

Our study presents several important novel insights to XCI evaluation in female FD patients. First, results of methylation-based methods and ASE protocols for XCI assessment tightly correlate. However, these tests may not be fully informative. Multiplication of tested loci allows correct identification of XCI patterns in a large majority of samples and minimizes potential biases. Second, the correct assessment of XCI in FD female patients may be hampered by cross-over event(s). To facilitate correct interpretation of the results, we suggest performing comparative *GLA* transcript expression analyses and/or measuring the residual AGAL enzymatic activity. Third, our data suggest that evaluation of XCI from a single tissue may be misleading. Moreover, tissue-specific XCI may change over time.

To conclude, studies correlating the phenotype of FD female patients and their XCI status require reliable data. Nonetheless, XCI evaluation in these patients is challenging. Our study demonstrates a clear benefit of the combined use of XCI assays, *GLA* expression analyses and enzyme activity assessment to attain correct results while minimizing the numerous technical and biological pitfalls.

ACKNOWLEDGMENTS

We thank Karolina Peskova for inspiring discussions and critical comments on the manuscript and to Michaela Hnizdova-Bouckova, Larisa Stolnaya and Jana Kmoskova for excellent technical assistance. The study was supported by the Ministry of Health of the Czech Republic—conceptual development of research organization: RVO-VFN 64165/2012 (a program of the General University Hospital in Prague) and by Ministry of Health of the Czech Republic, grant nr. NU21-08-00324.

CONFLICT OF INTEREST

The authors declare no conflict of interest.

AUTHOR CONTRIBUTIONS

Martin Řeboun performed X inactivation analyses, bioinformatic and statistical analyses, drafted the first version of the manuscript. Jakub Sikora played a key role in the evaluation and interpretation of the results, co-edited the final version of the manuscript. Martin Magner provided essential contribution to initial manuscript, co-edited the final version of the manuscript. Helena Wiederlechnerová and Alena Černá generated and analyzed data of X inactivation analyses. Helena Poupětová performed enzymatic activity measurements. Gabriela

Štorkánová performed mutation analyses. Dita Mušálková interpreted the results of X inactivation analyses, co-edited the manuscript. Gabriela Dostálová and Lubor Golán: ascertained and diagnosed patients, collected the patient samples, supplied clinical and laboratory data and co-edited the manuscript. Aleš Linhart: supervised the collection and presentation of the clinical and laboratory data, co-edited the final version of the manuscript. Lenka Dvořáková: designed and supervised the study, interpreted the results, co-drafted the initial version of the manuscript, co-edited the final version of the manuscript, submitted the manuscript. All authors revised the manuscript and agreed with submission.

DATA AVAILABILITY STATEMENT

The datasets generated for this study are available upon reasonable request to the corresponding author.

ORCID

Jakub Sikora  <https://orcid.org/0000-0003-4104-2023>

Lenka Dvořáková  <https://orcid.org/0000-0002-1620-3211>

REFERENCES

- Amos-Landgraf, J. M., Cottle, A., Plenge, R. M., Friez, M., Schwartz, C. E., Longshore, J., & Willard, H. F. (2006). X chromosome inactivation patterns of 1,005 phenotypically unaffected females. *The American Journal of Human Genetics*, 79(3), 493–499. <https://doi.org/10.1086/507565>
- Blaydon, D., Hill, J., & Winchester, B. (2001). Fabry disease: 20 novel GLA mutations in 35 families. *Human Mutation*, 18(5), 459. <https://doi.org/10.1002/humu.1219>
- Busque, L., Mio, R., Mattioli, J., Brais, E., Blais, N., Lalonde, Y., Maragh, M., & Gilliland, D. G. (1996). Nonrandom X-inactivation patterns in normal females: Lyonization ratios vary with age. *Blood*, 88(1), 59–65.
- Carrel, L., & Brown, C. J. (2017). When the Lyonized chromosome roars: Ongoing expression from an inactive X chromosome. *Philosophical Transactions of the Royal Society B: Biological Sciences*, 372(1733), 20160355. <https://doi.org/10.1098/rstb.2016.0355>
- Coop, G., & Przeworski, M. (2007). An evolutionary view of human recombination. *Nature Reviews Genetics*, 8(1), 23–34. <https://doi.org/10.1038/nrg1947>
- Davies, J. P., Winchester, B. G., & Malcolm, S. (1993). Mutation analysis in patients with the typical form of Anderson-Fabry disease. *Human Molecular Genetics*, 2(7), 1051–1053. <https://doi.org/10.1093/hmg/2.7.1051>
- Dobrovolny, R., Dvorakova, L., Ledvinova, J., Magage, S., Bultas, J., Lubanda, J. C., Elleder, M., Karetova, D., Pavlikova, M., & Hrebicek, M. (2005). Relationship between X-inactivation and clinical involvement in Fabry heterozygotes. Eleven novel mutations in the α -galactosidase a gene in the Czech and Slovak population. *Journal of Molecular Medicine*, 83(8), 647–654. <https://doi.org/10.1007/s00109-005-0656-2>
- Echevarria, L., Benistan, K., Toussaint, A., Dubourg, O., Hagege, A. A., Eladari, D., Jabbour, F., Beldjord, C., De Mazancourt, P., & Germain, D. P. (2016). X-chromosome inactivation in female patients with Fabry disease. *Clinical Genetics*, 89(1), 44–54. <https://doi.org/10.1111/cge.12613>
- Elstein, D., Schachamov, E., Beerli, R., & Altarescu, G. (2012). X-inactivation in Fabry disease. *Gene*, 505(2), 266–268. <https://doi.org/10.1016/j.gene.2012.06.013>
- Eng, C. M., Ashley, G. A., Burgert, T. S., Enriquez, A. L., D'Souza, M., & Desnick, R. J. (1997). Fabry disease: Thirty-five mutations in the alpha-galactosidase a gene in patients with classic and variant phenotypes. *Molecular medicine (Cambridge, MA)*, 3(3), 174–182.
- Ferreira, S., Reguenga, C., & Oliveira, J. P. (2015). The modulatory effects of the polymorphisms in GLA 5'-Untranslated region upon gene expression are cell-type specific. *JIMD Reports*, 23, 27–34. https://doi.org/10.1007/8904_2015_424
- Hoon, B. d., Monkhorst, K., Riegman, P., Laven, J. S. E., & Gribnau, J. (2015). Buccal swab as a reliable predictor for X inactivation ratio in inaccessible tissues. *Journal of Medical Genetics*, 52(11), 784–790. <https://doi.org/10.1136/jmedgenet-2015-103194>
- Hossain, M. A., Yanagisawa, H., Miyajima, T., Wu, C., Takamura, A., Akiyama, K., Itagaki, R., Eto, K., Iwamoto, T., Yokoi, T., Kurosawa, K., Numabe, H., & Eto, Y. (2017). The severe clinical phenotype for a heterozygous Fabry female patient correlates to the methylation of non-mutated allele associated with chromosome 10q26 deletion syndrome. *Molecular Genetics and Metabolism*, 120(3), 173–179. <https://doi.org/10.1016/j.ymgme.2017.01.002>
- Juchniewicz, P., Kloska, A., Tylki-Szymańska, A., Jakóbkiewicz-Banecka, J., Węgrzyn, G., Moskot, M., Gabig-Cimińska, M., & Piotrowska, E. (2018). Female Fabry disease patients and X-chromosome inactivation. *Gene*, 641, 259–264. <https://doi.org/10.1016/j.gene.2017.10.064>
- Lenders, M., Hennermann, J. B., Kurschat, C., Rolfs, A., Canaan-Kühl, S., Sommer, C., Üçeyler, N., Kampmann, C., Karabul, N., Giese, A. K., Duning, T., Stypmann, J., Krämer, J., Weidemann, F., Brand, S. M., Wanner, C., & Brand, E. (2016). Multicenter female Fabry study (MFFS)—Clinical survey on current treatment of females with Fabry disease. *Orphanet Journal of Rare Diseases*, 11(1), 88. <https://doi.org/10.1186/s13023-016-0473-4>
- Lidove, O., Jaussaud, R., & Aractingi, S. (2006). Dermatological and soft-tissue manifestations of Fabry disease: Characteristics and response to enzyme replacement therapy. In A. Mehta, M. Beck, & G. Sunder-Plassmann (Eds.), *Fabry disease: Perspectives from 5 years of FOS*. Oxford PharmaGenesis. Získáno z <http://www.ncbi.nlm.nih.gov/books/NBK11605/>
- Lukas, J., Giese, A. K., Markoff, A., Grittner, U., Kolodny, E., Mascher, H., Lackner, K. J., Meyer, W., Wree, P., Saviouk, V., & Rolfs, A. (2013). Functional characterisation of alpha-galactosidase a mutations as a basis for a new classification system in fabry disease. *PLoS Genetics*, 9(8), e1003632. <https://doi.org/10.1371/journal.pgen.1003632>
- Machado, F. B., Machado, F. B., Faria, M. A., Lovatel, V. L., Alves da Silva, A. F., Radic, C. P., De Brasi, C. D., Rios, A. F., de Sousa Lopes, S. M., da Silveira, L. S., Ruiz-Miranda, C. R., Ramos, E. S., & Medina-Acosta, E. (2014). 5mCpG epigenetic marks neighboring a primate-conserved core promoter short tandem repeat indicate X-chromosome inactivation. *PLoS One*, 9(7), e103714. <https://doi.org/10.1371/journal.pone.0103714>
- Maier, E. M., Osterrieder, S., Whybra, C., Ries, M., Gal, A., Beck, M., Roscher, A. A., & Muntau, A. C. (2006). Disease manifestations and X inactivation in heterozygous females with Fabry disease. *Acta Paediatrica (Oslo, Norway: 1992). Supplement*, 95(451), 30–38. <https://doi.org/10.1080/08035320600618809>
- Mauer, M., Glynn, E., Svarstad, E., Tøndel, C., Gubler, M. C., West, M., Sokolovskiy, A., Whitley, C., & Najafian, B. (2014). Mosaicism of podocyte involvement is related to podocyte injury in females with Fabry disease. *PLoS One*, 9(11), e112188. <https://doi.org/10.1371/journal.pone.0112188>
- Mayes, J. S., Scheerer, J. B., Sifers, R. N., & Donaldson, M. L. (1981). Differential assay for lysosomal alpha-galactosidases in human tissues and its application to Fabry's disease. *Clinica Chimica Acta*, 112(2), 247–251. [https://doi.org/10.1016/0009-8981\(81\)90384-3](https://doi.org/10.1016/0009-8981(81)90384-3)
- Morrone, A., Cavicchi, C., Bardelli, T., Antuzzi, D., Parini, R., Di Rocco, M., Feriozzi, S., Gabrielli, O., Barone, R., Pistone, G., Spisni, C., Ricci, R., & Zammarchi, E. (2003). Fabry disease: Molecular studies in Italian patients and X inactivation analysis in manifesting carriers. *Journal of Medical Genetics*, 40(8), e103.

- Mossner, M., Nolte, F., Hütter, G., Reins, J., Kläumünzer, M., Nowak, V., Obländer, J., Ackermann, K., Will, S., Röhl, H., Neumann, U., Neumann, M., Hopfer, O., Baldus, C. D., Hofmann, W. K., & Nowak, D. (2013). Skewed X-inactivation patterns in ageing healthy and myelodysplastic haematopoiesis determined by a pyrosequencing based transcriptional clonality assay. *Journal of Medical Genetics*, *50*(2), 108–117. <https://doi.org/10.1136/jmedgenet-2012-101093>
- Musalkova, D., Minks, J., Storkanova, G., Dvorakova, L., & Hrebicek, M. (2015). Identification of novel informative loci for DNA-based X-inactivation analysis. *Blood Cells, Molecules & Diseases*, *54*(2), 210–216. <https://doi.org/10.1016/j.bcmd.2014.10.001>
- Nowak, A., Mechtler, T. P., Hornemann, T., Gawinecka, J., Theswet, E., Hilz, M. J., & Kasper, D. C. (2018). Genotype, phenotype and disease severity reflected by serum LysoGb3 levels in patients with Fabry disease. *Molecular Genetics and Metabolism*, *123*(2), 148–153. <https://doi.org/10.1016/j.ymgme.2017.07.002>
- Ortiz, A., Germain, D. P., Desnick, R. J., Politei, J., Mauer, M., Burlina, A., Eng, C., Hopkin, R. J., Laney, D., Linhart, A., Waldek, S., Wallace, E., Weidemann, F., & Wilcox, W. R. (2018). Fabry disease revisited: Management and treatment recommendations for adult patients. *Molecular Genetics and Metabolism*, *123*(4), 416–427. <https://doi.org/10.1016/j.ymgme.2018.02.014>
- Palecek, T., Honzikova, J., Poupetova, H., Vlaskova, H., Kuchynka, P., Golan, L., Magage, S., & Linhart, A. (2014). Prevalence of Fabry disease in male patients with unexplained left ventricular hypertrophy in primary cardiology practice: Prospective Fabry cardiomyopathy screening study (FACSS). *Journal of Inherited Metabolic Disease*, *37*(3), 455–460. <https://doi.org/10.1007/s10545-013-9659-2>
- Pang, S., Chen, D., Zhang, A., Qin, X., & Yan, B. (2012). Genetic analysis of the LAMP-2 gene promoter in patients with sporadic Parkinson's disease. *Neuroscience Letters*, *526*(1), 63–67. <https://doi.org/10.1016/j.neulet.2012.07.044>
- Ploos van Amstel, J. K., Jansen, R. P., de Jong, J. G., Hamel, B. C., & Wevers, R. A. (1994). Six novel mutations in the alpha-galactosidase a gene in families with Fabry disease. *Human Molecular Genetics*, *3*(3), 503–505. <https://doi.org/10.1093/hmg/3.3.503>
- Racchi, O., Mangerini, R., Rapezzi, D., Rolfo, M., Gaetani, G. F., & Ferraris, A. M. (1998). X chromosome inactivation patterns in normal females. *Blood Cells, Molecules & Diseases*, *24*(4), 439–447. <https://doi.org/10.1006/bcmd.1998.0213>
- Řeboun, M., Rybová, J., Dobrovolný, R., Včelák, J., Veselková, T., Štorkánová, G., Mušálková, D., Hřebíček, M., Ledvinová, J., Magner, M., Zeman, J., Pešková, K., & Dvořáková, L. (2016). X-chromosome inactivation analysis in different cell types and induced pluripotent stem cells elucidates the disease mechanism in a rare case of Mucopolysaccharidosis type II in a female. *Folia Biologica*, *62*(2), 82–89.
- Redonnet-Vernhet, I., Ploos van Amstel, J. K., Jansen, R. P., Wevers, R. A., Salvayre, R., & Levade, T. (1996). Uneven X inactivation in a female monozygotic twin pair with Fabry disease and discordant expression of a novel mutation in the alpha-galactosidase a gene. *Journal of Medical Genetics*, *33*(8), 682–688.
- Rossanti, R., Nozu, K., Fukunaga, A., Nagano, C., Horinouchi, T., Yamamura, T., Sakakibara, N., Minamikawa, S., Ishiko, S., Aoto, Y., Okada, E., Ninchoji, T., Kato, N., Maruyama, S., Kono, K., Nishi, S., Iijima, K., & Fujii, H. (2021). X-chromosome inactivation patterns in females with Fabry disease examined by both ultra-deep RNA sequencing and methylation-dependent assay. *Clinical and Experimental Nephrology*, *25*, 1224–1230. <https://doi.org/10.1007/s10157-021-02099-4>
- Saito, S., Ohno, K., & Sakuraba, H. (2013). Comparative study of structural changes caused by different substitutions at the same residue on alpha-galactosidase a. *PLoS One*, *8*(12), e84267. <https://doi.org/10.1371/journal.pone.0084267>
- Rossanti, R., Nozu, K., Fukunaga, A., Nagano, C., Horinouchi, T., Yamamura, T., Sakakibara, N., Minamikawa, S., Ishiko, S., Aoto, Y., Okada, E., Ninchoji, T., Kato, N., Maruyama, S., Kono, K., Nishi, S., Iijima, K., & Fujii, H. (1990). Identification of point mutations in the alpha-galactosidase a gene in classical and atypical hemizygotes with Fabry disease. *American Journal of Human Genetics*, *47*(5), 784–789.
- Sandovici, I., Naumova, A. K., Leppert, M., Linares, Y., & Sapienza, C. (2004). A longitudinal study of X-inactivation ratio in human females. *Human Genetics*, *115*(5), 387–392. <https://doi.org/10.1007/s00439-004-1177-8>
- Shabbeer, J., Robinson, M., & Desnick, R. J. (2005). Detection of alpha-galactosidase a mutations causing Fabry disease by denaturing high performance liquid chromatography. *Human Mutation*, *25*(3), 299–305. <https://doi.org/10.1002/humu.20144>
- Shabbeer, J., Yasuda, M., Benson, S. D., & Desnick, R. J. (2006). Fabry disease: Identification of 50 novel alpha-galactosidase a mutations causing the classic phenotype and three-dimensional structural analysis of 29 missense mutations. *Human Genomics*, *2*(5), 297–309. <https://doi.org/10.1186/1479-7364-2-5-297>
- Shabbeer, J., Yasuda, M., Luca, E., & Desnick, R. J. (2002). Fabry disease: 45 novel mutations in the alpha-galactosidase a gene causing the classical phenotype. *Molecular Genetics and Metabolism*, *76*(1), 23–30. [https://doi.org/10.1016/S1096-7192\(02\)00012-4](https://doi.org/10.1016/S1096-7192(02)00012-4)
- Sharp, A., Robinson, D., & Jacobs, P. (2000). Age- and tissue-specific variation of X chromosome inactivation ratios in normal women. *Human Genetics*, *107*(4), 343–349.
- Stenson, P. D., Mort, M., Ball, E. V., Chapman, M., Evans, K., Azevedo, L., Hayden, M., Heywood, S., Millar, D. S., Phillips, A. D., & Cooper, D. N. (2020). The human gene mutation database (HGMD®): Optimizing its use in a clinical diagnostic or research setting. *Human Genetics*, *139*(10), 1197–1207. <https://doi.org/10.1007/s00439-020-02199-3>
- Swierczek, S. I., Piterkova, L., Jelinek, J., Agarwal, N., Hammoud, S., Wilson, A., Hickman, K., Parker, C. J., Cairns, B. R., & Prchal, J. T. (2012). Methylation of AR locus does not always reflect X chromosome inactivation state. *Blood*, *119*(13), e100–e109. <https://doi.org/10.1182/blood-2011-11-390351>
- Yanagisawa, H., Hossain, M. A., Miyajima, T., Nagao, K., Miyashita, T., & Eto, Y. (2019). Dysregulated DNA methylation of GLA gene was associated with dysfunction of autophagy. *Molecular Genetics and Metabolism*, *126*(4), 460–465. <https://doi.org/10.1016/j.ymgme.2019.03.003>

SUPPORTING INFORMATION

Additional supporting information may be found in the online version of the article at the publisher's website.

How to cite this article: Řeboun, M., Sikora, J., Magner, M., Wiederlechnerová, H., Černá, A., Poupětová, H., Štorkánová, G., Mušálková, D., Dostálová, G., Golán, L., Linhart, A., & Dvořáková, L. (2022). Pitfalls of X-chromosome inactivation testing in females with Fabry disease. *American Journal of Medical Genetics Part A*, 1–11. <https://doi.org/10.1002/ajmg.a.62728>

